Characterizing the role of accumbens medium spiny neurons in vulnerability to heroin addiction

Timothy J. O'Neal

A dissertation submitted in partial fulfillment
of the requirements for the degree of

Doctor of Philosophy

University of Washington
2021

Reading Committee:
Susan M. Ferguson, Chair
Larry S. Zweifel
Paul E. M. Phillips

Program authorized to offer degree:
Neuroscience

University of Washington

Abstract

Characterizing the role of accumbens medium spiny neurons
in vulnerability to heroin addiction

Timothy J. O'Neal

Chair of Supervisory Committee:
Associate Professor Susan M. Ferguson
Department of Psychiatry & Behavioral Sciences

Opioid addiction is a chronic, relapsing disorder that arises from dysregulation of the neural circuits responsible for reward processing, associative learning, and decision making, and is conceptualized as a three-stage, cyclical process encompassing drug consumption, withdrawal, and drug craving. Research into the neurobiological mechanisms that underlie addiction has demonstrated a central role for the cortico-basal ganglia circuit in the development and persistence of maladaptive addictive behaviors. The nucleus accumbens (NAc), which lies at the interface of the cortico-basal ganglia circuit, integrates cortical and subcortical inputs to guide behavioral output. The NAc is a heterogeneous structure containing two interspersed populations of medium spiny neurons (MSNs) with oppositional behavioral control: direct pathway MSNs (dMSNs) facilitate behavior and serve as a "go" signal; indirect pathway MSNs (iMSNs) suppress behavior and serve as a "stop" signal. Behavioral regulation is thought to rely on a balance between signaling of the direct and indirect pathways, and discrete behavioral aberrations, such as those associated with addiction, have been linked to disruptions of this balance. For example, driving NAc output (via dMSN activation or iMSN inhibition) facilitates drug taking and drug seeking, while dampening NAc output (via dMSN inhibition or iMSN activation) suppresses drug taking and drug seeking. Moreover, the excitability of iMSNs increases after cocaine exposure in cocaine-resistant mice, suggesting a role for MSNs in encoding individual vulnerability to addiction. It is important to note that most of our understanding of the role of these neuronal populations in regulating addictive behaviors is based on psychostimulant research, so their contribution to opioid addiction remains unknown. Furthermore, only a subset of individuals who use drugs medically or recreationally transition to addiction, so it is imperative to determine the neural correlates of vulnerability to addiction.

The overarching goal of this thesis was to combine innovative strategies for modulating and monitoring the activity of dMSNs and iMSNs with classic behavioral models of addiction that have been modified to highlight individual variability to the effects of heroin. In the first chapter, I will present an overview of the state of the opioid epidemic in the United States, introduce the primary nuclei of the cortico-basal ganglia circuit, and describe prominent mechanisms for modulating the excitability of dMSNs and iMSNs. The second chapter will introduce a model of intermittent-access heroin self-administration that produces subsets of addiction-resistant and addiction-sensitive rats, followed by a series of chemogenetic studies to assess the role of bidirectional modulation of dMSNs and iMSNs in the motivation to self-administer heroin and cue-induced heroin seeking after a period of abstinence. The third chapter will introduce a heroin conditioned place preference procedure that produces subsets of rats that are sensitive to and resistant to the reinforcing effects of heroin, followed by a series of fiber photometry studies to investigate the temporal signatures of dMSNs and iMSNs, as well as dopamine, during conditioned heroin reinforcement. The fourth chapter will describe a series of studies exploring sex differences in the behavioral effects of heroin following psychomotor sensitization or intermittent-access self-administration. The final chapter will summarize the main findings of these studies and describe a hypothetical model for the encoding of vulnerability to heroin addiction by dMSNs and iMSNs in the NAc, along with introducing multiple lines of future study stemming from these findings.

Timothy Joseph O'Neal

Education

August 2016 – Present
University of Washington | Seattle, WA
Doctorate of Philosophy, Neuroscience
Anticipated completion: March 2021

September 2010 – June 2014
Knox College | Galesburg, IL
Bachelor of Arts in Neuroscience & Biochemistry
Department Honors in Neuroscience & Biochemistry

Teaching

September 2017 – December 2017
TA, NEURO302 (Systems & Behavioral Neurobiology)
UW Department of Biology

May 2017 – August 2017
Instructor, Research Presentation & Communication
STEM-Prep Project

March 2014 – June 2014
TA, BCHM310 (Methods in Biochemistry)
Knox College Department of Biochemistry

March 2014 – June 2014
TA, NEUR340 (Methods in Neuroscience)
Knox College Department of Neuroscience

September 2012 – June 2014
Peer Tutor (CRLA Level 1)
Knox College Center for Teaching & Learning

Funding

January 2019 – Present
Predoctoral NRSA, F31 DA047012
National Institute on Drug Abuse

May 2018 – April 2019
ADAI Small Grants Program, ADAI-0318
UW Alcohol and Drug Abuse Institute

September 2017 – December 2018
UW Neuroscience Training Grant, T32 NS99578
National Institute of Neurological Disorders & Stroke

Research

August 2016 – Present
Doctoral Candidate
Department of Psychiatry & Behavioral Sciences, University of Washington
Center for Integrative Brain Research, Seattle Children's Research Institute
PI: Susan Ferguson

September 2014 – August 2016
Post-Baccalaureate Fellow
Eating and Addiction Section and Laboratory of Biology Modeling
National Institute of Diabetes and Digestive and Kidney Diseases
PI: Alexxai Kravitz, Kevin Hall

June 2014 – September 2014
Research Assistant
Human Behavioral Pharmacology Laboratory, University of Chicago
PI: Harriet de Wit, Emma Childs

August 2013 – May 2014
Honors Research Fellow
Department of Neuroscience, Knox College
PI: Heather Hoffmann

June 2013 – August 2013
Research Assistant
Department of Pharmacology, Universidade Federal de Santa Catarina
PI: Antonio Padua de Carobrez

June 2012 – August 2012
Research Assistant
Department of Neuroscience, Knox College
PI: Esther Penick

Skills

Addictive behaviors: **CPP, self-administration, sensitization**
Other behaviors: **Operant, Pavlovian**, locomotor/anxiety/depression
Biochemical/cellular assays: **IHC**, RNAscope, slice calcium imaging
Cell-type specific tools: Optogenetics, **DREADDs**, fiber photometry
Software: **MedAssociates**, Noldus, **Bonsai**, **Adobe CC**, R, **Python**, MATLAB
Surgery: **Viral infusion**, lens/cannula/**fiber implantation**, **catheterization**

Proficiency: moderate, **advanced**, **expert**

1900 9th Ave, Seattle, WA 98108 • timoneal@uw.edu • (815) 510–8408 • @tim.j.oneal

Publications

A conditioned place preference to heroin is signaled by increases in dopamine and direct pathway activity and decreases in indirect pathway activity in the nucleus accumbens. **O'Neal TJ**, Bernstein MX, Ferguson SM (2021). Neuropsychopharmacology, under review

Dopamine D2 receptor signaling on iMSNs is required for initiation and vigor of learned actions. Augustin SM, Loewinger GC, **O'Neal TJ**, Kravitz AV, Lovinger DM (2020). Neuropsychopharmacology, PMID 32811899.

One is not enough: Understanding and modeling polysubstance use. Crummy EA, **O'Neal TJ**, Baskin BM, Ferguson SM (2020). Frontiers in Neuroscience, PMID 32612502

Chemogenetic modulation of accumbens direct or indirect pathways bidirectionally alters reinstatement of heroin-seeking in high- but not low-risk rats. **O'Neal TJ**, Nooney M, Thien K, Ferguson SM (2020). Neuropsychopharmacology, PMID 31747681

Feeding Experimentation Device (FED): Construction and validation of an open-source device for measuring feeding behavior in rodents. Nguyen KP, Ali MA, **O'Neal TJ**, Szczot I, Licholai JA, Kravitz AV (2017). Journal of Visualized Experiments, PMID 28287564

Increases in wheel running result in diminishing increments in daily energy expenditure in mice. **O'Neal TJ***, Friend DM*, Guo J, Hall KD, Kravitz AV (2017). Current Biology, PMID 28111149

Basal ganglia dysfunction contributes to physical activity in obesity. Friend DM*, Devarakonda K*, **O'Neal TJ***, Skirzewski M, Kaplan A, Liow JS, Guo J, Rubenstein M, Alvarez VA, Hall KD, Kravitz AV (2017). Cell Metabolism, PMID 28041956

Do dopaminergic impairments underlie physical inactivity in people with obesity? Kravitz AV, **O'Neal TJ**, Friend DM (2016). Frontiers in Human Neuroscience, PMID 27790107

Feeding Experimentation Device (FED): A flexible open-source device for measuring feeding behavior. Nguyen KP, **O'Neal TJ**, Bolonduro R, White E, Kravitz AV (2016). Journal of Neuroscience Methods, PMID 27060385

Presentations

Talk Characterizing the role of accumbens medium spiny neurons in vulnerability to heroin addiction. UMN Medical Discovery Team on Addiction Seminar (Zoom; 12/11/20).

Poster Characterizing individual vulnerability and sex differences in heroin addiction. ACNP (Zoom; 12/09/20)

Talk Does the nucleus accumbens encode vulnerability to heroin addiction? UW Psychiatric Neuroscience Research Group (Zoom; 07/17/20).

Poster Female and male rats do not differ in vulnerability to heroin addiction. WCBR (Big Sky, MT; 01/27/20)

Talk Nucleus accumbens medium spiny neurons encode vulnerability to relapse in high-risk rats. WCBR (Snowmass Village, CO; 02/01/19), Seattle Children Research Institute's Graduate and Postdoc Symposium (Seattle, WA; 11/16/18)

Poster Striatal medium spiny neurons regulate reinstatement of heroin seeking. SfN (Washington, DC; 11/11/17), Seattle Children's Research Institute's Fall Symposium (Seattle, WA; 11/04/17)

Talk Dopamine D2 receptors on indirect pathway medium spiny neurons regulate motivation, but not learning, in a water T-maze. SfN (San Diego, CA; 11/15/16)

Talk Behavioral and physiological adaptation to voluntary exercise in mice. NIDDK Annual Scientific Meeting (Bethesda, MD; 04/07/16)

Poster Energetic cost of a running wheel: Implications for exercise-based weight loss interventions. SfN (Chicago, IL; 10/18/15), SSIB (Denver, CO; 07/07/15), NIH-Korea Collaborative Biomedical Research Symposium (Bethesda, MD; 04/16/15)

Poster Nicotine enhances initial sensitivity and acute functional tolerance to alcohol. RSA (San Antonio, TX; 06/21/15), ACNP (Hollywood, FL; 12/08/15)

Poster The sigma-1 receptor: A unique target for treatment of behavioral changes during methamphetamine addiction and withdrawal. SfN Chicago Chapter (Chicago, IL; 04/04/14).

Poster Interaction between the dorsolateral periaqueductal gray and glucocorticoids in the formation of aversive memories. SfN (San Diego, CA; 11/11/13), Midstates Consortium for Math and Science Research (St. Louis, MO; 11/02/13)

1900 9th Ave, Seattle, WA 98108 • timoneal@uw.edu • (815) 510–8408 • @tim.j.oneal

Awards

SfN Trainee Professional Development Award (2017)
NSF GRFP Honorable Mention (2017)
NIH Outstanding Poster Award (2015, 2016)
Frank & Ruth Schmitt Student Research Award (2014)
Richter Memorial Trust (2012, 2013, 2014)
Knox College Dean's List (2011 – 2014)
TRIO Achievement Program (2011 – 2014)
Hermann Muelder Scholarship (2010 – 2014)

Engagement

UW Neuroscience Graduate Recruitment Committee (2019)
UW Gray Matters (2018 – Present)
UW Advocates for Representation, Justice, & Equity (2018 – Present)
UW Graduate School Science & Policy Committee (2017 – Present)
UW Graduate & Professional Student Senate (2016 – Present)
UW Neuroscience Community Outreach Group (2016 – Present)
SfN Capitol Hill Day (2016)
NIDDK Fellows Advisory Board (2015 – 2016)

1900 9th Ave, Seattle, WA 98108 • timoneal@uw.edu • (815) 510–8408 • @tim.j.oneal

ACKNOWLEDGEMENTS

There were many times over the past four years that I doubted whether I was capable of finishing graduate school, including several moments when I was certain I would not. This thesis is the culmination of hundreds of hours of experiments, many of which kept me in lab until the middle of the night for weeks on end and some of which were done in their entirety during a pandemic. My experience in graduate school has been exhausting, overwhelming, and difficult, but through my many failures and an ongoing battle with imposter syndrome I do believe I have become a better scientist. Yet I firmly believe that none of this would have been possible if it had not been for the incredible group of individuals who supported me over the years; without them, none of this would have been possible.

To my advisor, Susan Ferguson: thank you for encouraging me to go outside my comfort zone and learn new skills, techniques, and ways of approaching problems; for trusting in me enough to give me the independence I needed to learn to fail and continue going; for giving me so many opportunities to explore my creativity and share my research; and for pushing me to find the work / life balance I needed to make it through grad school.

To my committee members, Larry Zweifel, Charley Chavkin, Paul Phillips, and Marti Bosma: thank you for your feedback, suggestions, and insight over the years. Your unique perspectives influenced my approach towards experimental design, analysis, and interpretation, and your confidence in my abilities gave me the assurance I needed to believe in myself.

To the many scientists who collaborated with me over the years, Abbie Schindler, Garret Stuber, Steve Smith, Whitney Heavner, Aguan Wei, and Liza Severs: thank you for your patience when teaching me new skills; for trusting me to tackle wild, unforeseen obstacles in our work together; and for treating me as an equal every step of the way.

To my labmates, Elizabeth Crummy, Aaron Garcia, Kanichi Nakata, Zackari Murphy, Brit Baskin, and Mollie Bernstein: thank you for being incredible teammates; for taking the time out of your days to help in a moment of crisis; for working around my often-unpredictable schedule; and for your kindness, sincerity, and generosity when things were rough.

To our undergraduate students, Reiley Duerre, Marlaena Nooney, Katie Thien, Grayson Bayden, and Jordyn Richardson: thank you for the tremendous amount of help over the years, and for giving me the chance to grow as a teacher and mentor.

To my incredible friends who provided endless love and support over the years, particularly Olivia Louko and Yael Cody: thank you for the thousands of games of euchre; for the countless hikes and adventures; for the pasta making and bread baking; for the puppy play dates; and for being the most supportive pals anyone could ask for.

And to my best friend and the love of my life, Rob Noland: thank you for taking a chance on me; for being willing to work around my schedule for late night walks and late morning breakfasts; for believing in me and helping me carry on when I was too exhausted to carry on; for helping on my long recovery after my shoulder injury; for getting a puppy with me in the middle of a pandemic; for being an endless source of joy, kindness, love, and comfort.

TABLE OF CONTENTS

CHAPTER 1

OPIOID ADDICTION, THE CORTICO-BASAL GANGLIA CIRCUIT, & MEDIUM SPINY NEURONS

With excerpts from:

Elizabeth A. Crummy, Timothy J. O'Neal, Britahny M. Baskin, Susan M. Ferguson

Frontiers in Neuroscience (2020) **14**: 569

THE OPIOID CRISIS

Epidemiology

Drug addiction is a heterogeneous disorder characterized by cyclic periods of drug use, withdrawal and abstinence, and drug-craving and recurrence of use[1]. Addiction is highly prevalent in our society, with 19.3 million people in the United States meeting the diagnostic criteria for a substance use disorder (SUD) in 2018 and ~10% of individuals developing a SUD during their lifetime[2,3]. Drug addiction is also one of the largest public health problems in the US, with an annual financial burden of $740 billion in costs related to treatment, lost work productivity, healthcare, and crime[4]. Notably, drug use has been rising worldwide in recent years, with ~250 million individuals reporting drug use in 2018 alone[5]. Although opioid use in the US has begun to plateau at ~11 million users, global opioid use has continued to rise; in 2018 alone, for example, 53 million people worldwide reported misusing opioids[5]. Additionally, opioid-associated mortality has continued to rise both globally and domestically, increasing >6-fold from 1999 to 2017[6] (**Figure 1.1**).

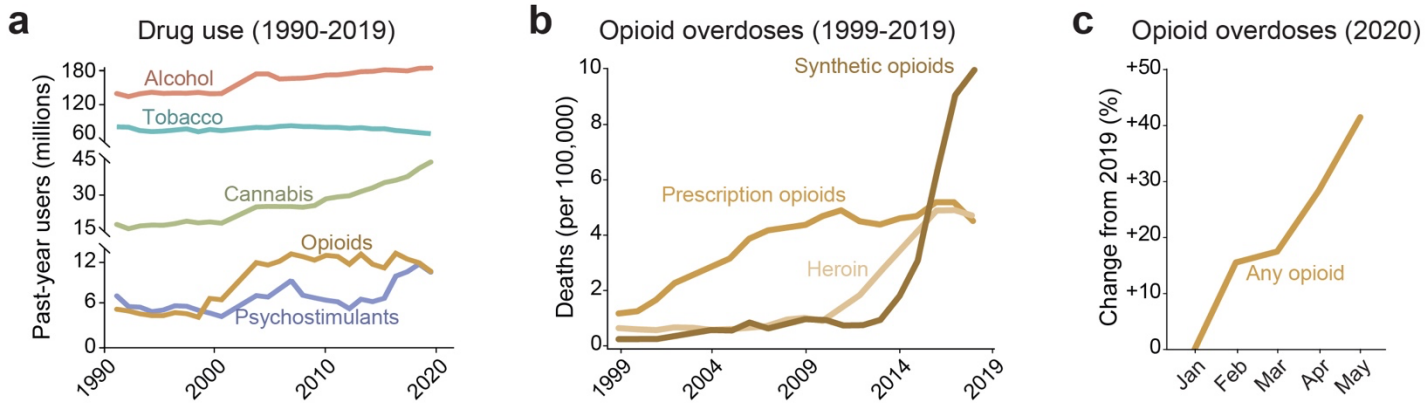

Figure 1.1 | Public health trends in opioid use. (**a**) Drug use in the United States from 1990 to 2019. Data from the National Household Survey on Drug Abuse and the National Survey on Drug Use and Health. (**b**) Drug overdose deaths in the United States from 1999 to 2019 involving opioids. Data from the Centers for Disease Control and Prevention. (**c**) Drug overdose deaths in the United States in 2020. Data from the Overdose Detection Mapping Application Program.

Although a rise in opioid-related mortality may seem contradictory to a plateau in opioid use, it can be explained by the trajectory of the opioid epidemic, which has occurred in three waves. Prior to the early 1990s, prescription of opioids for chronic pain outside of cancer treatment, palliative care, and end-of-life care was relatively uncommon. This began to change in the mid-1990s when pharmaceutical companies – particularly Purdue Pharma (the manufacturer of OxyContin) – employed a myriad of marketing strategies to increase prescription and use of opioids. These strategies, which included downplaying the addictive potential of these drugs to Congress, hosting all-expenses-paid symposia to influence prescribing habits, and offering lucrative bonuses to increase opioid sales, were remarkably successful, with sales of OxyContin alone growing from $48 million to $1.1 billion between 1996 and 2000[7]. These aggressive prescribing practices of opioids continued during the early 2000s and led to the first wave of the opioid epidemic, characterized by increased use of prescription opioids. The second wave of the opioid epidemic began ~2010 with the rise of heroin use. As regulators began to take steps towards stymying the flow of prescription opioids into particularly hard-hit communities, heroin became a cheaper, more easily attainable and potent alternative for opioid-dependent individuals. Deaths linked to heroin overdoses increased >250% from 2002 to 2013, and 80% of heroin users reported initial abuse of prescription opioids before switching to heroin[8,9]. The third wave of the opioid epidemic began in 2013 with a rise in deaths related to synthetic opioids – particularly fentanyl. Unlike earlier waves of the opioid epidemic, overdoses during the third wave have risen more rapidly, with an ~8-fold increase in overdose deaths since 2013[2]. This can be largely attributed to two factors: potency and distribution. Fentanyl has a remarkably high potency (~100x that of morphine), and fentanyl has increasingly been cut into other illicit opioids, particularly heroin[10]. This contributes to opioid users unknowingly taking fentanyl-laced opioids that are more potent than expected, leading to a greater risk of overdose and death. Following declaration of opioid addiction as a public health emergency in 2017, an increased focus on reducing opioid misuse and treating opioid addiction has contributed to a slow decline in overdose mortality. However, with the emergence of the COVID-19 pandemic and increased social isolation, overdose-related deaths have been on the rise – with a >40% rise in overdose mortality through May 2020[11]. The threat of overdose has always been disproportionately higher for isolated, socioeconomically disadvantaged individuals, and the gap between the privileged and disadvantaged has only widened during the COVID-19 pandemic.

Diagnosis and treatment

In 2013, the American Psychological Association released the updated Diagnostic and Statistical Manual of Mental Disorders (DSM) that included substantive changes in the characterization and diagnosis of SUDs. Unlike the prior DSM-IV that separately diagnosed substance abuse and substance dependence, the DSM-5 contains a spectrum for diagnosing SUDs that spans mild to severe, and is dependent on presence of specific criteria[12]. These criteria include escalation of drug intake, continued use despite negative consequences

(interpersonal, social, physical, or psychological), drug craving, emergence of tolerance, and withdrawal. While imperfect, the DSM-5's spectrum of addictive behaviors more closely captures the nature of addiction, regarded as a three-phase, cyclical process encompassing drug consumption, withdrawal, and drug craving[1]. Following bouts of excessive drug consumption, individuals undergo acute (i.e., minutes to hours) and chronic (i.e., hours to days) periods of withdrawal that are characterized by a negative affective state (e.g., dysphoria, heightened stress reactivity). Thereafter, individuals experience persistent drug-craving that increases over time, ultimately leading to relapse and propagation of the cycle. Rates of relapse are higher for opioids than for other drugs, with 59% of individuals relapsing within the first week of abstinence and 80% relapsing within the first month[13]. Notably, while prescription of opioids contributed to the onset and exacerbation of the current opioid crisis, development of pharmacotherapeutics for the treatment of opioid addiction has lagged behind. Today, FDA-approved medications for the treatment of opioid addiction are limited to those that reverse overdoses (naloxone) and those that work as opioid replacement therapies (e.g., methadone, buprenorphine). Importantly, there are currently no pharmacotherapeutics available to prevent binge opioid consumption or to alleviate opioid craving during abstinence, largely due to an incomplete understanding of the neural circuitry governing such behaviors.

THEORIES & MODELS OF ADDICTION

Theories of addiction

Over time, multiple theories of addiction have been proposed in an attempt to explain the various processes that contribute to the development and persistence of addiction. Several of these have gained prominence due to their elegant explanation of key components of the addiction cycle that are grounded in neuroscientific evidence: (1) incentive sensitization, (2) aberrant learning, (3) hedonic allostasis, and (4) frontostriatal dysfunction[14]. The incentive sensitization theory of addiction posits that potentially addictive drugs cause an initial increase in phasic dopamine (DA) release, which functions to attribute incentive salience (i.e., the psychological process that increases the valence of reward-associated cues) to cues, contexts, and other events associated with drug use. In addition, this theory posits that repeated exposure to drugs produces long-lasting adaptations in DA systems to sensitize responses to drugs and drug-associated stimuli[15]. The aberrant learning theory of addiction posits that repeated drug exposure enhances Pavlovian and instrumental sensitivity to drug-associated stimuli via neuroplastic adaptations in reward-associated nuclei, and that this heightened, targeted behavioral response is insensitive to outcome devaluation[16]. The hedonic allostasis theory, derived from the opponent-processes theory of motivation, proposes that while initial drug use is primarily due to the drug's rewarding effects, chronic drug use reduces the rewarding effects of drugs, recruits stress systems, and shifts the hedonic setpoint downward, such that continued drug use is driven by a desire to alleviate dysphoria, rather than enhance euphoria[17]. The frontostriatal dysfunction theory of addiction posits

that repeated drug exposure induces deficits in executive control that leads to exaggerated responsiveness to drugs and drug-associated stimuli, loss of impulse control, and overall impaired decision-making[18]. Drawing from these theories, prominent behavioral models have been developed over the years to investigate the contribution of specific neural circuits to addiction (**Figure 1.2**)[19]. Designed to assay specific addictive behaviors, these models have led to a substantial increase in our understanding of the neurobiology of addiction.

Psychomotor sensitization

The sensitizing properties of drugs of abuse have classically been used as a proxy for measuring progression of addiction pathology, including compulsive drug-seeking and psychosis. As proposed in the incentive sensitization theory, repeated exposure to drugs of abuse sensitizes the neural circuits underlying motivation, including those that illicit drug craving and seeking. Accordingly, psychomotor sensitization procedures involve repeated administration of a drug over multiple sessions, during which the locomotor response is monitored. Over time and with repeated drug exposure, the locomotor response becomes sensitized and stereotyped behaviors ("stereotypies") begin to develop, resulting in a hyperactive response to drug exposure[20]. In addition to measuring direct sensitization in response to repeated drug exposure, sensitization procedures frequently include a period of drug abstinence and withdrawal, followed by a challenge session that can provide insight into the persistent adaptations resulting from drug sensitization.

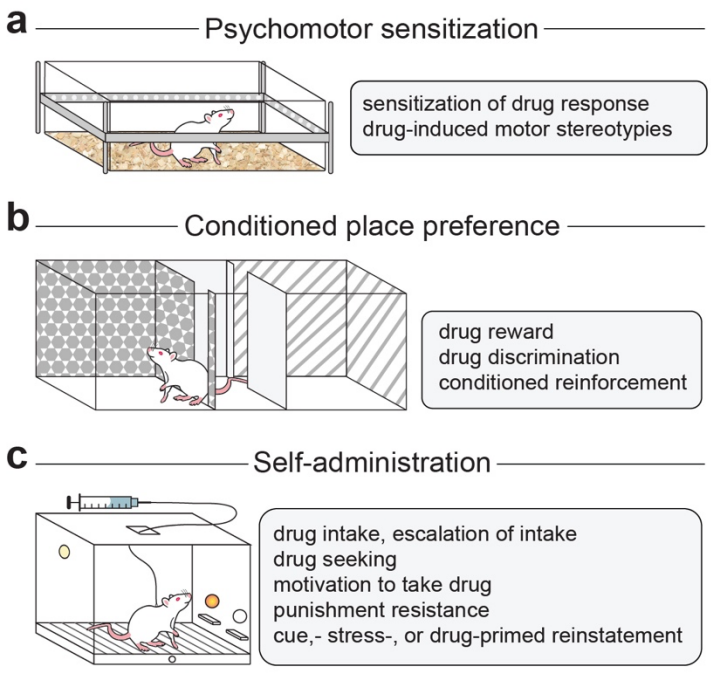

Figure 1.2 | Animal models of addiction. Schematics and example behavioral metrics assessed with (**a**) psychomotor sensitization, (**b**) conditioned place preference, and (**c**) self-administration procedures.

Conditioned place preference

In accordance with the aberrant learning theory of addiction, it is hypothesized that pairing drug exposure with specific stimuli produces an association that is insensitive to devaluation or extinction, facilitating the persistence of stimuli-induced drug craving. For decades, conditioned place preference (CPP) procedures have been used to investigate the neural circuits underlying this form of associative learning and have provided extensive insight into the development of conditioned drug seeking behaviors. CPP procedures involve two visually distinct chambers, with or without a smaller center chamber, that can be open for free exploration

or closed for confinement. During conditioning, subjects are alternatively confined to each chamber following non-contingent exposure to a drug and a non-drug reward, such as saline. Following conditioning, subjects are then allowed to freely explore the entire apparatus and spend time where they choose, which is often in the drug-paired chamber[21]. CPP procedures can also be modified to compare the rewarding effects of different types of drugs, different doses of the same drug, or drugs and non-drug rewards (e.g., highly palatable food), and can be extended to examine the persistence of the conditioned response.

Self-administration

While useful for answering specific questions about the sensitizing and rewarding properties of drugs, locomotor sensitization and CPP procedures are inherently limited due to the non-contingent (i.e., researcher-administered) route of drug administration. Contingent administration of drugs provides the opportunity to investigate a much broader set of questions around drug use, including drug-seeking and -taking, motivation to take drug, continued drug seeking despite negative consequences, and drug-seeking after a period of abstinence[22]. Moreover, self-administration of drugs can provide tremendous insight into individual differences associated with drug use and can help identify neural mechanisms that contribute to an individual's vulnerability to addiction. Self-administration procedures typically involve learning an action-outcome pairing of a drug reward delivered after completion of a response contingency (e.g., nose poke, lever press). Classic self-administration involves short-access sessions of continuous drug access for the length of a session (~1-3 hours)[23]. These sessions typically require a fixed number of responses for drug delivery, known as the fixed ratio (FR) of reinforcement. Depending on the nature of the experiment, the FR can begin low (e.g., FR1) and increase over time to assess willingness to work for drug at an increased cost. In addition to modifying the FR, self-administration procedures have been developed to lengthen the duration of each session (long-access), interleave periods of drug-availability with periods of drug-unavailability within a single session (intermittent-access), or increase training to >30 sessions to look at long-term patterns of drug use (extend-access). Unlike short-access self-administration, these variants more easily produce variability in the development and expression of addiction severity, allowing researchers to selectively study drug-induced alterations in vulnerable versus resilient groups[24–27] and model DSM criteria[28,29]. Once self-administration has been acquired through FR training, subjects can then undergo a plethora of additional tests to assay specific addiction-like behaviors, including: progressive ratio, a test of motivation in which the response contingency increases with successive reward deliveries; behavioral economics, a test of motivation in which the response contingency remains constant but the reward size decreases with successive trials; and punishment sessions, a test of sensitivity to negative consequences in which infusions are paired with a footshock[22]. Additionally, self-administration experiments can include extinction/reinstatement sessions, in which the action/outcome relationship is initially devalued (i.e., responding no longer results in drug delivery or presentation of drug-

paired cues) and the sensitivity to reinitiate drug-seeking is assessed following re-exposure to drug-associated stimuli (e.g., cues, context) or a stressor. Alternatively, self-administration can be followed by a period of abstinence (either forced or voluntary) prior to re-exposure to drug-associated stimuli. This abstinence period is known as incubation of craving[30,31], and drug craving has been shown to progressively increase with longer incubation periods. In combination with targeted (e.g., pharmacology, optogenetics, chemogenetics) or gross (e.g., lesions, ablations) manipulations of neural activity, these behavioral paradigms have revealed tremendous insight into the neural basis of addictive behaviors.

NEUROBIOLOGY OF ADDICTION

The development and maintenance of addictive behaviors arises in part from maladaptive neuroplasticity within the neural circuits responsible for decision making, associative learning, motivation, and reward processing. In particular, alterations in the cortico-basal ganglia circuit (C-BG) are known to contribute to the development and persistence of addictive behaviors[1]. The C-BG is a heavily interconnected network that integrates sensory and interoceptive cues to drive motivated behavioral output. The striatum, which serves as the interface of the C-BG, receives extensive glutamatergic input from cortical and subcortical regions (e.g., amygdalar, thalamic, and hippocampal nuclei), along with dopaminergic modulation from the ventral tegmental area (VTA) and substantia nigra in the midbrain[32,33] (**Figure 1.3**). Integration of glutamatergic and dopaminergic inputs with lateral inhibition in the striatum contributes to the initiation or suppression of behavioral output, and imbalanced signaling between the two striatal output pathways can drive addictive behaviors[34–36].

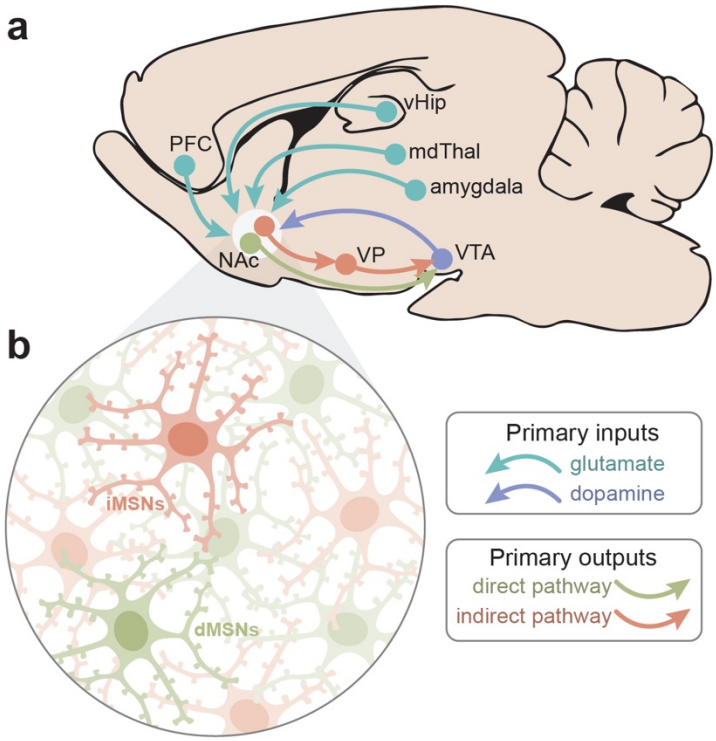

Figure 1.3 | Cortico-basal ganglia circuitry. (**a**) Prominent glutamatergic (blue) and dopaminergic (purple) inputs to the nucleus accumbens (NAc). (**b**) Local connectivity between direct pathway medium spiny neurons (dMSNs) and indirect pathway medium spiny neurons (iMSNs) in the NAc.

Prefrontal cortex

The prefrontal cortex (PFC) is centrally involved in reward learning, decision making, and outcome valuation[37]. It is a highly heterogenous structure, which adds to the complexity in understanding its role in normal cognition, as well as how its dysregulation contributes to drug use and addiction. In general, the medial prefrontal cortex (mPFC) – encompassing the anterior cingulate, prelimbic, and infralimbic cortices – regulates motivation and seeking of both natural and drug rewards via

excitatory glutamatergic projections to the NAc and VTA[1]. Notably, projections from the mPFC to the NAc are topographically and functionally organized, with the prelimbic cortex preferentially innervating the NAc core and encoding reward-associated cues and the infralimbic cortex preferentially innervating the NAc shell and encoding reward-associated contextual information[14,38,39]. The PFC is comprised of six layers, each with unique connectivity patterns and distinct cell types. Specifically, the PFC contains large pyramidal output cells that make up ~75% of all cortical cells, as well as several subtypes of interneurons[40]. Pyramidal cells in layers II/III send local projections within cortex, while those in layers V-VI send projections throughout the C-BG, including to the striatum, midbrain, amygdala, hippocampus, and thalamus[40,41]. Pyramidal cells can be further subdivided into intratelencephalic, pyramidal tract, and corticothalamic cells, each with distinct physiology and connectivity[42–46]. Recent studies have begun to characterize the anatomical, electrophysiological, and molecular profiles of each of these cell types[43,47–50], though how they each regulate behavior remains poorly understood. Finally, the PFC contains multiple populations of interneurons that heavily regulate cortical output via projections to both pyramidal neurons and interneurons[51,52].

Ventral tegmental area

The VTA, together with the substantia nigra, sends dopaminergic projections throughout the C-BG to modulate network activity and behavioral output[53]. Dopaminergic projections from the substantia nigra pars compacta to the dorsal striatum regulate action initiation, while those from the VTA to the NAc regulate goal-directed behaviors[54]. Recently identified subtypes of DA neurons with unique molecular profiles preferentially project to the NAc core or NAc shell, and regulate reward learning or motivation, respectively, yet co-activation of both populations appears to be necessary for robust reinforcement[55]. DA neurons receive dense glutamatergic input from the PFC, bed nucleus of the stria terminalis, and periaqueductal gray, as well as GABAergic input from a variety of sources[56], including the NAc and local GABA neurons. GABA neurons maintain tonic DA levels via inhibition of DA neurons, and brief disinhibition of DA neurons results in phasic DA release into the NAc. DA neurons receive glutamatergic input from the PFC and a number of subcortical nuclei, as well as GABAergic input from throughout the brain, including the NAc[56]. The VTA also contains glutamatergic neurons that project to striatal interneurons[57,58], though the inputs to and behavioral relevance of these neurons is unknown. Notably, the VTA contains subpopulations of DA neurons that can release glutamate and/or GABA[56,59,60], allowing the VTA to modulate C-BG activity at multiple levels and time scales. In addition to local inhibition from GABA neurons and the NAc, the activity of DA neurons undergoes dopaminergic modulation from D2 autoreceptors on DA terminals and cholinergic modulation from striatal cholinergic interneurons[56].

Striatum

The striatum is a heterogeneous structure comprised primarily of two interspersed populations of GABAergic medium spiny neurons (MSNs) that can bidirectionally regulate behavioral output. Direct pathway MSNs (dMSNs) express dopamine D1 receptors and the neuropeptides dynorphin and substance P, project directly to the midbrain, and can promote behavioral output by serving as a “go” signal. Conversely, indirect pathway MSNs (iMSNs) express dopamine D2 receptors and the neuropeptide enkephalin, project indirectly to the midbrain via the pallidum, and can suppress behavioral actions by serving as a “stop” signal[32,34]. The striatum contains dorsal and ventral compartments, with further subdivisions based on connectivity and function. The dorsal striatum receives dopaminergic modulation from the substantia nigra pars compacta and glutamatergic input from sensorimotor and associative cortices[61]. The ventral striatum, comprised of the olfactory tubercule, nucleus accumbens (NAc) core, and NAc shell, receives dopaminergic modulation from the VTA and glutamatergic input from the PFC, as well as thalamic, hippocampal, and amygdala nuclei[62]. In general, the dorsal striatum regulates motor planning, action selection, and locomotion, while the ventral striatum regulates motivated behavior and reward learning[34,63]. However, it has been hypothesized that an ascending loop between ventral and dorsal striatum facilitates information consolidation during learning, whereby habitual behaviors transition from the ventral striatum to the dorsal striatum[61,64]. Importantly, while dMSNs and iMSNs have historically been differentiated by downstream targets and expression of dopamine receptors, dorsal and ventral striatal dMSNs send collaterals to the pallidum[65,66], and D1 and D2 receptors are co-expressed by MSNs in the dorsal striatum (2-5%), NAc core (6-7%), and NAc shell (12-15%)[67,68]. In addition to MSNs, the striatum contains large, tonically-active cholinergic interneurons and multiple subtypes of GABAergic interneurons with distinct electrophysiological properties and peptide expression patterns[61]. MSNs also receive cholinergic modulation via projections from the pedunculopontine tegmentum and laterodorsal tegmentum[69], though the relevance of such input to local or network dynamics remains uncertain. Interestingly, each MSN receives ~5000-15000 excitatory inputs in addition to ~1200-1800 GABAergic inputs from other MSNs, so modulation of MSN activity via cholinergic and dopaminergic inputs are necessary for signal integration and effective synaptic plasticity[61,70]. Indeed, MSNs exhibit bi-stability, residing almost exclusively in either a down-state (-80 mV) or an up-state (-50 mV, near threshold) in the absence of external input. In addition, the maintenance of bi-stability and intrinsic excitability relies on the activity of cation channels that are under robust dopaminergic and cholinergic modulation[70,71]. Maintenance of intrinsic excitability within MSNs is critical for normal regulation of behavioral output, and dysregulation of NAc microcircuitry contributes to the development and expression of addictive behaviors[36,72,73].

DIRECT & INDIRECT PATHWAY MEDIUM SPINY NEURONS

Intrinsic excitability

Midbrain DA release into the striatum differentially impacts the activity of MSNs, facilitating dMSN activity and suppressing iMSN activity (**Figure 1.4**). D1 receptors (D1, D5) are excitatory $G\alpha_{olf}$-coupled receptors that enhance intrinsic excitability of dMSNs, while D2 receptors (D2, D3, D4) are inhibitory $G\alpha_{i/o}$-coupled receptors that reduce intrinsic excitability of iMSNs. D1 receptor activation increases production of cAMP via $G\alpha_{olf}$-mediated activation of adenylyl cyclase, promoting downstream activity of PKA to augment excitability; in particular, PKA activity reduces Na^+ channel conductivity, enhances NMDA receptor currents, and enhances L-type Ca^{2+} currents[74]. Additionally, D1 receptor activation enhances dMSN excitability by inactivating N-type and P/Q-type voltage-gated Ca^{2+} channel currents that subsequently suppresses small-conductance Ca^{2+}-dependent K^+ channel current[70]. Conversely, D2 receptor activation reduces cAMP production via $G\alpha_{i/o}$-mediated inhibition of adenylyl cyclase and inhibits the opening of N-type and P/Q-type Ca^{2+} channels via direct binding of $G\beta\gamma$ heterodimers[75]. D2 receptor activation also triggers stimulation of PLCβ via direct activation by $G\beta\gamma$, driving the mobilization of intracellular Ca^{2+} stores and activation of the calcium-dependent phosphatase calcineurin, which ultimately suppresses L-type Ca^{2+} channel currents[76]. Notably, while DA is capable of modulating intrinsic excitability via multiple mechanisms in both dMSNs and iMSNs, the net effect of these modulations appears to be negligible on the whole cell level; rather, it appears that dopaminergic modulation of MSNs regulates Ca^{2+} influx into dendritic spines to influence synaptic plasticity, with D1 receptors facilitating and D2 receptors suppressing plasticity[70]. Specifically, D1 receptor activation facilitates

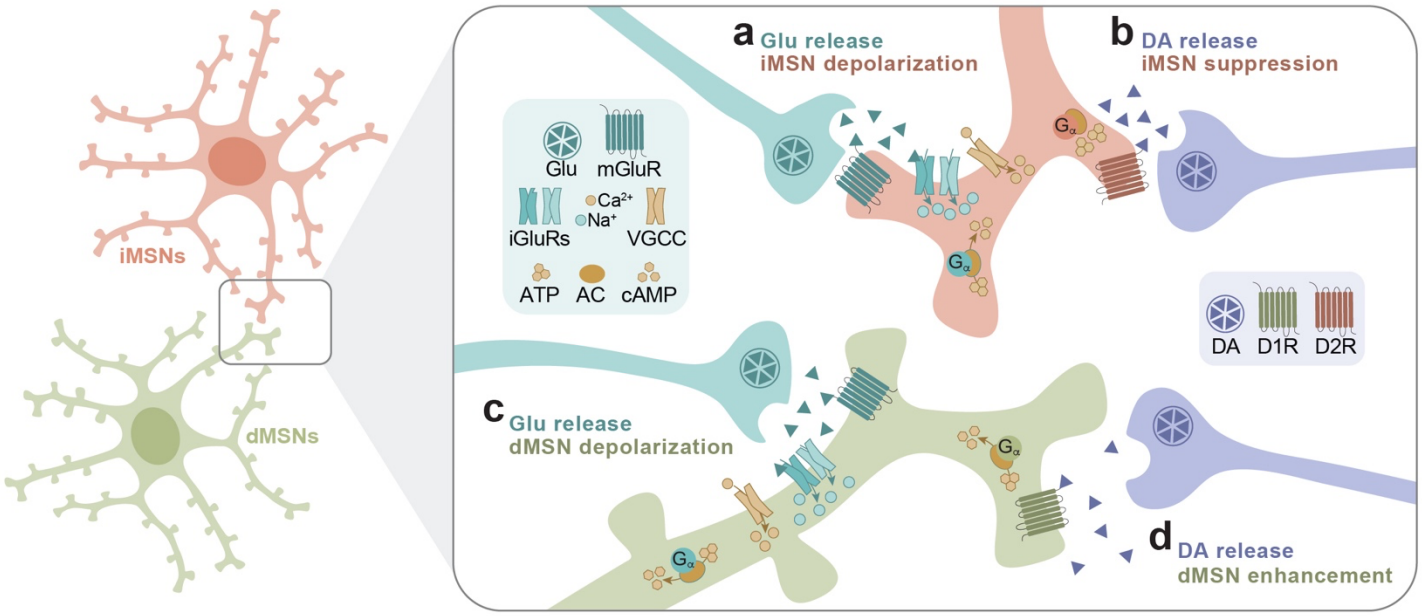

Figure 1.4 | Glutamatergic and dopaminergic modulation of MSN excitability. (**a, c**) Glutamate release increases the excitability of both (**a**) iMSNs and (**c**) dMSNs, facilitating depolarization. (**b, d**) Dopamine releases bidirectionally modulates MSNs, (**b**) suppressing iMSNs and (**d**) enhancing dMSNs.

up-state transitions and enhances up-state spiking in dMSNs, while D2 receptor activation impedes state transitions and suppresses up-state spiking[77].

In addition to dopaminergic modulation, the intrinsic excitability of MSNs is modulated via acetylcholine (ACh) released from cholinergic interneurons, which acts on two families of muscarinic ACh receptors: M1 receptors (M1, M5) are $G\alpha_{q/11}$-coupled receptors that increase intracellular [Ca^{2+}] and activate PLCβ and PKC, while M2 receptors (M2, M3, M4) are $G\alpha_{i/o}$-coupled receptors that inhibit cAMP production and inactivate voltage-gated Ca^{2+} channels[78,79]. Passive efflux of K^+ through constitutively active inwardly rectifying K^+ (KIR), A-type K^+ (KA), and KCNQ channels maintains the hyperpolarized down-state of MSNs, which is directly modulated by M1 receptors[80]. Phosphorylation by PKC reduces opening of KA channels and disrupts their voltage dependence, while PLCβ-mediated depletion of phosphatidylinositol 4,5-bisphosphate, inactivates KCNQ and KIR channels, collectively leading to MSN depolarization[81–83]. M1 receptor activation also inactivates L-type Ca^{2+} channels via a Ca^{2+}-dependent, G-protein-independent pathway, potentially via activity of calcineurin[84]. MSNs normally integrate synaptic input over a time window of 40-60ms, acting as input integrators rather than coincidence detectors[70]. CINs are relatively sparse within the striatum but are large, tonically active, and have largely branching dendritic arbors, so M1 receptor-dependent modulation of MSNs may serve to enhance signal integration within a local cluster of MSNs[61,85]. Additionally, M1 receptor-mediated suppression of L-type Ca^{2+} channels during MSN spiking attenuates Ca^{2+}-dependent K^+ currents (e.g., small conductance K^+ channels) to expand the window of integration[84]. M2 receptors are also capable of modulating MSN activity, via two distinct mechanisms: M2 and M3 receptors regulate synaptic input onto MSNs via presynaptic inhibition of glutamatergic, GABAergic, and Dopaminergic afferents, while M4 receptors regulate intrinsic excitability via direct inhibition of N-type and P/Q-type voltage-gated Ca^{2+} channels via G$\beta\gamma$ binding to shape the spiking of MSNs[61,80]. Notably, M4 receptors are more heavily expressed in dMSNs than iMSNs, indicating cell type-specific output filtering via CIN activity[76]. MSNs receive 5000-15000 glutamatergic inputs and 1200-1800 GABAergic inputs from other MSNs, so extensive cholinergic and dopaminergic modulation of a single MSN is likely necessary for signal integration and effective synaptic plasticity[61,70].

Synaptic plasticity

Unlike induction of synaptic plasticity in other cells types that requires the combination of strong somatic depolarization with high-frequency stimulation of afferent fibers, regulation of synaptic plasticity in striatal MSNs requires the convergence of back-propagating action potentials (bAPs) and synaptic input onto MSN dendrites[86]. Synaptic plasticity in MSNs generally employs a phenomenon known as spike timing-dependent plasticity (STDP) that determines the direction of plasticity: synaptic stimulation followed by trailing bAPs (+5 ms) induces long-term potentiation (LTP), while bAPs preceding synaptic stimulation (-10 ms) induces long-

term depression (LTD). Additionally, the mechanisms underlying the modulation of striatal synaptic plasticity differ between dMSNs and iMSNs. LTD in iMSNs requires stimulation of both presynaptic glutamatergic afferents and *en passant* dopaminergic afferents, which result in the activation of $G\alpha_{q/11}$-coupled group I metabotropic glutamate receptors (mGluRs), $G\alpha_{i/o}$-coupled D2 receptors, L-type voltage-gated Ca^{2+} channels, and CB1 endocannabinoid (eCB) receptors, but not NMDA receptors[87]. bAPs decrementally back-propagate into dendrites, providing local depolarization that is sufficient to open L-type Ca^{2+} channels and facilitate dendritic Ca^{2+} influx, resulting in ryanodine receptor-dependent Ca^{2+}-induced Ca^{2+} release from intracellular stores[87,88]. Additionally, glutamate binding to $mGluR_{1/5}$ and DA binding to D2 receptors both activate PLCβ via direct binding of G$\beta\gamma$ dimers, enhancing production of IP_3 and src kinase to facilitate Ca^{2+} entry via L-type Ca^{2+} channels and IP_3 receptors[88]. These signaling mechanisms collectively enhance the production of eCBs (e.g., anandamide, 2-arachidonylglycerol) that are released from iMSN dendritic spine heads to act on presynaptic CB_1 receptors[89]. Activation of D2 receptors also decreases surface expression of AMPA receptors to reduce iMSN synaptic strength, which together with presynaptic CB1 receptor activation depresses synaptic plasticity[90]. Unlike iMSN LTD that is expressed presynaptically and is dependent on D2 receptors, iMSN LTP is dependent on activation of NMDA receptors and $G\alpha_{olf}$-coupled adenosine A2A receptors. Stimulation of A2A receptors augments adenylyl cyclase-dependent production of cAMP to enhance activity of PKA, though the exact mechanisms through which this produces LTP remains uncertain. PKA phosphorylates a number of signaling molecules that have been implicated in synaptic plasticity, including DARPP-32 and MAPKs, though future work is needed to fully understand the role of such signaling in iMSN LTP[32]. Notably, enhancing D2 receptor activity via an LTP protocol induces LTD, while enhancing A2A receptor activity via an LTD protocol induces LTP, emphasizing the critical balance between G-protein signaling cascades, presynaptic activity, and postsynaptic excitability required for proper modulation of iMSN synaptic plasticity[86].

Similar to LTP in iMSNs, LTP in dMSNs is dependent on activation of NMDA receptors and a $G\alpha_{olf}$-coupled receptor, though dMSN LTP requires activation of D1 receptors rather than A2A receptors. Employing an STDP protocol with synaptic stimulation and trailing postsynaptic stimulation induces LTP in dMSNs that is dependent on activation of D1 receptors, likely requiring downstream activity of cAMP and PKA. D1 receptor activation also enhances surface expression of AMPA and NMDA receptors through a PKA-dependent mechanism, potentially via activation of striatal-enriched phosphatase and the tyrosine kinase Fyn, to enhance excitability of dMSNs[32,90]. However, using the same stimulation protocol in the presence of a D1 receptor antagonist induces dMSN LTD that is dependent bAP-driven Ca^{2+} influx through L-type Ca^{2+} channels, glutamatergic activation of $mGluR_{1/5}$, and presynaptic CB1 receptor activation[86]. Collectively, these mechanisms provide a framework through which DA can induce bidirectional Hebbian plasticity at glutamatergic synapses on MSNs, despite differing DA receptor expression at dMSNs and iMSNs. D2

receptors have a high affinity for DA and are the primary target of tonic DA release from the midbrain, while D1 receptors have a low affinity for DA and generally only activate following phasic DA spikes. Additionally, iMSNs and dMSNs can have opposing control of behavioral output, with iMSN activity suppressing behavior and dMSN activity facilitating behavior. Thus, in the absence of behaviorally relevant stimuli, low levels of tonic DA primarily activate iMSN D2 receptors to enable bidirectional STDP plasticity, while the absence of dopaminergic modulation of dMSN D1 receptors selectively facilitates LTD. During phasic DA release – triggered by behaviorally relevant stimuli – dMSN D1 receptors can be transiently activated to facilitate LTP, thereby affording behaviorally mediated mechanisms for bidirectional Hebbian plasticity in striatal MSNs.

MECHANISMS OF CALCIUM SIGNALING

Ca^{2+} is a ubiquitous second messenger molecule that can regulate nearly all forms of neuronal activity, including membrane excitability, neurotransmitter release, short- and long-term synaptic plasticity, gene expression, and apoptosis[91]. Given the broad impacts that fluctuations in intracellular Ca^{2+} may have on the activity of an individual neuron or local neural networks, cellular mechanisms have evolved to regulate local Ca^{2+} via chemical and ionic concentration gradients across the plasmalemma, sequestration within intracellular storage organelles, and binding to cytosolic Ca^{2+} buffers. In particular, the expression of electrophysiologically and pharmacologically distinct Ca^{2+} channels in distinct subcellular compartments provides mechanisms for rapid, localized, and transient spikes in intracellular Ca^{2+} that can be time-locked to discrete signaling events (e.g., action potential arrival, G-protein activation)[92,93]. Collectively, these mechanisms facilitate transient, temporally precise fluctuations in intracellular Ca^{2+} that can either be restricted to isolated neuronal compartments during discrete signaling events or propagate towards the soma to induce long-term changes in gene expression, as determined by the source and conditions of Ca^{2+} release.

Calcium channels

Plasmalemmal Ca^{2+} channels can be divided into two superfamilies, based on mechanism of activation: voltage-gated Ca^{2+} channels that are dependent on local membrane depolarization, and ligand-gated Ca^{2+} channels that are dependent on neurotransmitter binding. Voltage-gated Ca^{2+} channels are differentiated based on their electrophysiological and pharmacological properties, as well as on their subcellular distribution[92]. T-type Ca^{2+} channels (also known as low voltage-activated channels) activate at hyperpolarized membrane potentials (i.e., positive to -70mV), rapidly inactivate, and have low ionic conductance. T-type Ca^{2+} channels are expressed both somatically and dendritically, and are primarily responsible for regulating excitability in pace-making cells, such as interneurons[94]. High voltage-activated (HVA) Ca^{2+} channels activate at depolarized membrane potentials (positive to -20mV) and can be further subdivided into four subtypes: N- and P/Q-type Ca^{2+} channels are predominately expressed at presynaptic terminals and initiate

neurotransmitter release, L-type Ca^{2+} channels are expressed both dendritically and somatically and initiate Ca^{2+}-dependent transcription events, and R-type Ca^{2+} channels are expressed both presynaptically and postsynaptically and mediate neurotransmitter release and synaptic plasticity[92,95]. Ligand-gated Ca^{2+} channels are ionotropic glutamate receptors that provide the primary source of excitatory input for most neurons, and include AMPA receptors and NMDA receptors[93]. AMPA receptors are tetrameric ionophores composed of four GluR1-4 subunits that determine cation selectivity: AMPA receptors that lack the GluR2 subunit have fast gating kinetics, exhibit inward rectification, and gate Na^+, K^+, and Ca^{2+}, and are thus termed Ca^{2+}-permeable AMPA (CP-AMPA) receptors; GluR2-containing AMPA receptors are weakly-conductive, gate Na^+ and K^+, and are referred to as Ca^{2+}-impermeable AMPA (CI-AMPA) receptors[93]. CI-AMPA receptors predominate in mature neurons under normal physiological circumstances, though certain conditions induce synaptic expression of CP-AMPA receptors[96]. In particular, withdrawal from heavy psychostimulant intake and incubation of psychostimulant craving upregulate CP-AMPA receptor expression in NAc MSNs, presumably enhancing neuronal excitability to drug-related cues[96–99]. NMDA receptors are also tetrameric ionophores composed of GluNR1 and GluNR2 subunits, and all NMDA receptors are permeable to both Na^+ and Ca^{2+}, with Ca^{2+} accounting for 6-12% of the total cation current through NDMA receptors[100]. While AMPA and NMDA receptors similarly use glutamate as their endogenous agonist, activation of NMDA receptors also requires co-agonism by glycine or serine along with coincident depolarization to remove a Mg^{2+} block from within the conductive pore[93]. Intracellular Ca^{2+} channels mediate Ca^{2+} release from internal storage organelles (e.g., SER, endosomes) and include inositol 1,4,5-trisphosphate (IP_3) receptors, localized in dendritic shafts and near the soma, and ryanodine receptors, localized in dendritic spines and axons[101]. Whereas transient activation of plasmalemmal Ca^{2+} channels rapidly and transiently increases local Ca^{2+}, activation of intracellular Ca^{2+} channels occurs downstream of primary signaling events (e.g., plasmalemmal ion channel opening, G-protein activation) to generate Ca^{2+} waves that are capable of propagating throughout the neuron to induce long-lasting changes in neuronal plasticity and gene expression[102].

Calcium release

When an action potential invades a presynaptic terminal, local Na^+ current-induced depolarization triggers the opening of voltage-gated Ca^{2+} channels (N-type and P/Q-type) clustered near the readily-releasable pool of neurotransmitter to provide a rapid spike in intracellular Ca^{2+} near the synaptic cleft, with the Ca^{2+} near voltage-gated Ca^{2+} channels rising from 50nM to >50μM in ~5ms[103]. This localized increase in presynaptic Ca^{2+} binds to low-affinity Ca^{2+} sensors (e.g., synaptotagmins) to initiate vesicular release machinery (i.e., zippering of α-helical SNARE motifs on the plasma membrane and the synaptic vesicle, membrane fusion) and ultimately induces neurotransmitter release within several milliseconds of the action potential's arrival. In contrast to the rapid rise in Ca^{2+} upon action potential arrival, removal of Ca^{2+} from the presynaptic bouton occurs more slowly

(~100s of milliseconds) and relies primarily on two mechanisms: Ca^{2+} chelation and Ca^{2+} extrusion[104]. Endogenous Ca^{2+} buffers (e.g., parvalbumin, calretinin, calbindin) sequester free Ca^{2+} with high-affinity Ca^{2+} binding sites, whereas Ca^{2+} extruders either actively pump Ca^{2+} out of the presynaptic bouton and into the extracellular space (e.g., K^+-dependent and K^+-independent Na^+/Ca^{2+} exchangers, plasma membrane Ca^{2+}-ATPases) or pump Ca^{2+} into intracellular storage organelles, such as the SER (e.g., sarco-/endoplasmic reticulum Ca^{2+} ATPase)[91,100]. Under normal physiological conditions, glutamate released from a presynaptic terminal can bind to both CI-AMPA and NMDA receptors, opening CI-AMPA receptors to allow influx of Na^+ into the dendrite and facilitating subsequent depolarization. Following sufficient CI-AMPA receptor-mediated depolarization or during coincident glutamate release and local depolarization bAPs from within the postsynaptic neuron, NMDA receptors open to facilitate robust Ca^{2+} influx into the cell, driven by the steep concentration gradient of Ca^{2+}. Under these conditions, NMDA receptors are the primary source of glutamate induced Ca^{2+} influx in neurons and act as coincidence detectors to selectively gate Ca^{2+} when both pre- and post-synaptic regulatory conditions are met. Conversely, glutamatergic excitation of CP-AMPA receptors can result in Ca^{2+} influx independent of postsynaptic depolarization and NMDA receptor activation, providing a mechanism through which subthreshold (e.g., mEPSP rather than full depolarization) stimulation of a dendritic spine can result in Ca^{2+} influx and activation of Ca^{2+}-dependent intracellular signaling events. In addition to directly driving Ca^{2+} influx via CP-AMPA or NMDA receptors, glutamate-mediated dendritic depolarization can also indirectly open L-type Ca^{2+} channels in the perisynaptic membrane to further enhance local, intracellular Ca^{2+}.

While CP-AMPA receptors, NMDA receptors, and L-type Ca^{2+} channels are efficient for producing acute, transient spikes in dendritic Ca^{2+}, whole-cell Ca^{2+} events (also known as Ca^{2+} waves) can be generated by either IP_3-dependent Ca^{2+}-induced Ca^{2+} release (ICICR) via IP_3 receptor or Ca^{2+}-induced Ca^{2+} release (CICR) via ryanodine receptors[102,105]. ICICR requires the coincidence of bAP-triggered Ca^{2+} influx via voltage-gated (L-type and R-type) Ca^{2+} channels and activation of postsynaptic $G\alpha_{q/11}$-coupled metabotropic receptors. Agonist binding to $G\alpha_{q/11}$ receptors (e.g., glutamate binding to mGluR1) triggers the activation of PLCβ, which hydrolyzes phosphatidylinositol 4-5-bisphosphate into diacylglycerol and IP_3. IP_3 binds to IP_3 receptors on the SER to facilitate Ca^{2+} release from internal stores, resulting in a substantial rise in intracellular Ca^{2+} within the dendritic spine, referred to as the trigger zone for ICICR[102]. Similar to ICICR, CICR requires bAP-triggered Ca^{2+} influx and results in release of Ca^{2+} from intracellular stores, but unlike ICICR, mGluR1 activation enhances but is not necessary for CICR, as CICR induces Ca^{2+} release from ryanodine receptor-sensitive Ca^{2+} stores rather than IP_3 receptors[88]. Once Ca^{2+} within a trigger zone reaches threshold, Ca^{2+}-gated K^+ currents activate to modulate bidirectional transfer of synaptic currents toward distal dendrites and the soma[102]. Somatic Ca^{2+} signals generally have a delayed onset, greater amplitude, and longer duration than dendritic Ca^{2+} signals, and

Ca^{2+} within the nucleus can regulate CREB-mediated gene expression directly or indirectly via Ca^{2+}/calmodulin-dependent protein kinases[106]. Ca^{2+} waves are more likely to fully propagate to the soma when Ca^{2+} reaches threshold within the trigger zone of multiple, proximal dendrites, indicating a potential role for Ca^{2+} waves in encoding synergistic, global Ca^{2+} signaling events. Ca^{2+} waves have therefore been proposed to be a mechanism for heterosynaptic plasticity, by which changes in synaptic strength spread from one synapse to neighboring synapses[107]. Strong activation of $G\alpha_{q/11}$ receptors is also capable of inducing ICICR and subsequent Ca^{2+}-mediated K^+ currents independent of action potential-evoked Ca^{2+} release[108,109]. This phenomenon is also subject to modulation by other neurotransmitters, including dopamine: in the NAc, phasic dopamine enhances ICICR-mediated Ca^{2+} signals in D1 receptor-expressing dMSNs but reverses adenosine A2A receptor/ICICR-mediated Ca^{2+} signals in D2 receptor-expressing iMSNs. D1 and A2A receptors are both $G\alpha_s$-coupled receptors that facilitate cAMP production and PKA activation, each of which have been shown to increase cytosolic Ca^{2+} via IP_3-sensitive Ca^{2+} stores independent of IP_3 production[110,111].

Calcium imaging

As cytosolic Ca^{2+} can be influenced by such a range of signaling mechanisms, it is unsurprising that the significance of *in vivo* Ca^{2+} signals monitored via genetically encoded Ca^{2+} sensors (e.g., GCaMP) in a specific brain region and/or genetically defined cell type remains uncertain. However, careful experimental design can resolve some of the conflicts when considering the information outlined above. Ca^{2+} signaling in the axonal bouton, for example, is predominated by voltage-gated N-type and P/Q-type Ca^{2+} channels that activate during firing of an action potential, so *in vivo* Ca^{2+} imaging in the downstream target region of a neuronal population of interest can be used as a proxy for action potential firing. Similarly, somatic Ca^{2+} signaling, driven by L-type Ca^{2+} channels and CICR via Ca^{2+} waves, drives transcriptional regulation, so single cell Ca^{2+} imaging with ROI's centered near the nucleus and soma can provide insight into such processes. Finally, while individual dendritic Ca^{2+} signaling drives homosynaptic plasticity, Ca^{2+} waves across a population of dendrites may be linked to heterosynaptic plasticity associated with dramatic changes in neuronal signaling, so the use of fiber photometry can inform the influence that external, behaviorally relevant stimuli have on a population of neurons.

MECHANISMS OF OPIOID ACTION

Pharmacology

Mu opioid (μO) receptors are widely expressed throughout the central, peripheral, and enteric nervous systems, and can be distributed both somatodendritically and axonally[112]. While expression of μO receptors in axons is weaker than expression in proximal dendrites and the soma, μO receptor activity in the presynaptic bouton substantially impacts local and network neuronal activity via presynaptic inhibition. μO receptors are

$G\alpha_{i/o}$-coupled receptors that affect neuronal activity via four distinct mechanisms, mediated by activity of the $G\alpha$ and $G\beta\gamma$ subunits: (1) inhibition of cAMP-mediated signaling cascades, (2) activation of GIRK channels, (3) inhibition of voltage-gated Ca^{2+} channels, and (4) inhibition of soluble N-ethylmaleimide-sensitive factor attachment protein receptor (SNARE)-dependent vesicle release[113,114]. Prior to ligand binding, heterotrimeric G-protein complex ($G\alpha\beta\gamma$) are coupled to *μ*O receptors. Agonist binding results in a conformational change that activates the $G\alpha$ subunit, facilitating exchange of a bound GDP for a GTP and inducing dissociation of the $G\alpha$/GTP complex and the $G\beta\gamma$ dimer from the *μ*O receptor. $G\alpha_{i/o}$ translocates to the membrane-delimited enzyme adenylyl cyclase, inhibiting the enzymatic conversion of ATP to cAMP. cAMP is a ubiquitous second messenger responsible for activating protein kinases (e.g., PKA) and transcription factors (e.g., CREB), so *μ*O receptor agonist-induced suppression of cAMP activity can result in medium- and long-term changes in neuronal activity. Conversely, the $G\beta\gamma$ dimer acutely impacts neuronal excitability by translocating to GIRKs and voltage gated Ca^{2+} channels near the synaptic bouton. $G\beta\gamma$ dimers can directly bind to and open GIRK channels, causing hyperpolarization in the presynaptic terminal and inhibiting neural activity until either the $G\alpha$/GTP complex undergoes hydrolysis to $G\alpha$/GDP and re-associates with $G\beta\gamma$ or a $G\beta\gamma$ scavenger (e.g., G-protein regulated kinase [GRK] 2 or GRK3) binds $G\beta\gamma$ subunits via their carboxy termini[113,115]. $G\beta\gamma$ dimers can also directly bind to the I-II linker of α_{1A}/α_{1B} subunits of N-type and P/Q-type Ca^{2+} channels to disrupt channel gating, slow activation kinetics, and shift the current/voltage relationship of the channel, effectively occluding Ca^{2+} influx[116,117]. Finally, $G\beta\gamma$ dimers can directly disrupt presynaptic vesicular release machinery by binding to vesicular SNARE proteins and preventing zippering of α-helical SNARE motifs on the synaptic vesicle and the plasma membrane, thereby obstructing neurotransmitter release[114]. Collectively, these mechanisms afford opioids with broad-reaching potential for *μ*O receptor-mediated presynaptic inhibition that impacts not only *μ*O receptor-expressing neurons but also their downstream targets to disrupt local circuit dynamics.

Respiratory depression

Opioids are capable of disrupting many aspects of respiration (e.g., tidal volume, respiratory rate), but opioid-induced respiratory depression is predominately caused by desynchronization of respiratory rhythm. Respiration is controlled by nuclei within the brainstem and ventrolateral medulla that receive ascending input from peripheral and central chemoreceptors that detect changes in blood O_2 and CO_2 content, respectively. Oxygen-sensing type I cells of peripheral carotid bodies are responsible for triggering the hypoxic ventilatory response, a chemoreflex that upregulates respiration when O_2 levels begin to decline. During a hypoxic event, reduced O_2 availability triggers the opening of L-type and P/Q-type Ca^{2+} channels in type I cells, and the influx of Ca^{2+} drives neurotransmitter release and excitation of postsynaptic carotid sinus nerves within the carotid body. Glutamatergic stimulation by carotid sinus nerves excites neurons of the nucleus tractus solitarius (NTS) within the brainstem and subsequently upregulates respiratory rate via connections between the NTS and the

pre-Bötzinger complex (preBötC) in the ventrolateral medulla. μO and kappa opioid (κO) receptors are widely expressed throughout the respiratory system, including in oxygen-sensing type I cells of the carotid body, the NTS, and the preBötC, and opioid-induced respiratory depression is thought to be due to direct activity at each of these sites. DAMGO and U50-488 (full agonists for μO and κO receptors) facilitate activation of $G\alpha_{i/o}$-coupled signal transduction in μO/κO receptor-expressing type I cells of the carotid body, resulting in presynaptic inhibition via activation of GIRKs and inhibition of voltage gated Ca^{2+} channels by the $G\beta\gamma$ dimer. This presynaptic inhibition reduces excitability of NTS neurons and protracts the duration of a hypoxic ventilatory response, which is independently capable of disrupting respiration. However, μO receptors are also densely expressed in the commissural subdivision of the NTS (comNTS), which receives direct glutamatergic input from the carotid sinus nerve to induce a hypoxic ventilatory response. Intra-comNTS administration of DAMGO hyperpolarizes comNTS neurons and inhibits presynaptic glutamate release, attenuating the hypoxic ventilatory response; moreover, intra-comNTS administration of CTAP, a selective μO receptor antagonist, rescues depression of the hypoxic ventilatory response induced by systemic DAMGO injection, implicating the comNTS as an essential site for opioid-induced respiratory depression. Glutamatergic projections from the NTS innervate the preBötC, which is responsible for the generation of respiratory rhythm via oscillatory activity with the nearby retro-trapezoid and parafacial respiratory group (RTN/pFRG). Treatment of *in vitro* preparations of intact preBötC/RTN/pFRG with DAMGO reduces inspiratory frequency that is not due to faulty rhythmicity, as subthreshold action potentials can still be recorded in the absence of inspiration. Similar disruptions in respiratory rhythmicity can be seen *in vivo* in rats treated with fentanyl, indicating that opioid-induced respiratory disruption is mediated in part by stochastic, intermittent attenuation of preBötC output. However, intra-preBötC injection of the μO receptor antagonist naloxone fails to reverse opioid-induced respiratory depression, suggesting that disrupted preBötC rhythmicity may be a consequence of opioid action upstream in the respiratory pathway. Collectively, this body of research indicates that opioids are capable of inducing respiratory depression at multiple, synergistic levels, including: (1) impaired peripheral chemosensation of hypoxia, (2) weakened hypoxic ventilatory response generation within the NTS, and (3) disrupted respiratory rhythm generation by the preBötC. μO and κO receptors are expressed in additional sites throughout the respiratory system and while it is possible that there are additional neural loci responsible for disrupting respiration, the action of opioids at these sites is sufficient for opioid-induced respiratory depression. Notably, highly efficacious μO receptor agonists (e.g., fentanyl, sufentanil) with biased β-arrestin2 signaling pose a greater risk for respiratory depression, and respiratory depression is attenuated in β- arrestin2-KO mice. Thus, both G-protein and β-arrestin2 signaling appear to influence respiratory depression through distinct mechanisms.

POLYDRUG USE WITH OPIOIDS

Although studies of drug addiction and its impacts are often centered around individual drugs, drug use frequently involves multiple substances[118–120]. Indeed, drug-dependent individuals report an average use of 3.5 substances[121], including both simultaneous and sequential polydrug use. In addition, the likelihood of developing comorbid substance dependencies is high in clinical populations[122,123]. Although which substances are co-used can vary, primary drug dependencies are typically found for alcohol, opioids, amphetamine, and methamphetamine, while cannabis and cocaine are more often reported as secondary- or tertiary-used substances[118]. The high prevalence of polysubstance use is particularly concerning given the impact that this can have on both SUD severity and treatment outcomes. For example, a polysubstance history is associated with greater unmet physical and mental health care needs, increased risk behavior, violence, and increased overdose and mortality risk compared to single substance use[123–125]. Although the majority of research on SUDs has focused on individual substances in isolation, with a multiple drug use history often considered an exclusion criterion for clinical studies, it is important to recognize that many drug users engage in polysubstance use. For instance, 30% to 80% of heroin users also use cocaine[126], and deaths involving both cocaine and opioids more than doubled between 2010 to 2015.. A person is considered a polysubstance user if they use more than one substance, including use of multiple drugs on separate occasions (sequential use) or at the same time (concurrent/simultaneous). Limiting studies to individual drugs risks overlooks interactions between substances, limits translatability of preclinical research, and can impede the efficacy of resulting treatments for SUDs. Indeed, polysubstance use has consistently been associated with worse treatment outcomes, including poorer treatment retention, higher rates of relapse, and a three-fold higher mortality rate compared to mono-substance use[127–129].

Epidemiology of polydrug opioid use

The prevalence of opioid misuse (i.e., use outside of prescribed use) has risen dramatically in recent years, with ~53 million adults (1.1% of global population) reporting past-year non-medical use of an opioid[5]. North America has the highest rate of opioid misuse, with ~11 million past-year users[130]; however, this estimate is conservative as it does not include homeless or incarcerated individuals, who have disproportionately higher levels of opioid use. In addition, the rate of first-time heroin users rose in parallel with non-medical use of prescription opioids from 2002 to 2011[5], a reflection that individuals with past-year prescription opioid misuse are 19 times more likely to initiate heroin use than those without such a history[9,131]. Studies have investigated polydrug use among heroin and prescription opioid misusers, and found that there are higher frequencies of opioid use in people that also use cocaine (>33%) or methamphetamine (>20%)[132,133], but reduced odds for primary opioid use in those that have secondary alcohol and cannabis use[133,134] (**Figure 1.5**). In addition, first-time methamphetamine use is more prevalent following past-month opioid use[134]. Of those entering treatment

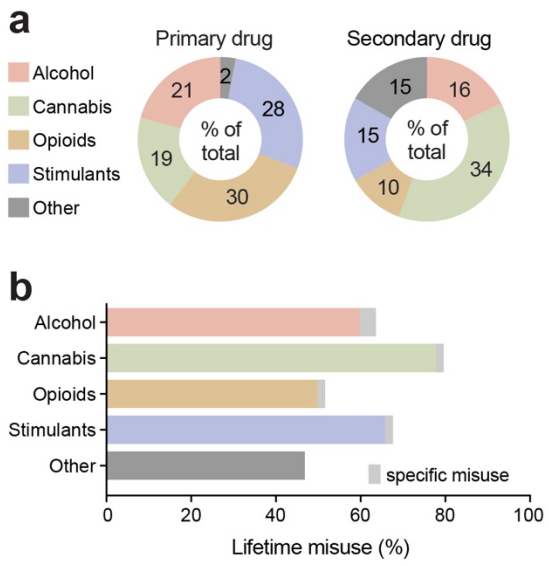

Figure 1.5 | Polysubstance use. Unspecified polysubstance use in treatment-seeking drug users in Finland from 1997 to 2008. *Top*: Primary (left) and secondary (right) drugs used by treatment-seeking drug users, shown as percent of total users. *Bottom*: Percent of users reporting exclusive misuse of one drug (white bars) or misuse of a given drug along with polysubstance use of another (colored bars).

for heroin use, it has been found that 91% of people reported a lifetime history of cocaine use[128], and in the UK, 54% of opioid users in treatment between 2017-2018 also had a comorbid cocaine use disorder[135]. Nonetheless, simultaneous use of heroin with alcohol and/or cannabis is more common than with psychostimulants[136,137], suggesting that a sequential pattern of drug use is preferable for opioids and psychostimulants.

In the US, opioid use is a national public health emergency, responsible for more than 1.6 million years of life lost from 2001 to 2016[138]. Moreover, opioid overdose deaths are currently the leading cause of accidental death among US adults, with 68% of all drug overdose deaths involving an opioid[5]. Given that nearly 80% of fatal opioid overdoses also involved another substance, it appears that there is a greater risk of death when opioids are used in combination with other opioids and/or other drugs[139]. Specifically, of these deaths, 78% involved another opioid, while 21.6% involved cocaine, 11.1% involved alcohol, and 5.4% involved a psychostimulant other than cocaine[139]. In addition, opioid-related emergency room visits also involved tobacco (51.1%), cocaine (36.9%) or other stimulants (22.6%), cannabis (25.1%), and alcohol (16.9%). Substantial polysubstance use of three or more of these substances has also been reported for opioid-related emergency room visits[140], and the likelihood of these visits has been associated with the degree of severity of other SUDs[141,142]. Taken together, these reports suggest that combining opioid use with other substances is frequently involved with the deleterious consequences of opioid use. In addition to overdose risk, opioid users face very high rates of relapse, with 59% of individuals relapsing in the first week and 80% relapsing in the first month of abstinence[13]. Past use of other substances, including the degree of cocaine use, increases relapse susceptibility[128]. Methamphetamine use among those seeking treatment for opioid use has also been on the rise[5], and it has recently been reported that methamphetamine use is associated with a discontinuation of buprenorphine treatment in people with an opioid use disorder[143]. Thus, a better understanding of the impact of multi-substance use in the context of opioids is crucial for more successful emergency responses and long-term treatment outcomes.

Behavioral effects of polydrug opioid use

Given the unique neurobiological alterations that can occur with exposure to multiple drugs, along with the high prevalence of polysubstance use disorders, there is a strong need to develop polydrug paradigms that have high translational value. These paradigms are critical for fully understanding the behavioral changes and addiction-related phenotypes that develop following polydrug use. However, given the vast number of potential substance combinations and the variability in methodologies that exist across studies, there are mixed results and interpretations to date regarding the impact of polydrug history on addiction-related behaviors. Nonetheless, some general trends in drug consumption, drug preference and drug-seeking have been demonstrated in commonly investigated substance combinations (**Figure 1.6**).

Sequential use of heroin and cocaine has not been found to alter heroin self-administration or reinstatement of heroin-seeking[144]. Although alcohol pretreatment can prevent the conditioned morphine seeking[145], adolescent alcohol exposure enhances the development of conditioned morphine seeking[146]. Interestingly, co-administration of morphine & THC prevents the development of the analgesic tolerance that normally accompanies long-term exposure to either drug alone[147–149]. In addition, the analgesic effects of THC and oxycodone co-administration are additive to oxycodone alone[150]. Moreover, administration of either THC or THC & CBD attenuates naloxone-precipitated withdrawal without impacting the development of conditioned

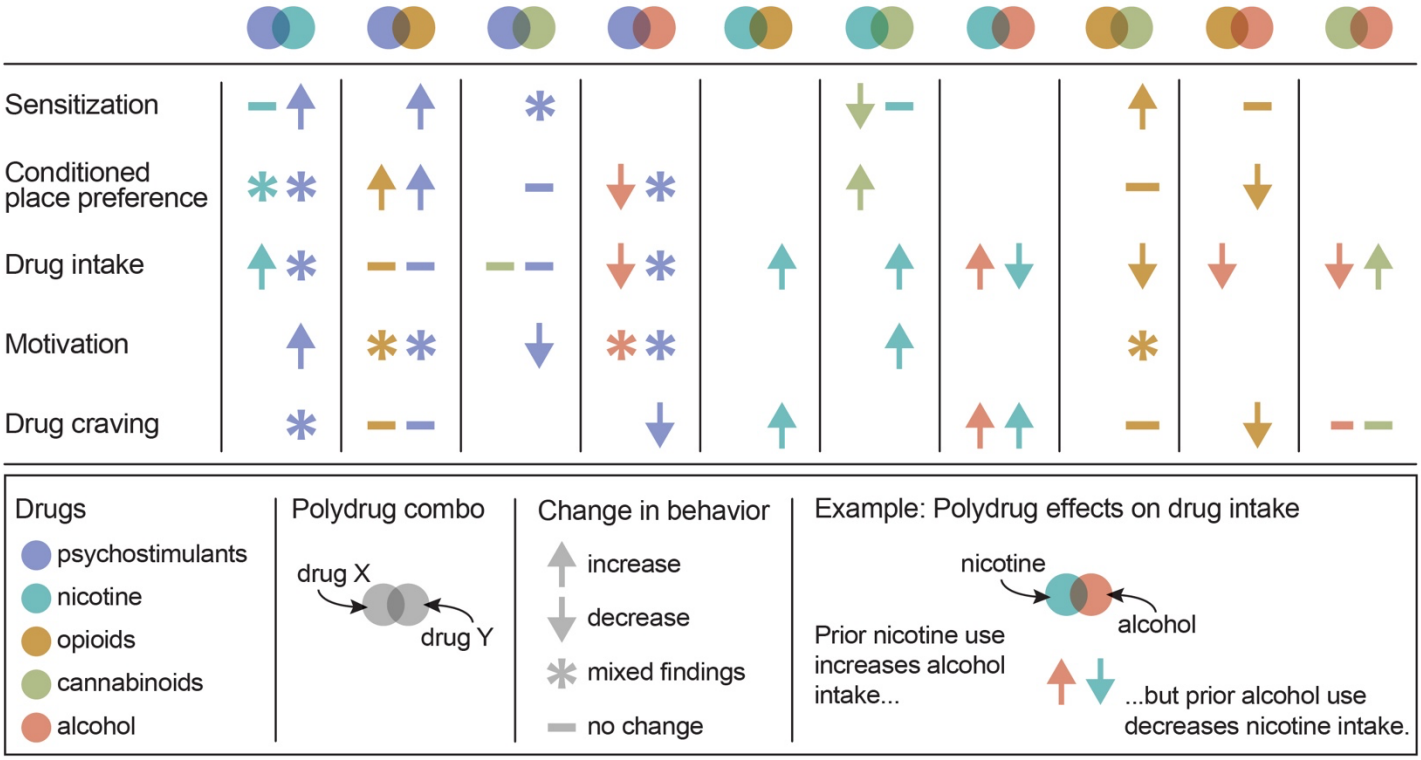

Figure 1.6 | Net effects of polydrug combinations on addiction behaviors. Summary of the effects of specific polydrug combinations on assays of addiction-like behavior in animal studies.

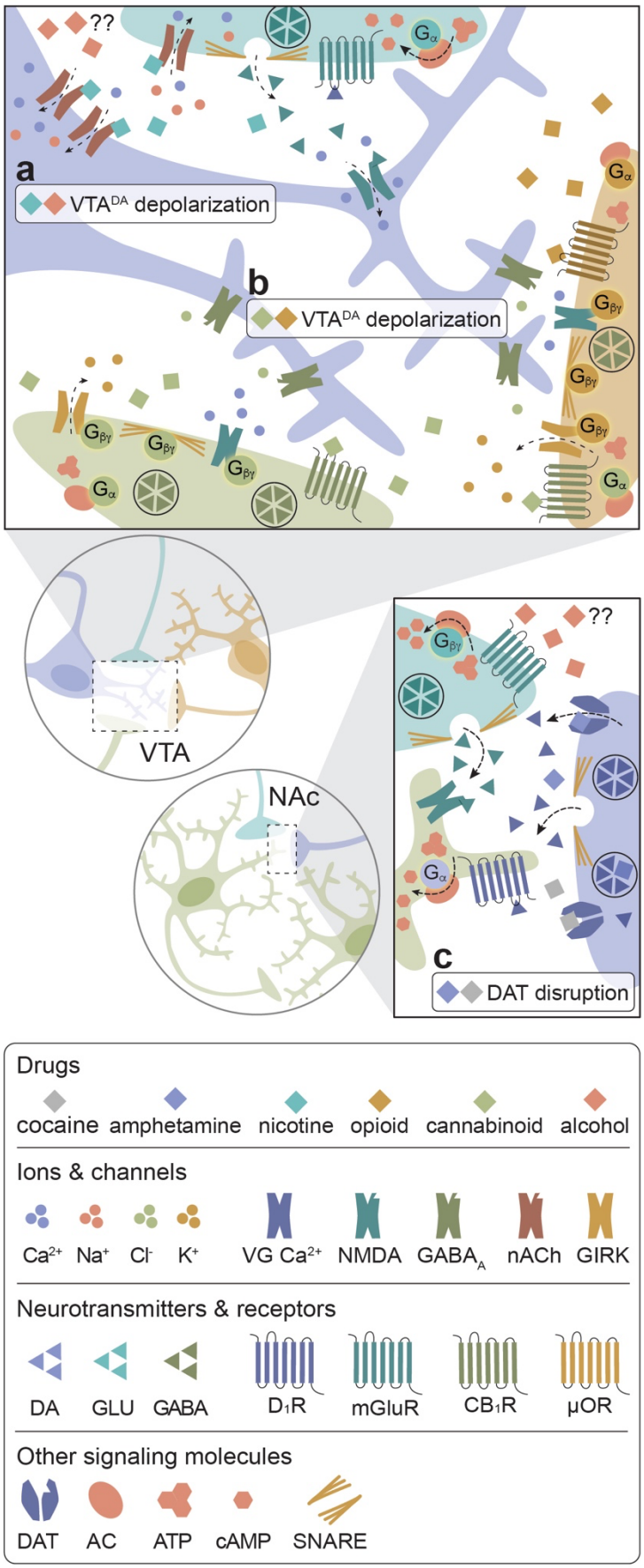

morphine seeking[151,152]. These data suggest a potential role for cannabinoids in regulating a physical dependence to opioids without altering their reinforcing properties. In support of this, repeated THC administration has no effect on the motivation to self-administer heroin or relapse to heroin-seeking, although it produces a small reduction in both heroin[153] and oxycodone[150] intake. The effects of opioid and cannabis polydrug use, however, appear to be dose-dependent as systemic administration of THC prior to heroin self-administration reduces responding for large doses of heroin, but has no effect on responding for lower doses in both monkeys and rats[153,154].

Mechanisms of polydrug opioid use

A unique feature of all potentially addictive drugs is the ability to evoke phasic DA release into the NAc, yet the underlying mechanisms vary across drugs (**Figure 1.7**). Psychostimulants disrupt DA reuptake into VTA^{DA} terminals[155], nicotine and alcohol directly activate VTA^{DA} neurons[156,157], and opioids and cannabinoids disinhibit VTA^{DA} neurons[156,158]. The

Figure 1.7 | Primary mechanisms of potentially addictive drugs on DA release. (**a**) Nicotine activates DA neurons via direct activation of somatodendritic nACh receptors and activation of glutamatergic inputs. Alcohol directly activates DA cell bodies, but the mechanism is not understood. (**b**) Opioids and cannabinoids disinhibit DA neurons via presynaptic inhibition of dMSN inputs and local GABA interneurons through four mechanisms: inhibition of VGCCs, activation of GIRKs, inactivation of AC, and inhibition of GABA release. (**c**) Psychostimulants impair DA reuptake by blocking DAT (cocaine) or reversing the activity of DAT and facilitating DA release (amphetamine), leading to increased dopaminergic tone in the NAc. Alcohol also targets glutamatergic inputs NAc, but the mechanism is unknown.

synergistic and antagonistic interactions between different drugs within the C-BG lends complexity to the study of polydrug use, and little is known about the mechanisms underlying the acute effects of specific polydrug combinations. However, *in vivo* extracellular recordings in rats that alternatively self-administered cocaine and heroin in the same session found that only ~20% of PFC and NAc neurons responded similarly to both drugs[159], indicating divergent engagement of the C-BG by these drugs. Thus, examining the synergistic and antagonistic mechanisms of different drugs can guide our understanding of how specific polydrug combinations may disrupt C-BG network dynamics and contribute to the manifestation of addiction behaviors.

Although opioids are differentiated by their origin, potency, and receptor bias factor[160], all opioids exert their rewarding effects via activation of μO receptors. μO receptors are expressed both somatodendritically and axonally[112], but the primary mechanism of opioid-induced DA release relies on presynaptic inhibition of VTA^{GABA} neurons. μO receptors are inhibitory G protein-coupled receptors, and their activation reduces neuronal excitability via four mechanisms: (1) Gα-mediated inhibition of cAMP-dependent signaling cascades, (2) Gβγ-mediated activation of GIRK channels, (3) Gβγ-mediated inactivation of voltage-gated Ca^{2+} channels, and (4) Gβγ-mediated inhibition of SNARE-dependent vesicle release[113–117]. Acute exposure to opioids inhibits VTA^{GABA} neurons[161,162], resulting in subsequent disinhibition of VTA^{DA} neurons and phasic DA release into the NAc[155,163]. Nonetheless, although opioids facilitate DA release into the striatum, whether this DA transmission is necessary for opioid reward remains a point of debate[14]. Opioids activate VTA^{DA} neurons *in vivo* and increase DA in the NAc[162,164], but lesions of the NAc or systemic antagonism of DA receptors blockade has no effect on opioid reward[165–168]. Given the divergent mechanism of action for opioids compared to psychostimulants and nicotine, it is not surprising that co-administration of these drugs augments the acute effects of opioids. Indeed, simultaneous administration of opioids and psychostimulants produces an additive increase in DA release in the NAc, and prolongs elevated levels of DA and its metabolites, DOPAC and HVA[169]. Similarly, simultaneous administration of opioids and nicotine enhances opioid-evoked DA release in the NAc and dorsal striatum[170]. Cross-tolerance to opioid-mediated analgesia has also been shown following pre-exposure to nicotine and cannabis[171], and chronic nicotine treatment dose-dependently reduces analgesic tolerance to opioids in a nACh receptor-dependent manner[172,173]. Interestingly, pretreatment with Ca^{2+} channel blockers or naloxone prevents this tolerance, suggesting a complex pharmacological interaction between opioids and nicotine[174]. Notably, cross-tolerance to opioid analgesia is mediated via divergent mechanisms for different polydrug combinations. Nicotine and opioid cross-tolerance is mediated by μO and nACh receptors[172,173] while cannabinoid and opioid cross-tolerance is mediated by μO receptors and CB1 receptors[175,176].

Neuroplasticity of polydrug opioid use

Long-term use of psychostimulants, nicotine, opioids, cannabinoids, and alcohol results in widespread and disparate changes throughout the C-BG network, yet there are notable alterations that are shared across drugs (**Figure 1.8**). For example, acute withdrawal produces a transient reduction in tonic DA levels in the NAc[177–180]. This is followed by a persistent increase in excitability of VTA^{DA} neurons[181–185], which contributes to enhanced cue-evoked phasic DA release during abstinence[186]. Conversely, withdrawal also produces a persistent reduction in LTD and intrinsic excitability in NAc MSNs, as well as a reduction in striatal D2 receptor binding[187]. As described earlier, striatal D2 receptors are primarily expressed on iMSNs, can serve as a "stop" signal on the C-BG circuit, and reduced D2 receptor availability has been ubiquitously linked to range of addictive diseases, including drug addiction and obesity[188–190]. Finally, these drugs all drive a persistent increase in ΔFosB expression in cortical pyramidal cells and NAc dMSNs[191], which has been linked to drug-seeking during abstinence[192].

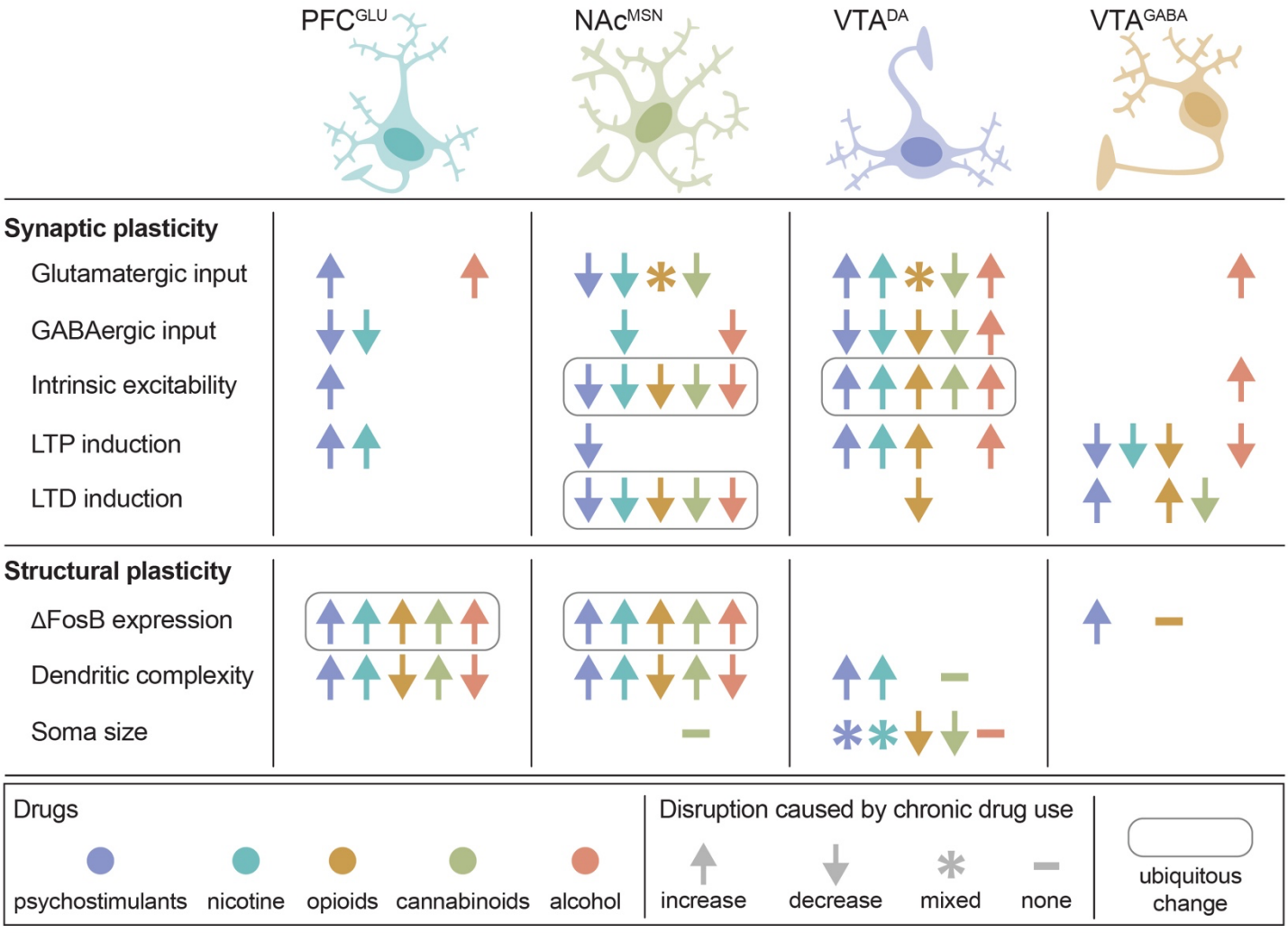

Figure 1.8 | Persistent disruptions in synaptic and structural plasticity caused by long-term use of potentially addictive drugs. Summary of disruptions in synaptic and structural plasticity following chronic drug exposure.

Similar to psychostimulants and nicotine, long-term exposure to opioids strengthens glutamatergic input to VTA^{DA} neurons[193,194]. They also weaken GABAergic inhibition of VTA^{DA} neurons[182,195,196] via a reduction of dMSN-mediated $GABA_B$ inhibition[193]. This effect is largely driven by MSNs in the NAc[197], indicating a persistent disruption in NAc output. Unlike psychostimulants and nicotine, however, long-term exposure to opioids decreases dendritic branching and spine density in NAc MSNs and mPFC pyramidal cells[198–200]. Within the NAc, long-term opioid exposure weakens glutamatergic input to NAc shell iMSNs[201,202] and induces silent synapses on iMSNs via AMPA internalization[203]. Moreover, during withdrawal, opioid-generated silent synapses on iMSNs are eliminated[203], and the intrinsic excitability of iMSNs is weakened[202]. Given that MSNs create a dense network of lateral inhibition within the NAc, with ~30% of iMSNs synapsing onto other iMSNs or dMSNs[204], it is possible that opioid-induced disruptions in iMSN signaling could disrupt local NAc microcircuitry and facilitate aberrant C-BG network dynamics.

THESIS OVERVIEW

The overarching goal of this thesis is to combine novel techniques for manipulating and monitoring neuronal activity with classic behavioral models in order to understand the role of NAc dMSNs and iMSNs in encoding individual vulnerability to heroin addiction. Chapter 2 will describe an intermittent-access heroin self-administration procedure that produces subsets of high-risk and low-risk rats, based on individual differences in addictive behaviors. In combination with targeted chemogenetic manipulations, I will describe a role for dMSNs and iMSNs in cue-induced heroin seeking, selectively in high-risk rats. Chapter 3 will describe a heroin conditioned place preference procedure that produces subsets of heroin-preferring and saline-preferring rats. In combination with fiber photometry for *in vivo* monitoring of dMSNs, iMSNs, and DA release, I will describe NAc activity dynamics during conditioned heroin seeking and present evidence of basal differences in relative dMSN and iMSN strength in drug-naïve rats, based on their sensitivity to the rewarding effects of heroin. Chapter 4 will explore potential sex differences in the behavioral effects of heroin using locomotor sensitization and intermittent-access self-administration procedures. Chapter 5 will provide a discussion of major findings, describe a potential model for the NAc in encoding individual vulnerability to the addictive effects of heroin, and present preliminary data for future directions stemming from this work.

REFERENCES

1. Koob, G. F. & Volkow, N. D. Neurobiology of addiction: a neurocircuitry analysis. *The Lancet Psychiatry* (2016). doi:10.1016/S2215-0366(16)00104-8
2. Substance Abuse and Mental Health Services Administration. *Key substance use and mental health indicators in the United States: Results from the 2018 National Survey on Drug Use and Health*. (2019).
3. Grant, B. F. *et al.* Epidemiology of DSM-5 drug use disorder results from the national epidemiologic survey on alcohol and related conditions-III. *JAMA Psychiatry* **73**, 39–47 (2016).
4. National Institute on Drug Abuse. *Trends & Statistics*. (2020).
5. United National Office on Drugs and Crime. *World Drug Report 2019*. (2019).
6. Centers for Disease Control. Multiple Cause of Death 1999-2016. *CDC WONDER Online Database* (2018).
7. Van Zee, A. The promotion and marketing of oxycontin: Commercial triumph, public health tragedy. *American Journal of Public Health* (2009). doi:10.2105/AJPH.2007.131714
8. Jones, C. M. Heroin use and heroin use risk behaviors among nonmedical users of prescription opioid pain relievers - United States, 2002-2004 and 2008-2010. *Drug Alcohol Depend.* (2013). doi:10.1016/j.drugalcdep.2013.01.007
9. Muhuri, P. K., Gfroerer, J. C. & Davies, C. *Associations of nonmedical pain reliever use and initiation of heroin use in the United States*. (2013).
10. Ciccarone, D. Fentanyl in the US heroin supply: A rapidly changing risk environment. *International Journal of Drug Policy* (2017). doi:10.1016/j.drugpo.2017.06.010
11. CDC. *Overdose Deaths Accelerating During COVID-19*. (2020).
12. American Psychiatric Association. *Diagnostic and statistical manual of mental disorders : DSM-5. American Psychiatric Association*. *DSM* (2014). doi:10.1176/appi.books.9780890425596.744053
13. Smyth, B. P., Barry, J., Keenan, E. & Ducray, K. Lapse and relapse following inpatient treatment of opiate dependence. *Ir. Med. J.* (2010).
14. Badiani, A., Belin, D., Epstein, D., Calu, D. & Shaham, Y. Opiate versus psychostimulant addiction: The differences do matter. *Nature Reviews Neuroscience* (2011). doi:10.1038/nrn3104
15. Robinson, T. E. & Berridge, K. C. The neural basis of drug craving: An incentive-sensitization theory of addiction. *Brain Research Reviews* (1993). doi:10.1016/0165-0173(93)90013-P
16. Everitt, B. J., Dickinson, A. & Robbins, T. W. The neuropsychological basis of addictive behaviour. *Brain Research Reviews* (2001). doi:10.1016/S0165-0173(01)00088-1
17. Koob, G. F. & Le Moal, M. Drug addiction, dysregulation of reward, and allostasis. *Neuropsychopharmacology* (2001). doi:10.1016/S0893-133X(00)00195-0
18. Jentsch, J. D. & Taylor, J. R. Impulsivity resulting from frontostriatal dysfunction in drug abuse:

Implications for the control of behavior by reward-related stimuli. *Psychopharmacology* (1999). doi:10.1007/PL00005483

19. Everitt, B. J., Giuliano, C. & Belin, D. Addictive behaviour in experimental animals: Prospects for translation. *Philosophical Transactions of the Royal Society B: Biological Sciences* (2018). doi:10.1098/rstb.2017.0027
20. Anagnostaras, S. G. & Robinson, T. E. Sensitization to the psychomotor stimulant effects of amphetamine: Modulation by associative learning. *Behav. Neurosci.* (1996). doi:10.1037/0735-7044.110.6.1397
21. Bardo, M. T. & Bevins, R. A. Conditioned place preference: What does it add to our preclinical understanding of drug reward? *Psychopharmacology* (2000). doi:10.1007/s002130000569
22. Panlilio, L. V. & Goldberg, S. R. Self-administration of drugs in animals and humans as a model and an investigative tool. *Addiction* (2007). doi:10.1111/j.1360-0443.2007.02011.x
23. Spealman, R. D. & Goldberg, S. R. Drug Self-Administration by Laboratory Animals: Control by Schedules of Reinforcement. *Annu. Rev. Pharmacol. Toxicol.* (1978). doi:10.1146/annurev.pa.18.040178.001525
24. O'Neal, T. J., Nooney, M. N., Thien, K. & Ferguson, S. M. Chemogenetic modulation of accumbens direct or indirect pathways bidirectionally alters reinstatement of heroin-seeking in high- but not low-risk rats. *Neuropsychopharmacology* **45**, 1251–1262 (2020).
25. Kawa, A. B., Bentzley, B. S. & Robinson, T. E. Less is more: prolonged intermittent access cocaine self-administration produces incentive-sensitization and addiction-like behavior. *Psychopharmacology (Berl).* (2016). doi:10.1007/s00213-016-4393-8
26. Oleson, E. B. *et al.* Dopamine uptake changes associated with cocaine self-administration. *Neuropsychopharmacology* (2009). doi:10.1038/npp.2008.186
27. Oleson, E. B. & Roberts, D. C. S. Cocaine self-administration in rats: Threshold procedures. *Methods Mol. Biol.* (2012). doi:10.1007/978-1-61779-458-2_20
28. Yager, L. M., Garcia, A. F., Donckels, E. A. & Ferguson, S. M. Chemogenetic inhibition of direct pathway striatal neurons normalizes pathological, cue-induced reinstatement of drug-seeking in rats. *Addict. Biol.* (2019). doi:10.1111/adb.12594
29. Deroche-Gamonet, V., Belin, D. & Piazza, P. V. Evidence for addiction-like behavior in the rat. *Science (80-.).* (2004). doi:10.1126/science.1099020
30. Shaham, Y. Incubation of craving and fear: Behavioral and neuronal mechanisms. *J. Mol. Neurosci.* (2013).
31. Lu, L., Grimm, J. W., Hope, B. T. & Shaham, Y. Incubation of cocaine craving after withdrawal: A review of preclinical data. *Neuropharmacology* (2004). doi:10.1016/j.neuropharm.2004.06.027

32. Gerfen, C. R. & Surmeier, D. J. Modulation of Striatal Projection Systems by Dopamine. *Annu. Rev. Neurosci.* (2011). doi:10.1146/annurev-neuro-061010-113641
33. Calabresi, P., Picconi, B., Tozzi, A., Ghiglieri, V. & Di Filippo, M. Direct and indirect pathways of basal ganglia: A critical reappraisal. *Nature Neuroscience* (2014). doi:10.1038/nn.3743
34. Kravitz, A. V. *et al.* Regulation of parkinsonian motor behaviours by optogenetic control of basal ganglia circuitry. *Nature* (2010). doi:10.1038/nature09159
35. Ferguson, S. M. *et al.* Transient neuronal inhibition reveals opposing roles of indirect and direct pathways in sensitization. *Nat. Neurosci.* **14**, 22–4 (2011).
36. O'Neal, T. J., Nooney, M. N., Thien, K. & Ferguson, S. M. Chemogenetic modulation of accumbens direct or indirect pathways bidirectionally alters reinstatement of heroin-seeking in high- but not low-risk rats. *Neuropsychopharmacology* (2019). doi:10.1038/s41386-019-0571-9
37. Garcia, A. F., Nakata, K. G. & Ferguson, S. M. Viral strategies for targeting cortical circuits that control cocaine-taking and cocaine-seeking in rodents. *Pharmacology Biochemistry and Behavior* (2018). doi:10.1016/j.pbb.2017.05.009
38. Brog, J. S., Salyapongse, A., Deutch, A. Y. & Zahm, D. S. The patterns of afferent innervation of the core and shell in the "Accumbens" part of the rat ventral striatum: Immunohistochemical detection of retrogradely transported fluoro-gold. *J. Comp. Neurol.* (1993). doi:10.1002/cne.903380209
39. McGlinchey, E. M., James, M. H., Mahler, S. V., Pantazis, C. & Aston-Jones, G. Prelimbic to Accumbens Core Pathway Is Recruited in a Dopamine-Dependent Manner to Drive Cued Reinstatement of Cocaine Seeking. *J. Neurosci.* (2016). doi:10.1523/jneurosci.1291-15.2016
40. Santana, N. & Artigas, F. Laminar and cellular distribution of monoamine receptors in rat medial prefrontal cortex. *Front. Neuroanat.* **11**, 87 (2017).
41. Gabbott, P. L. A., Warner, T. A., Jays, P. R. L., Salway, P. & Busby, S. J. Prefrontal cortex in the rat: Projections to subcortical autonomic, motor, and limbic centers. *J. Comp. Neurol.* **492**, 145–177 (2005).
42. Brown, S. P. & Hestrin, S. Intracortical circuits of pyramidal neurons reflect their long-range axonal targets. *Nature* **457**, 1133–6 (2009).
43. Kim, E. J., Juavinett, A. L., Kyubwa, E. M., Jacobs, M. W. & Callaway, E. M. Three Types of Cortical Layer 5 Neurons That Differ in Brain-wide Connectivity and Function. *Neuron* **88**, 1253–67 (2015).
44. Morishima, M. & Kawaguchi, Y. Recurrent connection patterns of corticostriatal pyramidal cells in frontal cortex. *J. Neurosci.* **26**, 4394–405 (2006).
45. Reiner, A., Hart, N. M., Lei, W. & Deng, Y. Corticostriatal projection neurons - Dichotomous types and dichotomous functions. *Front. Neuroanat.* (2010). doi:10.3389/fnana.2010.00142
46. Shepherd, G. M. G. Corticostriatal connectivity and its role in disease. *Nat. Rev. Neurosci.* **14**, 278–91 (2013).

47. Chen, X. *et al.* High-Throughput Mapping of Long-Range Neuronal Projection Using In Situ Sequencing. *Cell* **179**, 772-786.e19 (2019).
48. Kalmbach, B. E., Johnston, D. & Brager, D. H. Cell-type specific channelopathies in the prefrontal cortex of the fmr1-/y mouse model of fragile X syndrome. *eNeuro* **2**, ENEURO.0114-15.2015 (2015).
49. Saiki, A. *et al.* In Vivo Spiking Dynamics of Intra- and Extratelencephalic Projection Neurons in Rat Motor Cortex. *Cereb. Cortex* **28**, 1024–1038 (2018).
50. Winnubst, J. *et al.* Reconstruction of 1,000 Projection Neurons Reveals New Cell Types and Organization of Long-Range Connectivity in the Mouse Brain. *Cell* **179**, 268–81 (2019).
51. Batista-Brito, R. *et al.* Developmental Dysfunction of VIP Interneurons Impairs Cortical Circuits. *Neuron* **95**, 884–95 (2017).
52. van Versendaal, D. & Levelt, C. N. Inhibitory interneurons in visual cortical plasticity. *Cellular and Molecular Life Sciences* **73**, 3677–3691 (2016).
53. Koob, G. F. & Volkow, N. D. Neurocircuitry of addiction. *Neuropsychopharmacology* **35**, 217–38 (2010).
54. Saunders, B. T., Richard, J. M., Margolis, E. B. & Janak, P. H. Dopamine neurons create Pavlovian conditioned stimuli with circuit-defined motivational properties. *Nat. Neurosci.* (2018). doi:10.1038/s41593-018-0191-4
55. Heymann, G. *et al.* Synergy of distinct dopamine projection populations in behavioral reinforcement. *Neuron* (2019). doi:10.1016/j.neuron.2019.11.024
56. Morales, M. & Margolis, E. B. Ventral tegmental area: Cellular heterogeneity, connectivity and behaviour. *Nature Reviews Neuroscience* (2017). doi:10.1038/nrn.2016.165
57. Brown, M. T. C. *et al.* Ventral tegmental area GABA projections pause accumbal cholinergic interneurons to enhance associative learning. *Nature* (2012). doi:10.1038/nature11657
58. Qi, J. *et al.* VTA glutamatergic inputs to nucleus accumbens drive aversion by acting on GABAergic interneurons. *Nat. Neurosci.* (2016). doi:10.1038/nn.4281
59. Kim, J. I. *et al.* Aldehyde dehydrogenase 1a1 mediates a GABA synthesis pathway in midbrain dopaminergic neurons. *Science (80-.).* (2015). doi:10.1126/science.aac4690
60. Berrios, J. *et al.* Loss of UBE3A from TH-expressing neurons suppresses GABA co-release and enhances VTA-NAc optical self-stimulation. *Nat. Commun.* (2016). doi:10.1038/ncomms10702
61. Burke, D. A., Rotstein, H. G. & Alvarez, V. A. Striatal Local Circuitry: A New Framework for Lateral Inhibition. *Neuron* (2017). doi:10.1016/j.neuron.2017.09.019
62. Li, Z. *et al.* Cell-type-specific afferent innervation of the nucleus accumbens core and shell. *Front. Neuroanat.* (2018). doi:10.3389/fnana.2018.00084
63. Cui, G. *et al.* Concurrent activation of striatal direct and indirect pathways during action initiation. *Nature* (2013). doi:10.1038/nature11846

64. Dobbs, L. K. K. *et al.* Dopamine Regulation of Lateral Inhibition between Striatal Neurons Gates the Stimulant Actions of Cocaine. *Neuron* **90**, 1100–13 (2016).
65. Cazorla, M. *et al.* Dopamine d2 receptors regulate the anatomical and functional balance of basal ganglia circuitry. *Neuron* (2014). doi:10.1016/j.neuron.2013.10.041
66. Kupchik, Y. M. *et al.* Coding the direct/indirect pathways by D1 and D2 receptors is not valid for accumbens projections. *Nat. Neurosci.* (2015). doi:10.1038/nn.4068
67. Bertran-Gonzalez, J. *et al.* Opposing patterns of signaling activation in dopamine D1 and D2 receptor-expressing striatal neurons in response to cocaine and haloperidol. *J. Neurosci.* (2008). doi:10.1523/JNEUROSCI.1039-08.2008
68. Gagnon, D. *et al.* Striatal Neurons Expressing D1 and D2 Receptors are Morphologically Distinct and Differently Affected by Dopamine Denervation in Mice. *Sci. Rep.* (2017). doi:10.1038/srep41432
69. Dautan, D. *et al.* A major external source of cholinergic innervation of the striatum and nucleus accumbens originates in the Brainstem. *J. Neurosci.* (2014). doi:10.1523/JNEUROSCI.5071-13.2014
70. Moyer, J. T., Wolf, J. A. & Finkel, L. H. Effects of dopaminergic modulation on the integrative properties of the ventral striatal medium spiny neuron. *J. Neurophysiol.* (2007). doi:10.1152/jn.00335.2007
71. Plenz, D. & Kitai, S. T. Up and down states in striatal medium spiny neurons simultaneously recorded with spontaneous activity in fast-spiking interneurons studied in cortex-striatum-substantia nigra organotypic cultures. *J. Neurosci.* (1998). doi:10.1523/jneurosci.18-01-00266.1998
72. Bock, R. *et al.* Strengthening the accumbal indirect pathway promotes resilience to compulsive cocaine use. *Nat. Neurosci.* (2013). doi:10.1038/nn.3369
73. Stefanik, M. T. *et al.* Optogenetic inhibition of cocaine seeking in rats. *Addict. Biol.* (2013). doi:10.1111/j.1369-1600.2012.00479.x
74. Surmeier, D. J., Bargas, J., Hemmings, H. C., Nairn, A. C. & Greengard, P. Modulation of calcium currents by a D1 dopaminergic protein kinase/phosphatase cascade in rat neostriatal neurons. *Neuron* (1995). doi:10.1016/0896-6273(95)90294-5
75. Surmeier, D. J. *et al.* The role of dopamine in modulating the structure and function of striatal circuits. in *Progress in Brain Research* (2010). doi:10.1016/S0079-6123(10)83008-0
76. Yan, Z., Flores-Hernandez, J. & Surmeier, D. J. Coordinated expression of muscarinic receptor messenger RNAs in striatal medium spiny neurons. *Neuroscience* (2001). doi:10.1016/S0306-4522(01)00039-2
77. Surmeier, D. J., Ding, J., Day, M., Wang, Z. & Shen, W. D1 and D2 dopamine-receptor modulation of striatal glutamatergic signaling in striatal medium spiny neurons. *Trends in Neurosciences* (2007). doi:10.1016/j.tins.2007.03.008
78. Mamaligas, A. A., Cai, Y. & Ford, C. P. Nicotinic and opioid receptor regulation of striatal dopamine D2-

receptor mediated transmission. *Sci. Rep.* (2016). doi:10.1038/srep37834

79. Mamaligas, A. A. & Ford, C. P. Spontaneous Synaptic Activation of Muscarinic Receptors by Striatal Cholinergic Neuron Firing. *Neuron* (2016). doi:10.1016/j.neuron.2016.06.021
80. Oldenburg, I. A. & Ding, J. B. Cholinergic modulation of synaptic integration and dendritic excitability in the striatum. *Current Opinion in Neurobiology* (2011). doi:10.1016/j.conb.2011.04.004
81. Nakamura, T. Y., Coetzee, W. A., De Miera, E. V. S., Artman, M. & Rudy, B. Modulation of Kv4 channels, key components of rat ventricular transient outward K+ current, by PKC. *Am. J. Physiol. - Hear. Circ. Physiol.* (1997). doi:10.1152/ajpheart.1997.273.4.h1775
82. Shen, W., Hamilton, S. E., Nathanson, N. M. & Surmeier, D. J. Cholinergic suppression of KCNQ channel currents enhances excitability of striatal medium spiny neurons. *J. Neurosci.* (2005). doi:10.1523/JNEUROSCI.1381-05.2005
83. Shen, W. *et al.* Cholinergic modulation of Kir2 channels selectively elevates dendritic excitability in striatopallidal neurons. *Nat. Neurosci.* (2007). doi:10.1038/nn1972
84. Howe, A. R. & Surmeier, D. J. Muscarinic Receptors Modulate N-, P-, and L-type Ca2+ Currents in Rat Striatal Neurons through Parallel Pathways. *J. Neurosci.* (1995). doi:10.1523/jneurosci.15-01-00458.1995
85. Lv, X. *et al.* M1 muscarinic activation induces long-lasting increase in intrinsic excitability of striatal projection neurons. *Neuropharmacology* (2017). doi:10.1016/j.neuropharm.2017.03.017
86. Shen, W., Flajolet, M., Greengard, P. & Surmeier, D. J. Dichotomous dopaminergic control of striatal synaptic plasticity. *Science (80-.).* (2008). doi:10.1126/science.1160575
87. Kreitzer, A. C. & Malenka, R. C. Striatal Plasticity and Basal Ganglia Circuit Function. *Neuron* (2008). doi:10.1016/j.neuron.2008.11.005
88. Plotkin, J. L. *et al.* Regulation of dendritic calcium release in striatal spiny projection neurons. *J. Neurophysiol.* (2013). doi:10.1152/jn.00422.2013
89. Giuffrida, A. *et al.* Dopamine activation of endogenous cannabinoid signaling in dorsal striatum. *Nat. Neurosci.* (1999). doi:10.1038/7268
90. Sun, X., Zhao, Y. & Wolf, M. E. Dopamine receptor stimulation modulates AMPA receptor synaptic insertion in prefrontal cortex neurons. *J. Neurosci.* (2005). doi:10.1523/JNEUROSCI.4603-04.2005
91. Saftenku, E. È. Models of calcium dynamics in cerebellar granule cells. *Cerebellum* (2012). doi:10.1007/s12311-010-0216-3
92. Lacinová, L. Voltage-dependent calcium channels. *General Physiology and Biophysics* (2005). doi:10.1016/0006-2952(94)90498-7
93. Dingledine, R., Borges, K., Bowie, D. & Traynelis, S. F. The glutamate receptor ion channels. *Pharmacological Reviews* (1999).

94. Talley, E. M. *et al.* Differential distribution of three members of a gene family encoding low voltage-activated (T-type) calcium channels. *J. Neurosci.* (1999). doi:10.1523/jneurosci.19-06-01895.1999
95. Metz, A. E., Jarsky, T., Martina, M. & Spruston, N. R-type calcium channels contribute to afterdepolarization and bursting in hippocampal CA1 pyramidal neurons. *J. Neurosci.* (2005). doi:10.1523/JNEUROSCI.0624-05.2005
96. Conrad, K. L. *et al.* Formation of accumbens GluR2-lacking AMPA receptors mediates incubation of cocaine craving. *Nature* (2008). doi:10.1038/nature06995
97. Lu, W. Y. *et al.* Activation of synaptic NMDA receptors induces membrane insertion of new AMPA receptors and LTP in cultured hippocampal neurons. *Neuron* (2001). doi:10.1016/S0896-6273(01)00194-5
98. Scheyer, A. F. *et al.* AMPA Receptor Plasticity in Accumbens Core Contributes to Incubation of Methamphetamine Craving. *Biol. Psychiatry* (2016). doi:10.1016/j.biopsych.2016.04.003
99. Purgianto, A. *et al.* Different adaptations in AMPA receptor transmission in the nucleus accumbens after short vs long access cocaine self-administration regimens. *Neuropsychopharmacology* (2013). doi:10.1038/npp.2013.78
100. Grienberger, C. & Konnerth, A. Imaging Calcium in Neurons. *Neuron* (2012). doi:10.1016/j.neuron.2012.02.011
101. Segal, M. & Korkotian, E. Endoplasmic reticulum calcium stores in dendritic spines. *Frontiers in Neuroanatomy* (2014). doi:10.3389/fnana.2014.00064
102. Barbara, J. G. IP3-dependent calcium-induced calcium release mediates bidirectional calcium waves in neurones: Functional implications for synaptic plasticity. in *Biochimica et Biophysica Acta - Proteins and Proteomics* (2002). doi:10.1016/S1570-9639(02)00439-9
103. Kaeser, P. S. & Regehr, W. G. Molecular mechanisms for synchronous, asynchronous, and spontaneous neurotransmitter release. *Annual Review of Physiology* (2014). doi:10.1146/annurev-physiol-021113-170338
104. Helmchen, F., Borst, J. G. G. & Sakmann, B. Calcium dynamics associated with a single action potential in a CNS presynaptic terminal. *Biophys. J.* (1997). doi:10.1016/S0006-3495(97)78792-7
105. Verkhratsky, A. The endoplasmic reticulum and neuronal calcium signalling. *Cell Calcium* (2002). doi:10.1016/S0143416002001896
106. Hardingham, G. E., Arnold, F. J. L. & Bading, H. Nuclear calcium signaling controls CREB-mediated gene expression triggered by synaptic activity. *Nat. Neurosci.* (2001). doi:10.1038/85109
107. Bailey, C. H., Giustetto, M., Huang, Y. Y., Hawkins, R. D. & Kandel, E. R. Is Heterosynaptic modulation essential for stabilizing hebbian plasiticity and memory. *Nat. Rev. Neurosci.* (2000). doi:10.1038/35036191

108. Hagenston, A. M., Fitzpatrick, J. S. & Yeckel, M. F. MGluR-mediated calcium waves that invade the soma regulate firing in layer V medial prefrontal cortical pyramidal neurons. *Cereb. Cortex* (2008). doi:10.1093/cercor/bhm075

109. Canepari, M. & Ogden, D. Kinetic, pharmacological and activity-dependent separation of two Ca2+ signalling pathways mediated by type 1 metabotropic glutamate receptors in rat Purkinje neurones. *J. Physiol.* (2006). doi:10.1113/jphysiol.2005.103770

110. Taylor, C. W. *et al.* Structural organization of signalling to and from IP3 receptors. *Biochem. Soc. Trans.* (2014). doi:10.1042/BST20130205

111. Tovey, S. C. *et al.* Regulation of inositol 1,4,5-trisphosphate receptors by cAMP independent of cAMP-dependent protein kinase. *J. Biol. Chem.* (2010). doi:10.1074/jbc.M109.096016

112. Arvidsson, U. *et al.* Distribution and targeting of a μ-opioid receptor (MOR1) in brain and spinal cord. *J. Neurosci.* (1995). doi:10.1523/jneurosci.15-05-03328.1995

113. Al-Hasani, R. & Bruchas, M. R. Molecular mechanisms of opioid receptor-dependent signaling and behavior. *Anesthesiology* (2011). doi:10.1097/ALN.0b013e318238bba6

114. Blackmer, T. *et al.* G protein βγ directly regulates SNARE protein fusion machinery for secretory granule exocytosis. *Nat. Neurosci.* (2005). doi:10.1038/nn1423

115. Blanchet, C. & Lüscher, C. Desensitization of μ-opioid receptor-evoked potassium currents: Initiation at the receptor, expression at the effector. *Proc. Natl. Acad. Sci. U. S. A.* (2002). doi:10.1073/pnas.072075399

116. Bourinet, E., Soong, T. W., Stea, A. & Snutch, T. P. Determinants of the G protein-dependent opioid modulation of neuronal calcium channels. *Proc. Natl. Acad. Sci. U. S. A.* (1996). doi:10.1073/pnas.93.4.1486

117. Zamponi, G. W. & Currie, K. P. M. Regulation of CaV2 calcium channels by G protein coupled receptors. *Biochimica et Biophysica Acta - Biomembranes* (2013). doi:10.1016/j.bbamem.2012.10.004

118. Substance Abuse and Mental Health Services Administration. *Treatment Episode Data Set (TEDS): 2004-2014. National Admissions to Substance Abuse Treatment*. (2016).

119. Gjersing, L. *et al.* Diversity in causes and characteristics of drug-induced deaths in an urban setting. *Scand. J. Public Health* **41**, 119–125 (2013).

120. Roy, élise, Richer, I., Arruda, N., Vandermeerschen, J. & Bruneau, J. Patterns of cocaine and opioid co-use and polyroutes of administration among street-based cocaine users in Montréal, Canada. *Int. J. Drug Policy* **24**, 142–149 (2013).

121. Onyeka, I. N. *et al.* Sociodemographic characteristics and drug abuse patterns of treatment-seeking illicit drug abusers in finland, 1997-2008: The huuti study. *J. Addict. Dis.* (2012). doi:10.1080/10550887.2012.735563

122. Leri, F., Stewart, J., Tremblay, A. & Bruneau, J. Heroin and cocaine co-use in a group of injection drug users in Montréal. *J. Psychiatry Neurosci.* **29**, 40–47 (2004).
123. Lorvick, J., Browne, E. N., Lambdin, B. H. & Comfort, M. Polydrug use patterns, risk behavior and unmet healthcare need in a community-based sample of women who use cocaine, heroin or methamphetamine. *Addict. Behav.* **85**, 94–99 (2018).
124. Gilmore, D. *et al.* Mortality risk in a sample of emergency department patients who use cocaine with alcohol and/or cannabis. *Subst. Abus.* **39**, 266–270 (2018).
125. Pennings, E. J. M., Leccese, A. P. & De Wolff, F. A. Effects of concurrent use of alcohol and cocaine. *Addiction* **97**, 773–783 (2002).
126. Leri, F., Bruneau, J. & Stewart, J. Understanding polydrug use: Review of heroin and cocaine co-use. *Addiction* **98**, 7–22 (2003).
127. Staiger, P. K., Richardson, B., Long, C. M., Carr, V. & Marlatt, G. A. Overlooked and underestimated? Problematic alcohol use in clients recovering from drug dependence. *Addiction* **108**, 1188–1193 (2013).
128. Williamson, A., Darke, S., Ross, J. & Teesson, M. The effect of persistence of cocaine use on 12-month outcomes for the treatment of heroin dependence. *Drug Alcohol Depend.* **81**, 293–300 (2006).
129. de la Fuente, L. *et al.* Mortality risk factors and excess mortality in a cohort of cocaine users admitted to drug treatment in Spain. *J. Subst. Abuse Treat.* **46**, 219–26 (2014).
130. Substance Abuse and Mental Health Services Administration. *Key substance use and mental health indicators in the United States: Results from the 2016 National Survey on Drug Use and Health*. (2017).
131. Cicero, T. J., Kasper, Z. A. & Ellis, M. S. Increased use of heroin as an initiating opioid of abuse: Further considerations and policy implications. *Addict. Behav.* (2018). doi:10.1016/j.addbeh.2018.05.030
132. Hedegaard, H., Bastian, B. A., Trinidad, J. P., Spencer, M. & Warner, M. Drugs most frequently involved in drug overdose deaths: United states, 2011–2016. *Natl. Vital Stat. Reports* **67**, (2018).
133. Wang, L. *et al.* Polydrug use and its association with drug treatment outcomes among primary heroin, methamphetamine, and cocaine users. *Int. J. Drug Policy* **49**, 32–40 (2017).
134. Cicero, T. J., Ellis, M. S. & Kasper, Z. A. Polysubstance use: A broader understanding of substance use during the opioid crisis. *Am. J. Public Health* **110**, 244–250 (2020).
135. Public Health England. *Drug Statistics from the National Drug Treatment Monitoring System (NDTMS)*. *UK National Statistics* (2018). doi:10.1038/1811181a0
136. Bobashev, G., Tebbe, K., Peiper, N. & Hoffer, L. Polydrug use among heroin users in Cleveland, OH. *Drug Alcohol Depend.* **192**, 80–87 (2018).
137. Kelly, P. J. *et al.* Polysubstance use in treatment seekers who inject amphetamine: Drug use profiles, injecting practices and quality of life. *Addict. Behav.* **71**, 25–30 (2017).
138. Gomes, T., Tadrous, M., Mamdani, M. M., Paterson, J. M. & Juurlink, D. N. The Burden of Opioid-

Related Mortality in the United States. *JAMA Netw. open* (2018). doi:10.1001/jamanetworkopen.2018.0217

139. Jones, C. M., Einstein, E. B. & Compton, W. M. Changes in synthetic opioid involvement in drug overdose deaths in the United States, 2010-2016. *JAMA - J. Am. Med. Assoc.* **319**, 1819–1821 (2018).
140. Liu, S. & Vivolo-Kantor, A. A latent class analysis of drug and substance use patterns among patients treated in emergency departments for suspected drug overdose. *Addict. Behav.* **101**, 106142 (2020).
141. John, W. S. *et al.* Prevalence and patterns of opioid misuse and opioid use disorder among primary care patients who use tobacco. *Drug Alcohol Depend.* **194**, 468–475 (2019).
142. Zale, E. L. *et al.* Tobacco smoking, nicotine dependence, and patterns of prescription opioid misuse: Results from a nationally representative sample. *Nicotine Tob. Res.* **17**, 1096–1103 (2015).
143. Tsui, J. I. *et al.* Association between methamphetamine use and retention among patients with opioid use disorders treated with buprenorphine. *J. Subst. Abuse Treat.* (2020). doi:10.1016/j.jsat.2019.10.005
144. Crummy, E. A., Donckels, E. A., Baskin, B. M., Bentzley, B. S. & Ferguson, S. M. The impact of cocaine and heroin drug history on motivation and cue sensitivity in a rat model of polydrug abuse. *Psychopharmacology (Berl).* (2019). doi:10.1007/s00213-019-05349-2
145. Zhu, S. *et al.* Alcohol inhibits morphine/cocaine reward memory acquisition and reconsolidation in rats. *Psychopharmacology (Berl).* (2020). doi:10.1007/s00213-019-05433-7
146. Molet, J., Hervé, D., Thiébot, M. H., Hamon, M. & Lanfumey, L. Juvenile ethanol exposure increases rewarding properties of cocaine and morphine in adult DBA/2J mice. *Eur. Neuropsychopharmacol.* **23**, 1816–1825 (2013).
147. Smith, P. A., Selley, D. E., Sim-Selley, L. J. & Welch, S. P. Low dose combination of morphine and Δ9-tetrahydrocannabinol circumvents antinociceptive tolerance and apparent desensitization of receptors. *Eur. J. Pharmacol.* (2007). doi:10.1016/j.ejphar.2007.06.001
148. Cichewicz, D. L. & McCarthy, E. A. Antinociceptive synergy between Δ9-tetrahydrocannabinol and opioids after oral administration. *J. Pharmacol. Exp. Ther.* **304**, 1010–1015 (2003).
149. Cox, M. L., Haller, V. L. & Welch, S. P. Synergy between Δ9-tetrahydrocannabinol and morphine in the arthritic rat. *Eur. J. Pharmacol.* **567**, 125–130 (2007).
150. Nguyen, J. D. *et al.* Δ 9 -tetrahydrocannabinol attenuates oxycodone self-administration under extended access conditions. *Neuropharmacology* **151**, 127–135 (2019).
151. Lichtman, A. H., Sheikh, S. M., Loh, H. H. & Martin, B. R. Opioid and cannabinoid modulation of precipitated withdrawal in δ9-tetrahydrocannabinol and morphine-dependent mice. *J. Pharmacol. Exp. Ther.* **298**, 1007–1014 (2001).
152. Valverde, O. *et al.* Δ9-tetrahydrocannabinol releases and facilitates the effects of endogenous enkephalins: Reduction in morphine withdrawal syndrome without change in rewarding effect. *Eur. J.*

Neurosci. **13**, 1816–1824 (2001).

153. Maguire, D. R. & France, C. P. Effects of daily delta-9-tetrahydrocannabinol treatment on heroin self-administration in rhesus monkeys. *Behav. Pharmacol.* **27**, 249–257 (2016).
154. Solinas, M., Panlilio, L. V. & Goldberg, S. R. Exposure to Δ-9-Tetrahydrocannabinol (THC) increases subsequent heroin taking but not heroin's reinforcing efficacy: A self-administration study in rats. *Neuropsychopharmacology* **29**, 1301–1311 (2004).
155. Pontieri, F. E., Tanda, G. & Di Chiara, G. Intravenous cocaine, morphine, and amphetamine preferentially increase extracellular dopamine in the 'shell' as compared with the 'core' of the rat nucleus accumbens. *Proc. Natl. Acad. Sci. U. S. A.* (1995). doi:10.1073/pnas.92.26.12304
156. Pidoplichko, V. I., DeBiasi, M., Wiliams, J. T. & Dani, J. A. Nicotine activates and desensitizes midbrain dopamine neurons. *Nature* (1997). doi:10.1038/37120
157. Brodie, M. S., Pesold, C. & Appel, S. B. Ethanol directly excites dopaminergic ventral tegmental area reward neurons. *Alcohol. Clin. Exp. Res.* (1999). doi:10.1111/j.1530-0277.1999.tb04082.x
158. Cheer, J. F., Marsden, C. A., Kendall, D. A. & Mason, R. Lack of response suppression follows repeated ventral tegmental cannabinoid administration: An in vitro electrophysiological study. *Neuroscience* (2000). doi:10.1016/S0306-4522(00)00241-4
159. Chang, J. Y., Janak, P. H. & Woodward, D. J. Comparison of mesocorticolimbic neuronal responses during cocaine and heroin self-administration in freely moving rats. *J. Neurosci.* (1998). doi:10.1523/jneurosci.18-08-03098.1998
160. Schmid, C. L. *et al.* Bias Factor and Therapeutic Window Correlate to Predict Safer Opioid Analgesics. *Cell* **171**, 1165–75 (2017).
161. Corre, J. *et al.* Dopamine neurons projecting to medial shell of the nucleus accumbens drive heroin reinforcement. *Elife* (2018). doi:10.7554/eLife.39945
162. Johnson, S. W. & North, R. A. Opioids excite dopamine neurons by hyperpolarization of local interneurons. *J. Neurosci.* (1992). doi:10.1523/jneurosci.12-02-00483.1992
163. Hemby, S. E., Martin, T. J., Co, C., Dworkin, S. I. & Smith, J. E. The effects of intravenous heroin administration on extracellular nucleus accumbens dopamine concentrations as determined by in vivo microdialysis. *J. Pharmacol. Exp. Ther.* (1995).
164. Di Chiara, G. & Imperato, A. Drugs abused by humans preferentially increase synaptic dopamine concentrations in the mesolimbic system of freely moving rats. *Proc. Natl. Acad. Sci. U. S. A.* (1988). doi:10.1073/pnas.85.14.5274
165. Olmstead, M. C. & Franklin, K. B. J. The development of a conditioned place preference to morphine: Effects of lesions of various CNS sites. *Behav. Neurosci.* (1997). doi:10.1037/0735-7044.111.6.1313
166. Sellings, L. H. L. & Clarke, P. B. S. Segregation of amphetamine reward and locomotor stimulation

between nucleus accumbens medial shell and core. *J. Neurosci.* (2003). doi:10.1523/jneurosci.23-15-06295.2003

167. Ettenberg, A., Pettit, H. O., Bloom, F. E. & Koob, G. F. Heroin and cocaine intravenous self-administration in rats: Mediation by separate neural systems. *Psychopharmacology (Berl).* (1982). doi:10.1007/BF00428151
168. Van Ree, J. M. & Ramsey, N. The dopamine hypothesis of opiate reward challenged. *Eur. J. Pharmacol.* (1987). doi:10.1016/0014-2999(87)90172-5
169. Zernig, G., O'Laughlin, I. A. & Fibiger, H. C. Nicotine and heroin augment cocaine-induced dopamine overflow in nucleus accumbens. *Eur. J. Pharmacol.* **337**, 1–10 (1997).
170. Vihavainen, T. *et al.* Chronic nicotine modifies the effects of morphine on extracellular striatal dopamine and ventral tegmental GABA. *J. Neurochem.* (2008). doi:10.1111/j.1471-4159.2008.05676.x
171. Schmidt, B. L., Tambeli, C. H., Gear, R. W. & Levine, J. D. Nicotine withdrawal hyperalgesia and opioid-mediated analgesia depend on nicotine receptors in nucleus accumbens. *Neuroscience* **106**, 129–136 (2001).
172. De Moura, F. B., Withey, S. L. & Bergman, J. Enhancement of opioid antinociception by nicotine. *J. Pharmacol. Exp. Ther.* **371**, 624–632 (2019).
173. Haghparast, A., Khani, A., Naderi, N., Alizadeh, A. M. & Motamedi, F. Repeated administration of nicotine attenuates the development of morphine tolerance and dependence in mice. *Pharmacol. Biochem. Behav.* **88**, 385–392 (2008).
174. Biala, G. & Weglinska, B. On the mechanism of cross-tolerance between morphine- and nicotine-induced antinociception: Involvement of calcium channels. *Prog. Neuro-Psychopharmacology Biol. Psychiatry* **30**, 15–21 (2006).
175. Pugh, G., Welch, S. P. & Bass, P. P. Modulation of free intracellular calcium and cAMP by morphine and cannabinoids, alone and in combination in mouse brain and spinal cord synaptosomes. *Pharmacol. Biochem. Behav.* **49**, 1093–1100 (1994).
176. Pugh, G., Smith, P. B., Dombrowski, D. S. & Welch, S. P. The role of endogenous opioids in enhancing the antinociception produced by the combination of Δ9-tetrahydrocannabinol and morphine in the spinal cord. *J. Pharmacol. Exp. Ther.* **279**, 608–616 (1996).
177. Weiss, F., Markou, A., Lorang, M. T. & Koob, G. F. Basal extracellular dopamine levels in the nucleus accumbens are decreased during cocaine withdrawal after unlimited-access self-administration. *Brain Res.* (1992). doi:10.1016/0006-8993(92)91327-B
178. Hildebrand, B. E., Nomikos, G. G., Hertel, P., Schilstrom, B. & Svensson, T. H. Reduced dopamine output in the nucleus accumbens but not in the medial prefrontal cortex in rats displaying a mecamylamine-precipitated nicotine withdrawal syndrome. *Brain Res.* (1998). doi:10.1016/S0006-

8993(97)01135-9

179. Diana, M., Melis, M. & Gessa, G. L. Increase in meso-prefrontal dopaminergic activity after stimulation of CB1 receptors by cannabinoids. *Eur. J. Neurosci.* (1998). doi:10.1111/j.1460-9568.1998.00292.x
180. Diana, M., Pistis, M., Carboni, S., Gessa, G. L. & Rossetti, Z. L. Profound decrement of mesolimbic dopaminergic neuronal activity during ethanol withdrawal syndrome in rats: Electrophysiological and biochemical evidence. *Proc. Natl. Acad. Sci. U. S. A.* (1993). doi:10.1073/pnas.90.17.7966
181. Creed, M. *et al.* Cocaine exposure enhances the activity of ventral tegmental area dopamine neurons via calcium-impermeable NMDARs. *J. Neurosci.* (2016). doi:10.1523/JNEUROSCI.1703-16.2016
182. Mansvelder, H. D. & McGehee, D. S. Long-term potentiation of excitatory inputs to brain reward areas by nicotine. *Neuron* (2000). doi:10.1016/S0896-6273(00)00042-8
183. Langlois, L. D. & Nugent, F. S. Opiates and Plasticity in the Ventral Tegmental Area. *ACS Chemical Neuroscience* (2017). doi:10.1021/acschemneuro.7b00281
184. Bloomfield, M. A. P., Ashok, A. H., Volkow, N. D. & Howes, O. D. The effects of δ9-tetrahydrocannabinol on the dopamine system. *Nature* (2016). doi:10.1038/nature20153
185. You, C., Vandegrift, B. & Brodie, M. S. Ethanol actions on the ventral tegmental area: novel potential targets on reward pathway neurons. *Psychopharmacology* (2018). doi:10.1007/s00213-018-4875-y
186. Volkow, N. D., Wang, G. J., Fowler, J. S., Tomasi, D. & Telang, F. Addiction: Beyond dopamine reward circuitry. *Proceedings of the National Academy of Sciences of the United States of America* (2011). doi:10.1073/pnas.1010654108
187. Trifilieff, P. & Martinez, D. *Cocaine: Mechanism and Effects in the Human Brain*. *The Effects of Drug Abuse on the Human Nervous System* (2013). doi:10.1016/B978-0-12-418679-8.00005-8
188. Volkow, N. D. & Morales, M. The Brain on Drugs: From Reward to Addiction. *Cell* (2015). doi:10.1016/j.cell.2015.07.046
189. Kravitz, A. V., O'Neal, T. J. & Friend, D. M. Do dopaminergic impairments underlie physical inactivity in people with obesity? *Front. Hum. Neurosci.* **10**, 514 (2016).
190. Friend, D. M. *et al.* Basal Ganglia Dysfunction Contributes to Physical Inactivity in Obesity. *Cell Metab.* (2017). doi:10.1016/j.cmet.2016.12.001
191. Lobo, M. K. *et al.* ΔFosB induction in striatal medium spiny neuron subtypes in response to chronic pharmacological, emotional, and optogenetic stimuli. *J. Neurosci.* (2013). doi:10.1523/JNEUROSCI.1875-13.2013
192. Nestler, E. J., Barrot, M. & Self, D. W. ΔFosB: A sustained molecular switch for addiction. *Proc. Natl. Acad. Sci. U. S. A.* (2001). doi:10.1073/pnas.191352698
193. Bonci, A. & Williams, J. T. A common mechanism mediates long-term changes in synaptic transmission after chronic cocaine and morphine. *Neuron* (1996). doi:10.1016/S0896-6273(00)80082-3

194. Saal, D., Dong, Y., Bonci, A. & Malenka, R. C. Drugs of abuse and stress trigger a common synaptic adaptation in dopamine neurons. *Neuron* (2003). doi:10.1016/S0896-6273(03)00021-7

195. Niehaus, J. L., Murali, M. & Kauer, J. A. Drugs of abuse and stress impair LTP at inhibitory synapses in the ventral tegmental area. *Eur. J. Neurosci.* (2010). doi:10.1111/j.1460-9568.2010.07256.x

196. Dacher, M. & Nugent, F. S. Morphine-induced modulation of LTD at GABAergic synapses in the ventral tegmental area. *Neuropharmacology* (2011). doi:10.1016/j.neuropharm.2010.11.012

197. Yang, H. *et al.* Nucleus Accumbens Subnuclei Regulate Motivated Behavior via Direct Inhibition and Disinhibition of VTA Dopamine Subpopulations. *Neuron* (2018). doi:10.1016/j.neuron.2017.12.022

198. Van Den Oever, M. C. *et al.* Prefrontal cortex AMPA receptor plasticity is crucial for cue-induced relapse to heroin-seeking. *Nat. Neurosci.* (2008). doi:10.1038/nn.2165

199. Badiani, A. *et al.* Environmental modulation of amphetamine-induced c-fos expression in D1 versus D2 striatal neurons. *Behav. Brain Res.* (1999). doi:10.1016/S0166-4328(99)00041-8

200. Robinson, T. E., Gorny, G., Savage, V. R. & Kolb, B. Widespread but regionally specific effects of experimenter- versus self-administered morphine on dendritic spines in the nucleus accumbens, hippocampus, and neocortex of adult rats. *Synapse* **46**, 271–9 (2002).

201. Hearing, M. C. *et al.* Reversal of morphine-induced cell-type-specific synaptic plasticity in the nucleus accumbens shell blocks reinstatement. *Proc. Natl. Acad. Sci. U. S. A.* **113**, 757–62 (2016).

202. McDevitt, D. S., Jonik, B. & Graziane, N. M. Morphine Differentially Alters the Synaptic and Intrinsic Properties of D1R- and D2R-Expressing Medium Spiny Neurons in the Nucleus Accumbens. *Front. Synaptic Neurosci.* (2019). doi:10.3389/fnsyn.2019.00035

203. Graziane, N. M. *et al.* Opposing mechanisms mediate morphine- and cocaine-induced generation of silent synapses. *Nat. Neurosci.* (2016). doi:10.1038/nn.4313

204. Taverna, S., Ilijic, E. & Surmeier, D. J. Recurrent collateral connections of striatal medium spiny neurons are disrupted in models of Parkinson's disease. *J. Neurosci.* (2008). doi:10.1523/JNEUROSCI.5493-07.2008

CHAPTER 2

CHEMOGENETIC MODULATION OF ACCUMBENS DIRECT OR INDIRECT PATHWAYS BIDIRECTIONALLY ALTERS REINSTATEMENT OF HEROIN-SEEKING IN HIGH- BUT NOT LOW-RISK RATS

Timothy J. O'Neal, Marlaena N. Nooney, Katie Thien, Susan M. Ferguson

Neuropsychopharmacology (2020) **45**: 1251-1262. PMID: 31747681

ABSTRACT

Opioid addiction has been declared a public health emergency, with fatal overdoses following relapse reaching epidemic proportions and disease-associated costs continuing to escalate. Relapse is often triggered by re-exposure to drug-associated cues, and though the neural substrates responsible for relapse in vulnerable individuals remains ambiguous, the nucleus accumbens (NAc) has been shown to play a central role. NAc direct and indirect pathway medium spiny neurons (dMSNs and iMSNs) can have oppositional control over reward-seeking and associative learning and are critically involved in reinstatement of psychostimulant-seeking. However, whether these pathways similarly regulate reinstatement of opioid-seeking remains unknown, as is their role in modulating motivation to take opioids. Here, we describe a method for classifying addiction severity in outbred rats following intermittent-access heroin self-administration that identifies subgroups as addiction-vulnerable (high-risk) or addiction-resistant (low-risk). Using dual viral-mediated gene transfer of DREADDs into dMSNs or iMSNs, we show that transient inactivation of dMSNs or activation of iMSNs is capable of suppressing cue-induced reinstatement of heroin-seeking in high- but not low-risk rats. Surprisingly, however, the motivation to self-administer heroin was unchanged, indicating a divergence in the encoding of heroin-taking and heroin-seeking in rats. We further show that transient activation of dMSNs or inactivation of iMSNs exacerbates cue-induced reinstatement of heroin seeking in high- but not low-risk rats, again with no effect on motivation in either group. These findings demonstrate a critical role for dMSNs and iMSNs in encoding vulnerability to reinstatement of heroin-seeking and provide much needed insight into the specific neurobiological changes that occur in vulnerable groups following heroin self-administration.

INTRODUCTION

Drug addiction is characterized by cycles of compulsive drug-taking and drug-seeking and high rates of relapse. Reported relapse rates for opioids are higher than any other drug class, with up to 59% of individuals relapsing in the first week of abstinence and 80% relapsing in the first month. Moreover, deaths linked to opioid overdoses are currently the leading cause of accidental death among American adults, and the recent sharp rise in opioid-related deaths have led to the opioid epidemic being declared a national emergency.

The cortico-basal ganglia (C-BG) circuit has been identified as a critical neural substrate in regulating the development and persistence of addiction. The striatum, which can be anatomically and functionally divided into the dorsal striatum and the nucleus accumbens (NAc), serves as the interface of the C-BG circuit, integrating cortical and subcortical inputs to guide a diverse set of behaviors including associative learning, decision-making, and motivation[1,2]. For example, the NAc is necessary for the development and expression of opioid-seeking[3,4], and the NAc has been shown to modulate opioid reward and opioid-taking[5–8]. However, the striatum is a heterogeneous structure containing two interspersed populations of GABAergic medium spiny neurons (MSNs): direct pathway MSNs (dMSNs) and indirect pathway MSNs (iMSNs). Both dMSNs and iMSNs receive extensive glutamatergic inputs from cortical, subcortical, and thalamic nuclei; GABAergic inputs from local striatal interneurons and other MSNs via lateral inhibition; and dopaminergic inputs from the ventral tegmental area (VTA) and substantia nigra[9]. However, NAc dMSNs project directly to the VTA, while NAc iMSNs project to the ventral pallidum (VP). As a result of this distinct connectivity, dMSNs and iMSNs can have opposing control over behavioral output, with stimulation of dMSNs facilitating behavior by serving as a “go” signal and stimulation of iMSNs suppressing behavior by serving as a “stop” signal[2,10]. With respect to addiction, it has been hypothesized that disruptions in the balance of signaling between dMSNs and iMSNs (i.e., excessive “go” signal or insufficient “stop” signal) could underlie development of the compulsive drug-taking and drug-seeking behaviors that are associated with compulsive drug use. Nonetheless, the role of these two striatal cell populations have not been examined in behaviors related to opioid addiction.

As only a subset of drug users transition from casual or medical use to addiction, it is essential to investigate whether addiction vulnerability is an intrinsic (e.g., genetically-defined) or acquired trait[11]. Thus, we have drawn from previous work investigating individual variability in addiction-like behavior[12–14] and developed a model for characterizing addiction severity using an intermittent-access (IntA) self-administration procedure that has been shown to produce distinct patterns of behavior in subsets of rats[13,14]. Additionally, we incorporated key components of the DSM diagnostic criteria for Opioid Use Disorder, including difficulty stopping or limiting drug intake, high motivation to obtain and consume drug, sustained drug craving during periods of abstinence, and relapse following abstinence into our severity classification model [15]. We then combined this model with dual-

viral mediated gene transfer techniques for selective expression of Gi/o- and Gq-DREADDs in NAc dMSNs and iMSNs to determine how transient, bidirectional changes in the activity of these cell populations[16,17] alters the motivation to take heroin and cue-induced reinstatement of heroin-seeking in rats expressing low and high levels of addiction-like behavior following heroin use.

METHODS

Subjects

Outbred male Sprague-Dawley rats (*n* = 133; Envigo) weighing 250-274 g upon arrival were pair-housed throughout testing in a temperature- and humidity-controlled vivarium on a 12 h light/dark cycle (lights off at 19:00). Rats were acclimated to the vivarium for ≥5 days and handled for ≥3 days prior to any experimentation. Rats were mildly food-restricted (~95-100% of initial body weight) 2 days prior to behavioral testing and were maintained on food restriction throughout testing to offset excessive weight gain. Behavioral testing occurred at the beginning of the dark cycle, and all experimental procedures were performed according to National Institutes of Health (NIH) guidelines and were approved by Seattle Children's Research Institute's Institutional Animal Care and Use Committee (IACUC).

Drugs

Diamorphine HCl (heroin) was obtained through the Drug Supply Program of the National Institute on Drug Abuse (NIDA) and was dissolved in sterile saline (0.9% NaCl) to a stock concentration of 5 mg/ml. For self-administration experiments, individual heroin syringes were prepared based on body weight for administration of 0.075 mg/kg heroin per infusion (50 *μ*l/infusion delivered over 2.8 s). D-amphetamine (Millipore-Sigma; A5880) was dissolved in sterile saline at a concentration of 2 mg/ml and administered at a dose of 1 ml/kg. Clozapine-*N*-oxide (CNO) was obtained through the Rapid Access to Investigate Drug Program of the National Institute of Neurological Disorders and Stroke (NINDS) of the NIH and was dissolved in dimethyl sulfoxide (DMSO; Sigma Aldrich, D650) in a hot water bath, then further diluted in sterile water to a final concentration of 6% DMSO. CNO was prepared fresh daily at a concentration of 5 mg/ml and administered *ip* at a dose of 1 ml/kg. Vehicle (VEH) injections consisted of DMSO dissolved in sterile water to a final concentration of 6% DMSO and were administered *ip* at a volume of 1 ml/kg.

Viral vectors

Adeno-associated viruses containing Cre-dependent Gi-coupled (pAAV-hSyn-DIO-hM$_4$D(Gi)-mCherry) and Gq-coupled (pAAV-hSyn-DIO-hM3D(Gq)-mCherry) DREADDs were acquired from Addgene (viral prep #44362-AAV8 and #44361-AAV8, respectively) and had titers of ≥4x10^{12} viral genomes/ml. Adeno-associated virus containing Cre-dependent eGFP (rAAV5-hSyn-DIO-eGFP) was acquired from the UNC Vector Core (lot

AV4497c) and had a titer of $4.1x10^{21}$ viral molecules/ml. Canine adenovirus containing retrogradely-transported Cre (CAV2-Cre) had a titer of ~$2.5x10^{9}$ viral genomes/μl and was prepared as previously described[18].

Surgical procedures

Rats were anesthetized with isoflurane (4-5% induction, 1-2% maintenance; Patterson Veterinary) for all surgical procedures. Rats received an injection of meloxicam (1 mg/ml, 1 ml/kg subcutaneously; Patterson Veterinary) prior to surgery for analgesia and an injection of sterile saline (1 ml/kg) when surgeries lasted ≥1 h to assist recovery. Post-operative recovery was monitored for a minimum of 3 days, and additional meloxicam and saline were administered as needed.

Catheter surgeries

Jugular catheterization surgeries were done as previously described[19]. Briefly, the right jugular vein was isolated and a custom-made silastic tubing catheter (ID = 0.51 mm, OD = 0.94 mm, length = 100 mm) was implanted, tied in place with non-absorbable silk sutures, and attached subcutaneously to a back-mounted port. Following surgery, catheters were flushed daily with a mixture of gentamicin (5 mg/ml) and heparin (3 U/ml) in sterile saline (0.2 ml/day, *iv*) to maintain patency. Catheter patency was checked prior to the first day of self-administration and following the final progressive ratio test with an infusion of brevital sodium (10 mg/ml in sterile saline, 0.05 – 0.2 ml/infusion, *iv*; Methohexital sodium, Patterson Veterinary); rats that became ataxic within 5 seconds of infusion were considered to have maintained patency. Rats that lost patency (n = 19) or whose catheters were damaged (n = 6) prior to the beginning of extinction training were excluded from all analyses.

Stereotaxic surgeries

Stereotaxic surgeries were done using standard surgical procedures[19]. Following head-fixation in a rat stereotax (Kopf Instruments), the skull was exposed and craniotomies were drilled above target regions of interest relative to bregma[20]. Viral vectors were delivered via 33-gauge needles attached to 10 μl gas-tight syringes (Hamilton Company) with PE20 tubing back-filled with sterile water. Viruses were infused at a volume of 500 nl/virus and a rate of 100 nl/min, unless otherwise specified. Coordinates for target brain regions (in mm, relative to bregma) were as follows: NAc [A/P +1.6, M/L ±1.5, D/V -7.3], VTA [A/P -5.0, M/L ±0.9, D/V -8.5], VP [A/P -0.1, M/L ±2.0, D/V -8.0]. For Fos experiments, CAV2-Cre was bilaterally infused into the VTA or VP, DIO-hM4Di or DIO-hM3Dq was unilaterally infused into the left NAc, and DIO-eGFP was unilaterally infused into the right NAc. For chemogenetic experiments targeting the direct pathway, CAV2-Cre was bilaterally infused into the VTA and DIO-hM4Di or DIO-hM3Dq was bilaterally infused into the NAc. For

chemogenetic experiments targeting the indirect pathway, CAV2-Cre was bilaterally infused into the VP and DIO-hM4Di or DIO-hM3Dq was bilaterally infused into the NAc. Injection needles were left in place for an additional 5 min following infusion to facilitate diffusion throughout the target nuclei, and needles were slowly retracted (~1 min) to prevent disruption of virus localization via capillary action.

Self-administration and severity classification

Self-administration apparatus

Behavioral testing was conducted in standard self-administration chambers equipped with two retractable levers, two white cue lights located above each lever, a house light, and a grid floor (MedAssociates). White cue lights were located on the front wall of the chamber above the levers for localized illumination, while the house light was located near the top of the back wall to illuminate the entire chamber. A syringe pump located outside each chamber was connected to a swivel within each chamber to permit *iv* drug infusions. Self-administration chambers were cleaned daily after each session with 70% ethanol.

Self-administration procedure

Following recovery from surgery, rats were trained to self-administer heroin using an intermittent access (IntA) procedure that produces spikes in brain drug concentration and results in individual variability of addiction severity in rodents[13]. Each self-administration (SA) session (6 h/day, 10 days) consisted of 12 repeating drug available (DA; 5 min) and drug unavailable (DU; 25 min) blocks; the length of each DU block ensured that brain concentrations for heroin and its two active metabolites (morphine and 6-monoacetylmorphine) were on the descending limb of their pharmacokinetic curves at the beginning of each DA block[21]. Daily IntA SA sessions were signaled by extinction of house lights and extension of two levers into the chamber: lever presses on the active lever resulted in drug delivery (FR1, 0.075 mg/kg/infusion over 2.8 s) and illumination of the cue light (3 s) over the drug lever, while lever presses on the inactive lever had no consequences. At the end of each DA block, house lights re-illuminated to signal the beginning of the DU block and levers remained extended to monitor drug-seeking during cued-unavailability, though lever presses resulted in neither drug delivery nor cue presentation. Following IntA self-administration, rats underwent a progressive ratio (PR) test in which the number of lever presses required for an infusion increased with each successive infusion (5, 10, 20, 45, 65, 85, 115, 145, 165, 185, 215, 245) until either 30 min passed without an infusion or 6 h total had elapsed[19]. Next, rats underwent daily extinction sessions (60 min/day, 9 days) during which lever presses no longer resulted in cue presentation or drug delivery; this was sufficient to reduce the responding of all rats to <20% of their final day of self-administration. Following extinction training, rats underwent a cue-induced reinstatement test (60 min), during which the drug-paired cue light was presented at the beginning of the session and active lever presses resulted in further cue presentations but no drug delivery.

Addiction severity classification

Six behavioral measures were collected and used to classify individual rats according to their overall addiction severity: (1) *Intake*, calculated as the total number of heroin infusions taken during IntA SA; (2) *Consistency*, calculated as the cumulative percentage of DA blocks across all IntA sessions in which at least one infusion was self-administered; (3) *Seeking*, calculated as the cumulative number of active presses during DU blocks across all IntA sessions; (4) *Motivation*, calculated as the breakpoint during PR testing; (5) *Extinction*, calculated as the total number of active lever presses during extinction training; and (6) *Relapse*, calculated as the total number of active lever presses during cue-induced reinstatement. The raw values for each behavior were converted to z-scores by subtracting the group mean from the individual values and dividing by the standard deviation of the group[22]. Individual z-scores for each animal were then combined to give a cumulative addiction severity score (SS), which was used to classify rats into low-risk ($SS < -1$), moderate-risk ($-1 \leq SS \leq 1$), and high-risk ($SS > 1$). The goal of the present study was to examine neurobiological differences between addiction-vulnerable (high-risk) and addiction-resilient (low-risk) rats, so those classified as moderate-risk were excluded from grouped analyses.

Anatomical tracing

To validate that the dual viral-mediated gene transfer of DREADDs strategy was capable of selectively targeting dMSNs, cholera toxin subunit B (CTB) conjugated to AlexaFluor (AF) 647 (CTB-647; C-34778, ThermoFisher) was mixed 1:1 with CAV2-Cre and infused into the VTA (700 nl total, 70 nl/min), CTB conjugated to AF488 (CTB-488; C-34775, ThermoFisher) was infused into the VP (350 nl, 70 nl/min), and DIO-hM4Di-mCherry was infused into the NAc. To validate that the viral strategy was capable of selectively targeting iMSNs, CTB-647 was mixed 1:1 with CAV2-Cre and co-infused into the VP (700 nl total, 70 nl/min), CTB-488 was infused into the VTA (350 nl total, 70 nl/min), and DIO-hM4Di-mCherry was infused into the NAc. Viruses were allowed to express for twenty-one days to allow sufficient DREADD expression and limit CTB-associated neurotoxicity. Following expression, rats were deeply anesthetized with Beuthanasia-D (2 ml/kg *ip*; 3.9 mg/ml pentobarbital sodium and 0.5 mg/ml phenytoin sodium; Patterson Veterinary) and transcardially perfused with phosphate-buffered saline (PBS; pH = 7.4) followed by paraformaldehyde (PFA; 4% in PBS). Brains were extracted, fixed overnight in 4% PFA, post-fixed for >48 h in sucrose (30% in PBS), and sectioned (50 μm) with a vibrating microtome. Z-stacks along the rostral/caudal axis of the NAc (A/P +2.5 through A/P +0.7) were collected with confocal microscopy (20x; Zeiss LSM 710), and neuronal localization of CTB-488, CTB-647, and hM4Di-mCherry was quantified using ImageJ (V1.49; NIH) and Adobe Illustrator (CC 2019).

Chemogenetic modulation of amphetamine stimulated Fos

To confirm that activation of Gi/o- and Gq-coupled DREADDs can modulate activity of NAc dMSNs and iMSNs, Fos levels in the NAc were measured following DREADD activation in an amphetamine plus novelty task that has previously been shown to induce Fos in both dMSNs and iMSNs[23]. Rats were injected with CNO (5 mg/kg, *ip*) and returned to their home cages for 30 min. Next, rats were moved to operant boxes in a new room, injected with d-amphetamine (2 mg/kg, *ip*), and allowed to freely explore. Fifty-five min later, rats were deeply anesthetized and perfused, and brain sections were collected as described above. To visualize Fos levels, floating sections were washed (PBS; 3 x 10 min), blocked (0.25% Triton-X, 5% normal goat serum, PBS; 120 min), and incubated with a primary antibody (1:800 rabbit anti-c-Fos, 0.25% Triton-X, 2.5% normal goat serum, PBS; 24 h; Cell Signaling #2250S, RRID: AB_2247211). Sections were then washed (PBS; 3 x 10 min) and incubated with a secondary antibody conjugated to AF-647 (1:500 goat-anti-rabbit, 0.25% Triton-X, 2.5% normal goat serum, PBS; 120 min; Life Technologies #A32733, RRID: AB_2633282). Finally, sections were washed (PBS; 3 x 10min), mounted on slides, and coverslipped with Vectashield mounting medium with DAPI (Vector Labs). Tri-color z-stacks (20x magnification) along the rostral/caudal axis of the NAc (A/P +2.7 through A/P +0.5) were collected via confocal microscopy and Fos+ cells were manually counted by three separate researchers who were blinded to experimental conditions.

Chemogenetic modulation of addiction-like behaviors

To assess the role of the NAc in driving motivation and relapse in low- and high-risk rats, dMSNs and iMSNs were selectively targeted with excitatory (Gq-coupled; hM3Dq) or inhibitory (Gi/o-coupled; hM4Di) DREADDs that were transiently activated with CNO prior to PR and cue-induced reinstatement tests. Unlike Gs-coupled DREADDs, which initiate Gs-coupled GPCR signaling cascades to broadly alter neuronal activity (via changes in gene transcription, protein trafficking etc.), Gq-coupled DREADDs directly increase neuronal firing via activation of Gq-coupled calcium channels[16]. This direct enhancement of neuronal firing aligned more closely with our experimental goals than a broad/general enhancement of activity. Moreover, Gs-coupled DREADDs have been shown to have a degree of constitutive activity[24,25], an effect that would have confounded our long-term behavioral study. CNO and VEH injections were administered 30 min prior to test sessions in a pseudo-randomized, within-subject design. Additional days of self-administration (3) and extinction (6) were interleaved between PR and cue-induced reinstatement tests, respectively, to re-baseline behavior. Unpaired *t*-tests (VEH first vs VEH second) revealed no significant effect of session order on progressive ratio ($t_{(75)} = 1.56$, $p = 0.12$) or cue-induced reinstatement of drug-seeking ($t_{(75)} = 1.61$, $p = 0.11$). Following completion of behavioral testing, rats were deeply anesthetized and perfused, and brain slices were collected as described above. To confirm DREADD expression, floating sections were washed (PBS; 3 x 10 min), blocked (0.25% Triton-X, 5% normal goat serum, PBS; 120 min), and incubated with a primary antibody (1:400 rabbit anti-DsRed, 0.25%

Triton-X, 2.5% normal goat serum, PBS; 24 h; Clontech #632496, RRID: AB_2737298). Sections were then washed (PBS; 3 x 10 min) and incubated with a secondary antibody conjugated to AF-568 (1:500 goat-anti-rabbit, 0.25% Triton-X, 2.5% normal goat serum; PBS, 120 min; Life Technologies #A11036, RRID: AB_10563566). Finally, sections were washed (PBS; 3 x 10min), mounted on slides, and coverslipped with Vectashield mounting medium with DAPI. Z-stacks along the rostral/caudal axis of the NAc (A/P +2.7 through A/P +0.5) were collected via confocal microscopy to confirm viral expression, quantified as the percent of rats with expression in a particular subregion of the NAc and pseudo-colored to correspond with each chemogenetic experiment. Rats with no detectable DREADD expression in NAc or other areas in examined brain slices (e.g., dorsal striatum, prefrontal cortex) were analyzed as a viral “miss” control group to assess the effects of CNO in rats not expressing DREADDs[19].

Statistical analysis

Behavioral data was collected using automated procedures (MedAssociates), processed using custom-written Python scripts, and analyzed using Python (V3.6) and GraphPad Prism (V8.0). Addiction severity measures were compared between low- and high-risk rats using unpaired two-tailed *t*-tests. The relative severity distribution was compared between groups using a frequency distribution (range: -10 to +17, bin size = 1) fit with a nonlinear regression (Gaussian), and the overlap coefficient was calculated between distributions using R (V3.5). The relative contribution of each severity metric to overall severity classification was analyzed using principal component analysis (PCA) in Python: raw behavioral data were normalized, the corresponding covariance matrix and eigens were calculated, and data was re-plotted on the resulting two-dimensional space. Principal components with an eigenvalue >1 were considered significant contributors to overall variance (**Tables 2.1, 2.2**). Fos+ cell counts along the rostral-caudal axis of the NAc were averaged into a single value per rat, and Fos+ cells were analyzed using paired two-tailed *t*-tests (eGFP vs DREADD). Lever presses during IntA SA and extinction training (severity x session) and lever presses during PR and cue-induced reinstatement tests (severity x treatment) were independently analyzed for each chemogenetic experiment using two-way repeated-measures analysis of variance (RM-ANOVA) followed by Sidak *post-hoc* tests. The relationship between severity metrics and the effect size of each chemogenetic manipulation on motivation and relapse were independently analyzed using multiple linear regressions. Statistical significance for all analyses was set at $p < 0.05$, and data are shown throughout as individual subjects, mean ± SEM, or best-fit line with 95% confidence intervals.

RESULTS

High-risk rats exhibit an addictive phenotype following heroin self-administration

Rats were implanted with indwelling jugular catheters and trained to self-administer heroin. IntA SA sessions consisted of twelve 5-min DA blocks on an FR1 schedule separated by 25-min DU blocks. Following IntA SA training, rats underwent a PR test, extinction training, and a cue-induced reinstatement test. Six behavioral metrics were extracted and used to classify individual addiction severity: (1) *intake*, (2) *consistency*, (3)

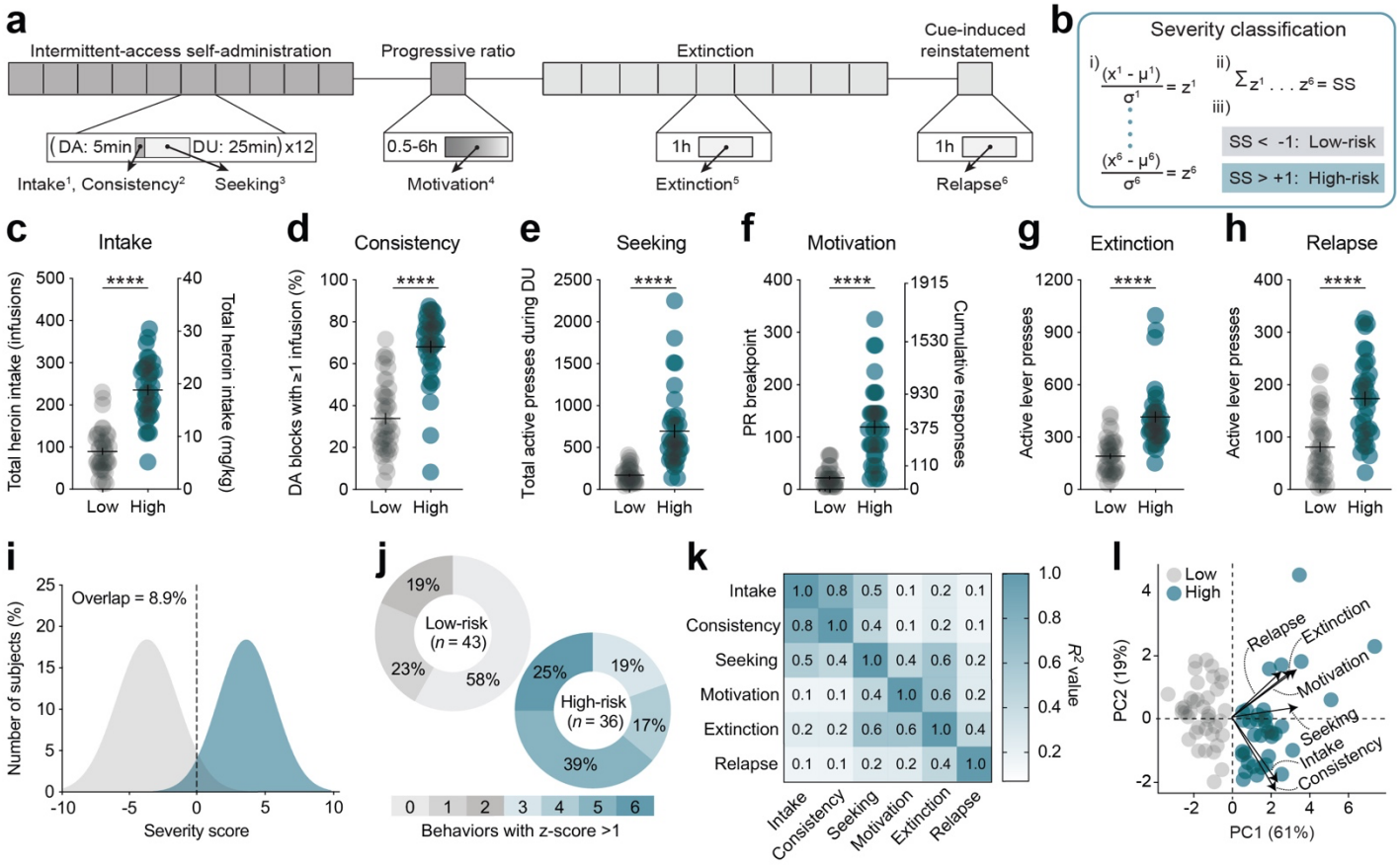

Figure 2.1 | Heroin self-administration procedure and addiction severity classification. (**a**) Timeline of self-administration procedure and behavioral metrics used to classify addiction severity. Dark grey: periods of drug availability (DA), light gray: periods of drug unavailability. (1) *Intake*: Total heroin intake; (2) *Consistency*: Percent (%) of DA blocks with ≥1 infusion; (3) *Seeking*: Total active presses during DU blocks; (4) *Motivation*: Breakpoint during PR; (5) *Extinction*: Total active presses during extinction; (6) *Relapse*: Total active presses during cue-induced reinstatement. (**b**) Severity classification: (i) raw behavioral data were converted to z-scores, (ii) z-scores were combined to give a cumulative severity score (SS), and (iii) individual rats were classified as low-risk (gray) or high-risk (green). (**c-h**) Compared to low-risk rats, high-risk rats (**c**) self-administered more heroin during IntA SA, (**d**) had a higher number of DA blocks where they engaged in drug-taking, (**e**) pressed the drug-paired lever more during DU blocks, (**f**) had higher breakpoints during a PR test, (**g**) pressed the drug-paired lever more during extinction sessions, and (**h**) during the cue-induced reinstatement test. (**i**) Classification produces largely non-overlapping severity distributions between groups. (**j**) High-risk rats scored positive on more severity metrics than low-risk rats. (**k**) Individual severity metrics are all significantly correlated (all $p < .05$), though the relationship between pairs of metrics are highly variable. (l) Principal component analysis of severity metrics, with individual rats and the original severity metrics (length = eigenvalue, angle = eigenvector) replotted on the resulting two-dimensional space. DA: drug available; DU: drug unavailable; IntA: intermittent-access PC: principal component; PR: progressive ratio; SA: self-administration; ****$p < .0001$ (low vs high).

seeking, (4) *motivation*, (5) *extinction*, and (6) *relapse* (**Figure 2.1a**). Severity metrics were normalized to z-scores and combined to give an overall addiction severity score (SS) that was used to classify addiction-resilient (i.e., low-risk; $n = 43$) and addiction-vulnerable (i.e., high-risk; $n = 36$) rats (**Figure 2.1b**). A small number of rats that did not express a strong severity phenotype ($n = 11$) were considered to represent a mixed group and were therefore excluded from analyses.

We identified two populations of rats with significantly different phenotypes that developed over the course of the experiment. Compared to low-risk rats, high-risk rats self-administered more heroin during IntA training (unpaired *t*-test: $t_{(77)} = 10.70$, $p < .0001$), engaged in more bouts of drug-taking during DA blocks (unpaired *t*-test: $t_{(77)} = 9.00$, $p < .0001$), had higher levels of drug-seeking during cued DU blocks (unpaired *t*-test: $t_{(77)} = 7.28$, $p < .0001$), showed higher motivation to self-administer heroin despite a rising cost for each infusion during PR testing (unpaired *t*-test: $t_{(77)} = 8.24$, $p < .0001$), exhibited higher levels of responding throughout extinction training (unpaired *t*-test: $t_{(77)} = 7.03$, $p < .0001$), and had greater rates of heroin-seeking during cue-induced reinstatement (unpaired *t*-test: $t_{(77)} = 5.90$, $p < 0.0001$; **Figure 2.1c-2.1h**). These behavioral differences resulted in largely non-overlapping addiction severity distributions between low-risk and high-risk rats (8.9% overlap; 95% CI: low [-4.1 to -3.2], high [3.4 to 4.0]). Nonetheless, there was variability within each subgroup for which severity metrics contributed to their classification and the number of positive severity metrics (low: 0.6 ± 0.1; high 4.7 ± 0.2; $t_{(77)} = 18.92$, $p < .0001$; **Figure 2.1i-2.1j**). While the six metrics used for severity classification were all highly correlated, the relationship between each metric was highly variable, indicating that the metrics were capturing distinct features of addiction-like behavior (**Figure 2.1k**). Dimensional reduction was performed on the severity metrics to identify the vectors accounting for the majority of the variance within the dataset. Distribution along the first principal component (PC1) corresponded with classification into low-risk ($PC1 < 0$) or high-risk ($PC1 > 0$) for all rats (**Figure 2.1l**). PC1 accounted for 61% of the cumulative variance and was positively correlated with all severity metrics, while PC2 accounted for 19% of all variance and was negatively correlated with *intake* and *consistency* but positively correlated with all other metrics.

Anatomical tracing of NAc direct and indirect pathways

Recent reports have indicated that the segregation of MSN output pathways may not be as complete as originally described – at least in mice – with one study finding that >90% of dMSNs send collaterals to the VP prior to synapsing in the VTA[26]. Thus, we first sought to determine whether DREADDs could be targeted selectively to MSNs projecting exclusively to the VTA (i.e., dMSNs) or the VP (i.e., iMSNs) in outbred Sprague Dawley rats. To verify DREADD expression in dMSNs, CTB-488 was infused into the VP, CTB-647 was co-infused into the VTA with CAV2-Cre, and Cre-dependent hM4Di-mCherry was infused into the NAc (**Figure 2.2a, 2.2c**). Using this method, 49.1% and 45.7% of neurons were labeled as putative dMSNs (CTB-647$^+$) and

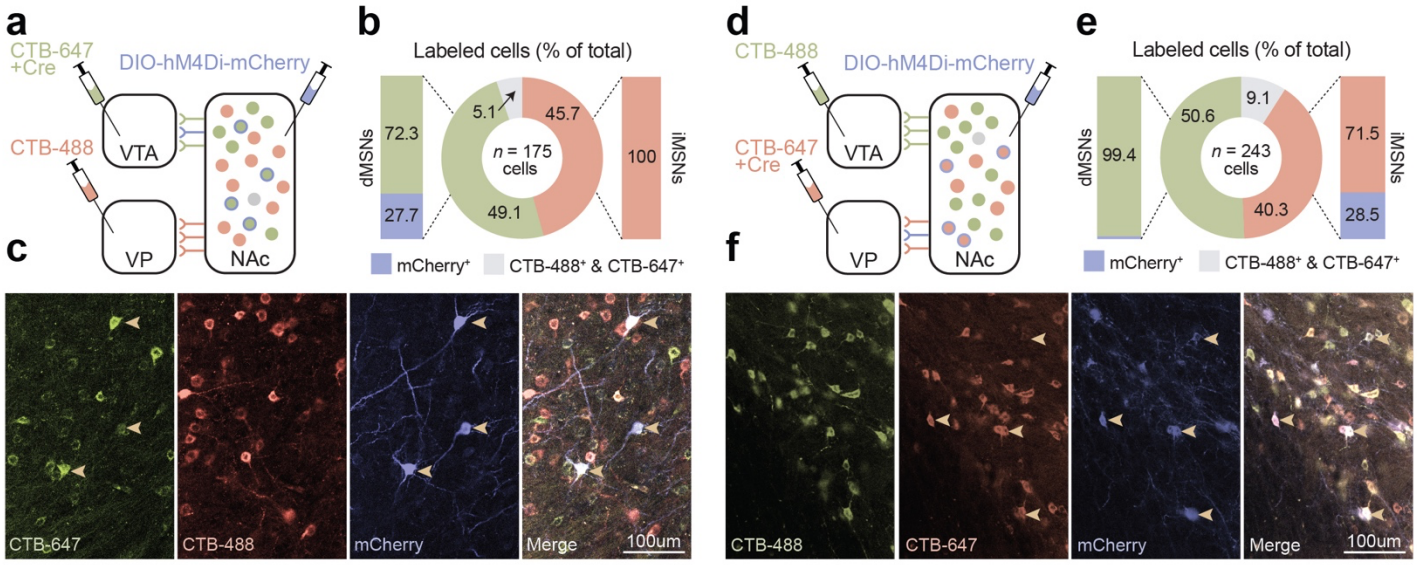

Figure 2.2 l Anatomical tracing of NAc direct and indirect pathways. (**a**) Viral strategy for anatomical tracing of NAc dMSNs. (**b**) Quantification of neuronal labeling. ~30% of putative dMSNs (green) and 0% of putative iMSNs (rerd) co-expressed DREADDs (purple). (**c**) Representative images of neuronal labeling and viral expression. (**d**) Viral strategy for anatomical tracing of NAc iMSNs. (**e**) Quantification of neuronal labeling. ~30% of putative iMSNs (red) and <1% of putative dMSNs (green) co-expressed DREADDs (purple). (**f**) Representative images of neuronal labeling and viral expression. Yellow arrow: DREADD expressed in cell type of interest; *n* = 4 rats, scale bar = 100 μm.

iMSNs (CTB-488$^+$), respectively, while 5.1% of neurons were co-labeled with both fluorophores. Importantly, 27.7% of dMSNs were positive for DREADDs, in contrast to 0% of iMSNs (**Figure 2.2b**). In contrast to what has been reported with mice[24], we did not detect any DREADD$^+$ terminals within the VP, suggesting that DREADD-transfected dMSNs were not sending collaterals to the VP in the rats[26]. A similar strategy was used to verify DREADD expression in iMSNs, with infusion of CTB-488 into the VTA, co-infusion of CTB-647 and CAV2-Cre into the VP, and infusion of hM4Di-mCherry into the NAc (**Figure 2.2d, 2.2f**). Comparable to labeling of the direct pathway, 40.3% and 50.6% of neurons were labeled as putative iMSNs (CTB-647$^+$) and dMSNs (CTB-488$^+$), respectively, with 9.1% of neurons co-labeled with both fluorophores. DREADD transfection in iMSNs was similar to dMSNs (28.5%), though a small number of dMSNs (< 1%) were found to be positive for DREADD expression (**Figure 2.2e**). Given the relatively high transfection rate within iMSNs, however, transfection in this small number of dMSNs is unlikely to contribute significantly to alterations in circuit function or behavior.

DREADDs bidirectionally regulate activity of NAc dMSNs and iMSNs

To validate that Gi/o- and Gq-DREADDs in NAc dMSNs and iMSNs can modulate neuronal activity, dual viral-mediated gene transfer was used to unilaterally express DREADDs (left NAc) and eGFP (right NAc) in each pathway. Rats received a home cage injection of CNO (5 mg/kg) 30 min prior to an injection of amphetamine

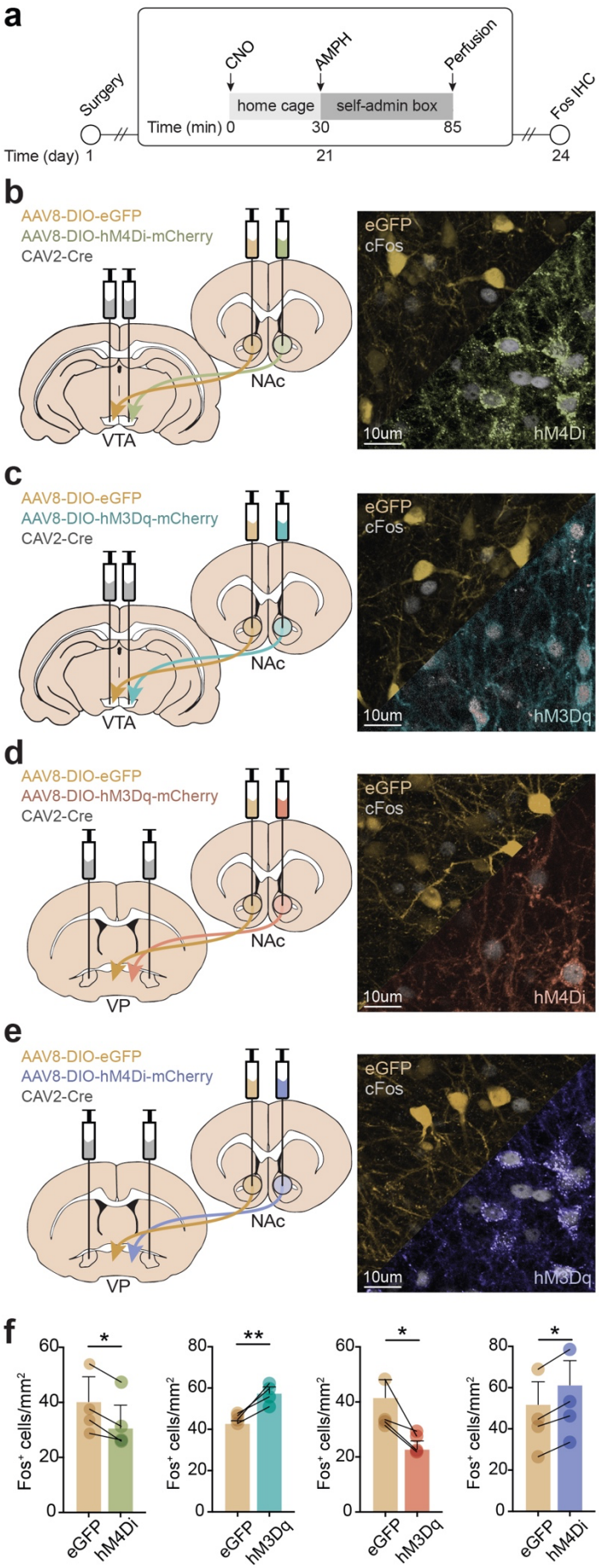

Figure 2.3 | DREADDs bidirectionally alter amphetamine stimulated Fos in MSNs. (**a**) Timeline for chemogenetic modulation of amphetamine stimulated Fos activation. (**b-e**) Viral strategy and representative histology for unilateral expression of GFP (left) and DREADDs (right) in (**b-c**) dMSNs and (**d-e**) iMSNs. (**f**) dMSN-hM4Di decreases, dMSN-hM3Dq increases, iMSN-hM3Dq decreases, and iMSN-hM4Di increases Fos activation, relative to GFP. n = 4/group; scale bar = 50 μm; *$p < .05$, **$p < .01$.

(2 mg/kg) in a novel environment, and 55 min later they were perfused for Fos analysis (**Figure 2.3a**). Inactivation of dMSNs via hM4Di significantly reduced the number of Fos+ cells in the NAc (paired t-test: $t_{(3)} = 5.00$, $p = .0154$), while activation of dMSNs via hM3Dq significantly enhanced the number of Fos$^+$ cells (paired t-test: $t_{(3)} = 5.11$, $p = .0145$; **Figure 2.3b-2.3c**). Similarly, inactivation of iMSNs via hM4Di significantly reduced Fos+ cells (paired t-test: $t_{(3)} = 3.26$, $p = .0473$), while activation of iMSNs via hM3Dq significantly enhanced the number of Fos$^+$ cells (paired t-test: $t_{(3)} = 7.58$, $p = .0048$; **Figure 2.3d-2.3e**). Together with our tracing data, these findings demonstrate the ability to selectively target and modify the activity of dMSNs or iMSNs with excitatory or inhibitory DREADDs.

dMSN inactivation suppresses reinstatement but not motivation in high-risk rats

To test the hypothesis that an imbalance of signaling between NAc dMSNs and iMSNs drives motivation for heroin self-administration under a PR schedule of reinforcement and reinstatement of heroin-seeking, dual viral-mediated gene transfer was used to selectively express Gi/o- or Gq-DREADDs in each pathway. Chemogenetic manipulations were performed in a counterbalanced, within-subject

design, wherein rats received an injection of either VEH or CNO (5 mg/kg) 30 min prior to two PR tests and two reinstatement tests, with additional days of IntA self-administration and extinction, respectively, between tests to re-baseline behavior (**Figure 2.4a, 2.5a**). Given prior work in our lab showing a role for dMSNs in cue-induced reinstatement of cocaine-seeking but not motivation to take cocaine[19], we first sought to determine if transient chemogenetic inhibition of dMSNs had similar effects following heroin self-administration (**Figure 2.4b**). As with the combined group data (**Figure 2.1**), high-risk rats ($n = 9$) exhibited a greater addiction severity profile compared to low-risk rats ($n = 9$), as they self-administered more heroin (severity x session interaction: $F_{(12, 180)} = 2.43$, $p = .0059$), showed greater motivation for heroin during PR testing (main effect of severity: active presses, $F_{(1, 16)} = 4.97$, $p = .0405$; breakpoint, $F_{(1, 16)} = 4.18$, $p = .0576$), and had higher levels of active lever pressing during extinction training (severity x session interaction: $F_{(14, 210)} = 2.80$, $p = .0007$) and during cue-induced reinstatement (main effect of severity: $F_{(1, 16)} = 12.92$, $p = .0024$; **Figure 2.4c-2.4f**). Importantly, both low- and high-risk rats discriminated between active and inactive levers during IntA SA and extinction training (**Figure S2.1**). Notably, increasing Gi/o signaling in NAc dMSNs had no effect on the motivation to self-administer heroin regardless of addiction severity (main effect of treatment: active presses, $F_{(1, 16)} = 0.28$, $p = .60$; breakpoint, $F_{(1, 16)} = 0.14$, $p = .71$; linear regression: $r^2 = 0.00$, $p = .98$; **Figure 2.4d**) but selectively attenuated reinstatement in high-risk rats (severity x treatment interaction: $F_{(1, 15)} = 9.86$, $p = .0067$), with the magnitude of attenuation significantly correlated with an individual's severity score (linear regression: $r^2 = 0.22$, $p = .0372$; **Figure 2.4f**).

dMSN activation exacerbates reinstatement but not motivation in high-risk rats

Given that increasing Gi/o-signaling in dMSNs was sufficient to attenuate reinstatement in high-risk rats, we next tested whether transient disruption of the balance between dMSNs and iMSNs by chemogenetic activation of dMSNs could drive reinstatement in low-risk rats (**Figure 2.4g**). As with the other experiments, compared to low-risk rats ($n = 11$), high-risk rats ($n = 6$) self-administered more heroin (severity x session interaction: $F_{(12, 180)} = 5.23$, $p < .0001$), had greater motivation for heroin during PR testing (main effect of severity: active presses, $F_{(1, 15)} = 38.73$, $p < .0001$; breakpoint, $F_{(1, 15)} = 23.18$, $p = .0002$), and had higher responding during extinction sessions (severity x session interaction: $F_{(14, 210)} = 3.96$, $p < .0001$) and during cue-induced reinstatement of drug-seeking (main effect of severity: $F_{(1, 15)} = 9.20$, $p = .0084$; **Figure 2.4h-2.4k**). Consistent with the inhibition experiment, chemogenetic activation of NAc dMSNs had no effect on the motivation to self-administer heroin regardless of addiction severity (main effect of treatment: active presses, $F_{(1, 15)} = 1.50$, $p = .24$; breakpoint, $F_{(1, 15)} = 0.21$, $p = .65$; linear regression: $r^2 = 0.0649$, $p = .28$; **Figure 2.4i**), but selectively enhanced reinstatement in high-risk rats (severity x treatment interaction: $F_{(1, 15)} = 5.41$, $p = .0344$), exacerbating reinstatement proportionally to individual severity scores (linear regression: $r^2 = 0.2122$, $p = .0410$; **Figure 2.4k**).

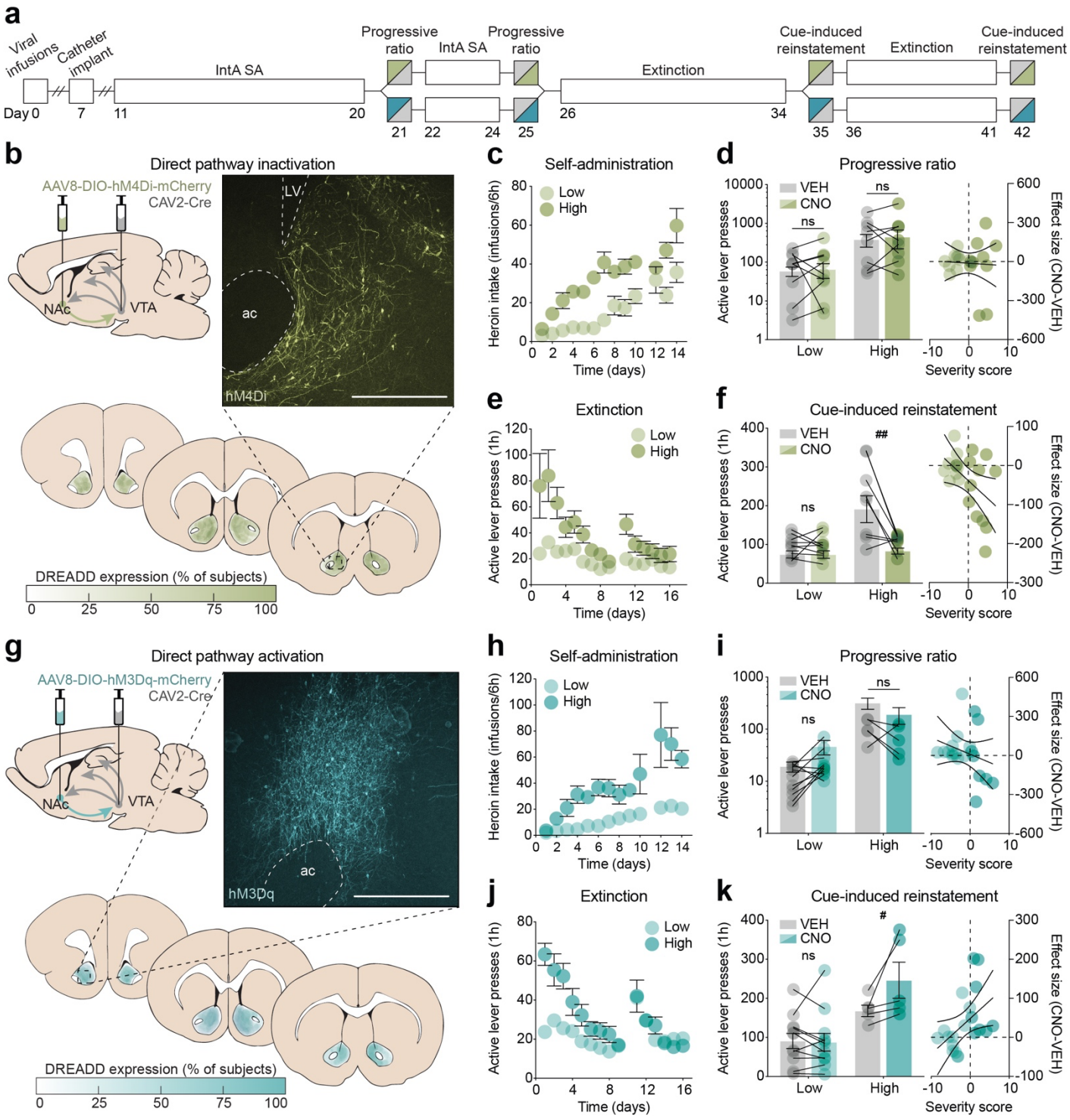

Figure 2.4 | Transient modulation of dMSNs bidirectionally alters reinstatement but not motivation in high-risk rats. (**a**) Timeline for chemogenetic modulation of motivation under a PR schedule of reinforcement and cue-induced reinstatement of drug-seeking. (**b**) Viral strategy, representative histology, and quantification of expression for dMSN inactivation. (**c-f**) Self-administration, progressive ratio, extinction, and reinstatement data for dMSN-hM4Di rats. (**d**) dMSN inactivation has no effect on motivation. (**e**) dMSN inactivation selectively reduces reinstatement in high-risk rats. (**f**) Viral strategy, representative histology, and quantification of expression for dMSN activation. (**h-k**) Self-administration, progressive ratio, extinction, and reinstatement data for dMSN-hM3Dq rats. (**i**) dMSN activation has no effect on motivation. (**k**) dMSN activation selectively enhances reinstatement in high-risk rats. Scale bar = 500 μm; ac = anterior commissure, LV = lateral ventricle; n = 6-11; $^{\#}p < .05$, $^{\#\#}p < .01$

iMSN activation attenuates reinstatement but not motivation in high-risk rats

Given the well-established role for oppositional control of behavioral output by NAc dMSNs and iMSNs, we next sought to determine whether chemogenetic activation of iMSNs would have similar effects following IntA heroin SA to inactivation of dMSNs (**Figure 2.5b**). Much like what we found with whole group analysis, high-risk rats ($n = 8$) developed a more addictive phenotype than low-risk rats ($n = 6$) (self-administration, severity x session interaction: $F_{(12, 144)} = 1.97$, $p = .0313$; PR active presses, main effect of severity: $F_{(1, 12)} = 10.98$, $p = .0062$; PR breakpoint, main effect of severity: $F_{(1, 12)} = 11.67$, $p = .0051$; extinction, severity x session interaction: $F_{(14, 168)} = 3.02$, $p = .0004$; cue-induced reinstatement, main effect of severity: $F_{(1, 12)} = 23.81$, $p = .0004$; **Figure 2.5c-2.5f**). Similar to our findings with inhibition of dMSNs, activation of NAc iMSNs had no effect on the motivation to self-administer heroin in high- or low-risk rats (main effect of treatment: active presses, $F_{(1, 12)} = 0.43$, $p = .52$; breakpoint, $F_{(1, 12)} = 0.54$, $p = 0.48$) (linear regression: $r^2 = 0.0027$, $p = .84$; **Figure 2.5d**); however, the manipulation selectively reduced reinstatement in high-risk rats (severity x treatment interaction: $F_{(1, 12)} = 20.15$, $p = .0007$), with the degree of reduction significantly correlating with addiction risk (linear regression: $r^2 = 0.2671$, $p = .0404$; **Figure 2.5f**). Together, these findings imply a critical role for NAc dMSNs and iMSNs in encoding drug/cue relationships that drive reinstatement of drug-seeking in high-risk individuals.

iMSN inactivation exacerbates reinstatement but not motivation in high-risk rats

To complement these findings, we examined the effect of transient chemogenetic inhibition of iMSNs following heroin self-administration (**Figure 2.5g**). Consistent with our severity classification group data, high-risk rats ($n = 8$) developed a greater addiction-like behavioral profile compared to low-risk rats ($n = 9$) (self-administration, severity x session interaction: $F_{(12, 180)} = 2.06$, $p = .0214$; PR active presses, main effect of severity: $F_{(1, 15)} = 26.57$, $p = .0001$; PR breakpoint, main effect of severity: $F_{(1, 15)} = 39.86$, $p < .0001$; extinction, severity x session interaction: $F_{(14, 210)} = 3.83$, $p < .0001$; cue-induced reinstatement, main effect of severity: $F_{(1, 15)} = 15.48$, $p = .0013$; **Figure 2.5h-2.5k**). While increasing Gi/o-signaling in iMSNs had no effect on the motivation to self-administer heroin in either high- or low-risk rats (main effect of treatment: active presses, $F_{(1, 15)} = 0.07$, $p = .80$; breakpoint, $F_{(1, 15)} = 0.12$, $p = .74$; linear regression: $r^2 = 0.0979$, $p = .19$; **Figure 2.5i**), it did selectively enhance reinstatement in high-risk rats (severity x treatment interaction: $F_{(1, 15)} = 7.62$, $p = .0146$), with the effect size significantly correlating with individual severity scores (linear regression: $r^2 = 0.383$, $p = .0047$; **Figure 2.5k**). Together, these findings suggest that while an imbalance of signaling between dMSNs and iMSNs is likely to contribute to reinstatement of drug-seeking in vulnerable individuals, artificially driving an imbalance is incapable of pushing resilient individuals to reinstate drug-seeking.

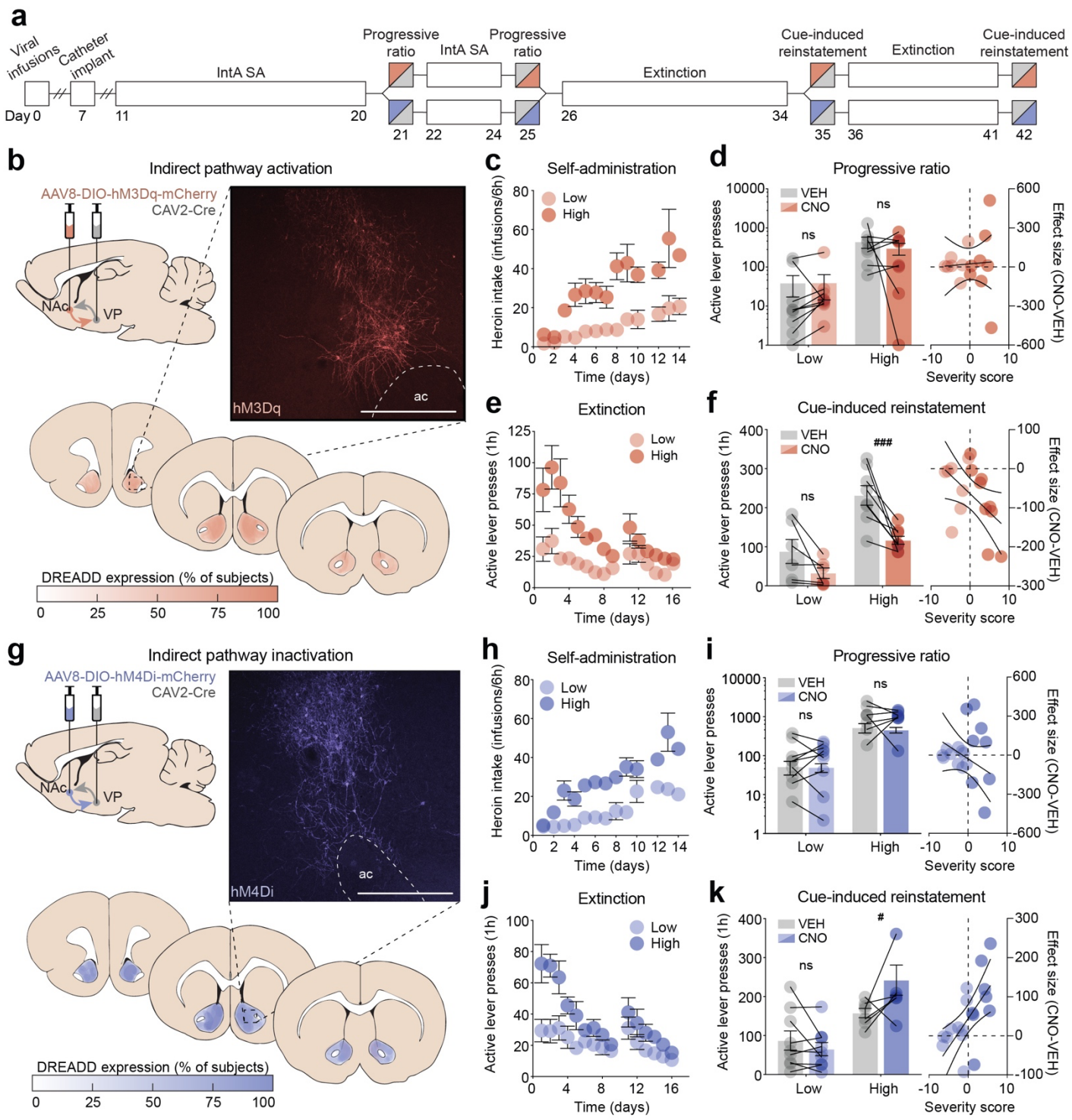

Figure 2.5 | Transient modulation of iMSNs bidirectionally alters reinstatement but not motivation in high-risk rats. (**a**) Timeline for chemogenetic modulation of motivation under a PR schedule of reinforcement and cue-induced reinstatement of drug-seeking. (**b**) Viral strategy, representative histology, and quantification of expression for iMSN activation. (**c-f**) Self-administration, progressive ratio, extinction, and reinstatement data for iMSN-hM3Dq rats. (**d**) iMSN activation has no effect on motivation. (**e**) iMSN activation selectively reduces reinstatement in high-risk rats. (**f**) Viral strategy, representative histology, and quantification of expression for iMSN inactivation. (**h-k**) Self-administration, progressive ratio, extinction, and reinstatement data for iMSN-hM4Di rats. (**i**) iMSN inactivation has no effect on motivation. (**k**) iMSN inactivation selectively enhances reinstatement in high-risk rats. Scale bar = 500 μm; ac = anterior commissure, LV = lateral ventricle; n = 6-9; $^{\#}p < .05$, $^{\#\#\#}p < .001$

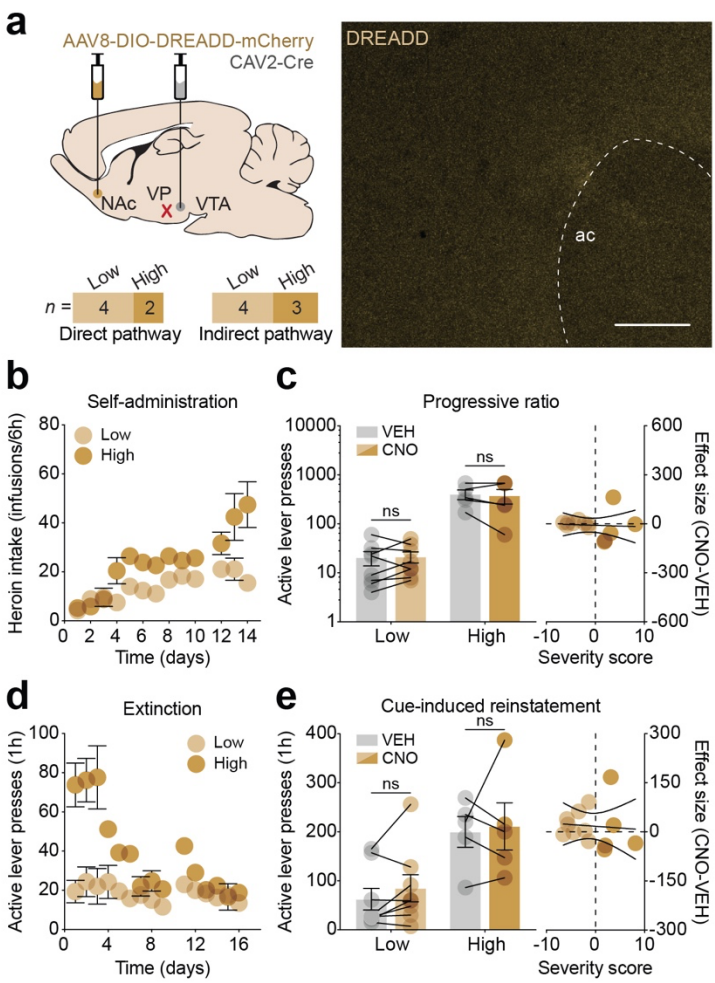

Figure 2.6 | CNO administration has no effect in animals lacking DREADDs. (a) Schematic illustrating viral "misses" from DREADD experiments, with representative lack of expression. Six rats were "misses" from direct pathway experiments (**Figure 2.4**), and seven rats were "misses" from indirect pathway experiments (**Figure 2.5**). (**b-e**) Self-administration, progressive ratio, extinction, and reinstatement data for viral "miss" rats. (**c**) CNO has no effect on motivation, regardless of addiction severity. (**e**) CNO has no effect on cue-induced reinstatement regardless of addiction severity. Scale bar = 500 μm; ac = anterior commissure.

CNO administration has no effects in rats lacking DREADD expression

Recent reports have found that CNO activation of DREADDs occurs indirectly, via retroconversion to clozapine [27]. To ensure that our results were not due to off-target effects of retroconverted clozapine, we examined the effects of CNO administration on motivation and cue-induced reinstatement in rats that had no detectable DREADD expression (viral "miss" rats). This was a heterogeneous group, with similar numbers of direct pathway (n = 6) and indirect pathway (n = 7) misses (**Figure 2.6a**). Consistent with other groups, high-risk rats (n = 5) developed a greater addiction-like behavioral profile compared to low-risk rats (n = 8) (self-administration, severity x session interaction: $F_{(12, 132)} = 3.11$, $p = 0.0007$; PR active presses, main effect of severity: $F_{(1, 11)} = 20.67$, $p = 0.0008$; PR breakpoint, main effect of severity: $F_{(1, 11)} = 28.15$, $p = 0.0003$; extinction, severity x session interaction: $F_{(14, 154)} = 8.95$, $p < 0.0001$; cue-induced reinstatement, main effect of severity: $F_{(1, 11)} = 10.34$, $p = 0.0082$; **Figure 2.6b-2.6e**). Importantly, CNO administration had no effect on motivation (main effect of treatment: active presses, $F_{(1, 11)} = 0.31$, $p = 0.59$; breakpoint, $F_{(1, 11)} = 0.65$, $p = 0.44$; linear regression: $r^2 = 0.001$, $p = 0.90$) or cue-induced reinstatement of heroin-seeking (main effect of treatment: $F_{(1, 11)} = 0.85$, $p = 0.38$; linear regression: $r^2 = 0.01$, $p = 0.73$) in high- or low-risk rats (**Figure 2.6c, 2.6e**). Thus, these results indicate that the observed behavioral effects in the other groups were likely due to the direct actions of CNO on DREADD receptors.

DISCUSSION

Using a dual viral-mediated gene transfer strategy to selectively target Gi/o- and Gq-DREADDs to direct and indirect pathway neurons, we show that dMSNs and iMSNs of the NAc have opposing roles in driving heroin-seeking in high-risk rats. These findings lend further support to the hypothesis that an imbalance in signaling between these two cell types underlies the development and persistence of addictive behaviors. Additionally, we demonstrate that although transient alterations in signaling activity in either pathway are sufficient to both attenuate and exacerbate cue-induced reinstatement of heroin-seeking in high-risk rats, reinstatement behavior was surprisingly unmodifiable in low-risk rats. Of note, chemogenetic modulation of dMSNs and iMSNs had no effect on the motivation to self-administer heroin across phenotype, indicating a divergence in the neural circuits responsible for encoding drug-seeking and drug-taking behaviors.

NAc MSNs regulate cue-induced reinstatement of heroin-seeking

The NAc plays a critical role in regulating cue-induced reinstatement of seeking across many types of rewards, including heroin[28], cocaine[29–32], methamphetamine[33], alcohol[34], and food[32,35]. Moreover, dMSNs and iMSNs have been shown to play oppositional roles in the rewarding and sensitizing effects of cocaine and amphetamine[22,36,37]. There has been no work, however, examining the role of NAc dMSNs and iMSNs in the context of opioid addiction. Our results show that altering the activity of either cell population is sufficient to modulate cue-induced reinstatement of heroin-seeking, complementing and expanding previous work showing a similar role for dorsal striatal dMSNs in cued-reinstatement of cocaine-seeking[19]. More surprisingly, though, these results were selective for high-risk rats, suggesting that their role in the encoding of drug cues is specific to conditions that promote the development of addiction-like behaviors. These findings are consistent with previous work demonstrating that synaptic strengthening of NAc iMSNs is enhanced in addiction-resilient mice following cocaine self-administration[22], and suggest a common role for iMSNs in encoding vulnerability to cue-induced reinstatement of drug-seeking. Notably, however, that same study found that chemogenetic inhibition of NAc iMSNs increased the motivation to self-administer cocaine[22], following previous work showing a role for iMSNs in cocaine-taking[38–40]. Additionally, a recent study from our lab using a polydrug procedure and behavioral economics found that rats had greater motivation for cocaine than heroin[41]. This suggests that psychostimulants and opioids differentially engage motivational circuits, likely due to their unique pharmacological properties (e.g., cocaine increases while morphine decreases Fos activation in iMSNs[42,43]). Thus, while dMSNs and iMSNs appear to play a common role in the encoding of drug-seeking, there appears to be divergence in the encoding of drug-taking across different classes of drugs.

The NAc receives strong glutamatergic input from the prelimbic (PrL) and infralimbic (IL) regions of the medial prefrontal cortex (mPFC), and previous work has found that mPFC, as well as its projections to the NAc, play a

critical role in the encoding of cue value and cue-induced reinstatement of drug-seeking. For example, reinstatement of heroin- or cocaine-seeking induces c-Fos expression in the PrL[44], and pharmacological inactivation of the PrL attenuates reinstatement of psychostimulant-seeking[33]. In addition, extracellular glutamate in the NAc increases following presentation of heroin cues during reinstatement[4], and chemogenetic inactivation of projections from the PrL or the IL to the NAc attenuates reinstatement of psychostimulant-seeking[33,45,46]. Thus, given that modulating activity of subpopulations of NAc MSNs had no effect on reinstatement of drug-seeking in low-risk rats, it is possible that the cue associations formed in mPFC to NAc projections of these rats were insufficiently strengthened during heroin self-administration.

The PrL and IL also differ in their projection patterns to the NAc, with the PrL preferentially innervating the central NAc core and the IL preferentially innervating the surrounding NAc shell. These divergent signaling pathways are generally thought to encode different types of drug-seeking, with the core encoding cue-induced[4,28,47,48] and the shell encoding context-induced[8,28,49] reinstatement. However, cue-induced reinstatement of cocaine[50,51] or ethanol[52,53] induces Fos activation in both the core and shell, and inactivation of either core or shell attenuates cue-induced reinstatement of sucrose-seeking[54]. Additionally, blockade of AMPA receptors in the IL[55] or inhibition of CaMKII activity in the shell[56] blocks cue-induced reinstatement of heroin- or morphine-seeking, respectively, indicating a role for the shell in reinstatement of opioid-seeking. Of note, there is extensive local connectivity between MSNs in the NAc[9], so manipulations of either core or shell are likely to alter overall signaling within the NAc. Consistent with these studies, we found no differences between rats with DREADD expression in both subregions compared to those with expression limited to the core or shell, though additional work specifically investigating the role of these subregions in cue-induced reinstatement of heroin-seeking will add clarity to our understanding of how the C-BG circuit encodes heroin cues.

Experimental caveats and limitations

The phenotyping approach was designed to capture baseline (i.e., genetic) differences in vulnerability, although with any procedure in outbred animals it is difficult to rule out interactions between genetic and environment factors. In addition, with any self-administration schedule, there is always an initial acquisition period, and this would be the case even if we started training on a continuous access schedule (as the rats would still have to learn a new set of contingencies when switched to IntA). Notably, there were no significant differences between high- and low-risk rats in active lever presses during early IntA SA, and there were no significant differences in inactive presses between groups at any point in IntA or extinction (**Figure S2.1**). Thus, this data suggests that the differences between low- and high-risk rats are likely due to differences in preference for the amount and/or pattern of heroin that is consumed, rather than differences in learning rates. However, we do acknowledge the possibility that the effects of our DREADD manipulations may have been

selective for rats with high levels of habitual responding (due to more stimulus-response pairings as a result of higher heroin intake), with the possibility that all rats would exhibit a DREADD-modifiable high-risk phenotype following enough drug-cue pairings.

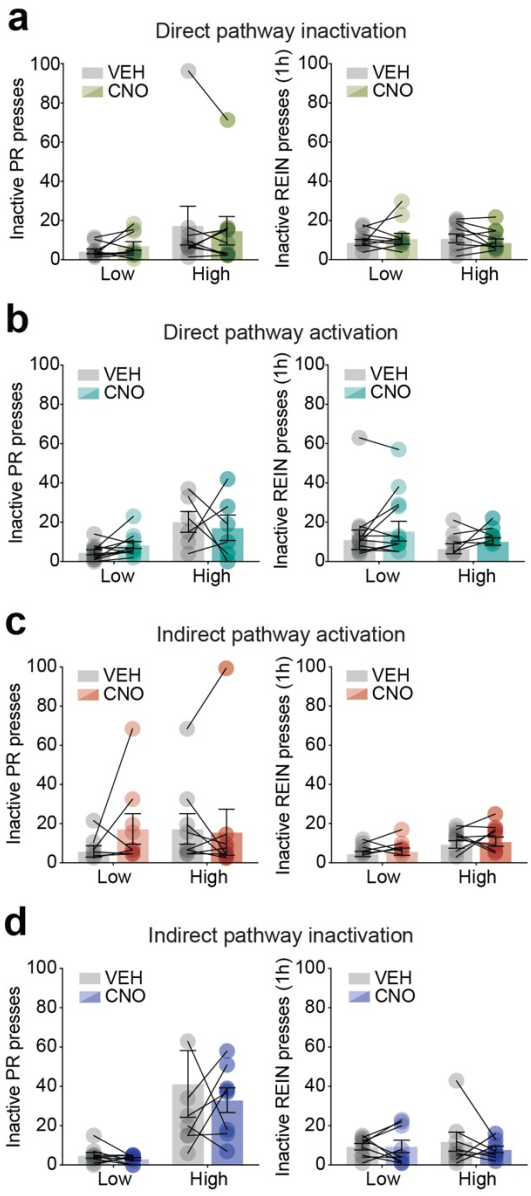

Figure S2.1 | Lever discrimination. Active and inactive lever presses during self-administration (left) and extinction (right). (**a**) dMSN-hM4Di (**b**) dMSN-hM3Dq (**c**) iMSN-hM3Dq, (**d**) iMSN-hM4Di

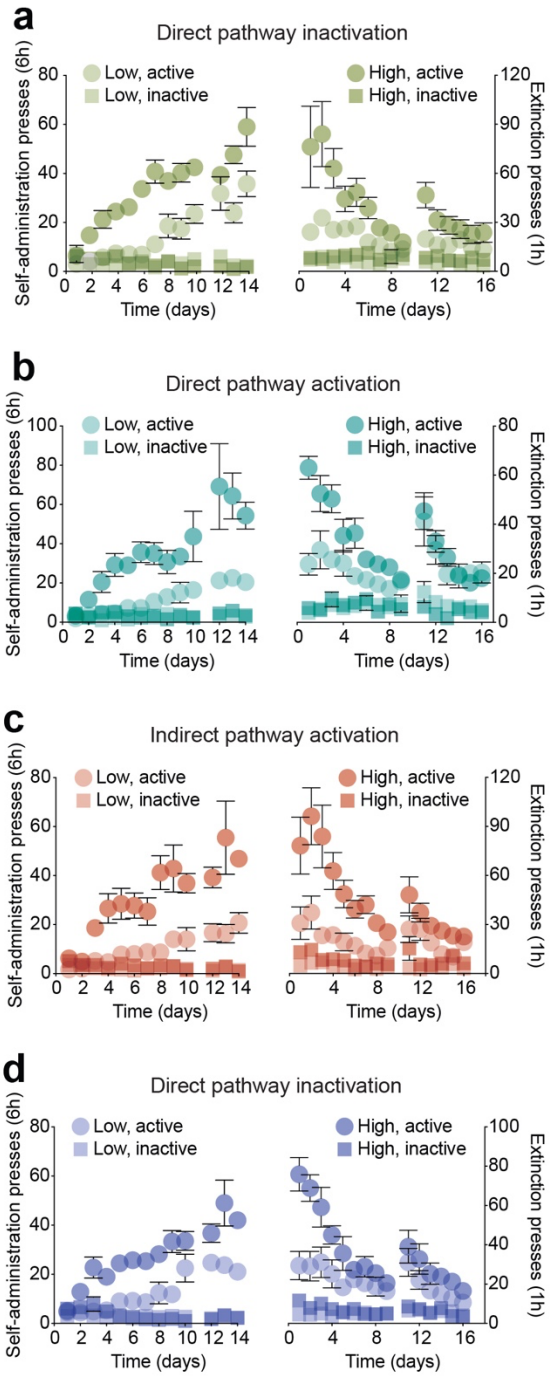

Figure S2.2 | DREADD activation has no effect on inactive lever pressing. Administration of CNO has no effect on inactive lever pressing during progressive ratio (left) or cue-induced reinstatement (right). (**a**) dMSN-hM4Di (**b**) dMSN-hM3Dq (**c**) iMSN-hM3Dq, (**d**) iMSN-hM4Di

It is worth noting that recent reports have shown that CNO activates DREADDs *in vivo* via retro-conversion to clozapine, an atypical antipsychotic with diverse pharmacology[27]. Importantly, while high doses of CNO are capable of having off-target behavioral effects[27,57], the dose of CNO used in these studies was chosen based on previous work in our lab and others showing no behavioral effects in control rats[19,36,58–67]. Moreover, in the present study, the behavioral effects of CNO were both severity- (high-risk but not low-risk) and behavior- (relapse but not motivation) dependent, and CNO treatment had no effect on inactive lever pressing in PR or reinstatement tests (**Figure S2.2**). Finally, CNO treatment had no effect on the

motivation to self-administer heroin or cue-induced reinstatement of heroin-seeking in high- or low-risk rats that were run in parallel to experimental rats but lacked DREADD expression (viral "miss" groups; **Figure 2.6**). Although the sample size of these viral "miss" groups is relatively small, the difference between low- and high-risk rats in behaviors contributing to the severity score was comparable to that from the groups expressing DREADDs (**Figures 2.4, 2.5**). Thus, it is unlikely that our observed effects on reinstatement in high-risk rats are due to non-DREADD mediated effects.

CONCLUSIONS

In summary, these data support a critical – and opposing – role for the direct and indirect pathways of the NAc in driving cue-induced reinstatement of heroin-seeking in high-risk rats. Interestingly, altering NAc output was unable to change reinstatement in low-risk rats, suggesting that NAc regulation of drug-seeking may be dependent on the strength of the associations that are formed between drugs and cues. Future work will investigate the role of discrete projections to the NAc (e.g., PrL, IL) in vulnerability to drug-seeking, since these projections are thought to regulate the consolidation of cue/drug relationships during initial drug use[45,47,68].

ACKNOWLEDGEMENTS

We thank Dr. John Neumaier and Dr. Michelle Kelly for providing the CAV2-Cre virus for this work, Dr. Scott Ng-Evans for designing MED-PC programs, and Jordyn Richardson and Grayson Baden for assistance with tissue sectioning and immunohistochemistry. This work was supported by grants from the National Institute on Drug Abuse (F31DA047012 to TJO, R01DA036582 to SMF) and the National Institute of Neurological Disorders (T32NS99578 to TJO).

REFERENCES

1. Calabresi, P., Picconi, B., Tozzi, A., Ghiglieri, V. & Di Filippo, M. Direct and indirect pathways of basal ganglia: A critical reappraisal. *Nature Neuroscience* (2014). doi:10.1038/nn.3743
2. Gerfen, C. R. & Surmeier, D. J. Modulation of Striatal Projection Systems by Dopamine. *Annu. Rev. Neurosci.* (2011). doi:10.1146/annurev-neuro-061010-113641
3. Peters, J. & De Vries, T. J. Glutamate mechanisms underlying opiate memories. *Cold Spring Harb. Perspect. Med.* (2012). doi:10.1101/cshperspect.a012088
4. LaLumiere, R. T. & Kalivas, P. W. Glutamate Release in the Nucleus Accumbens Core Is Necessary for Heroin Seeking. *J. Neurosci.* (2008). doi:10.1523/jneurosci.5129-07.2008
5. Suto, N., Wise, R. A. & Vezina, P. Dorsal as well as ventral striatal lesions affect levels of intravenous cocaine and morphine self-administration in rats. *Neurosci. Lett.* (2011). doi:10.1016/j.neulet.2011.02.011
6. Dworkin, S. I., Guerin, G. F., Goeders, N. E. & Smith, J. E. Kainic acid lesions of the nucleus accumbens selectively attenuate morphine self-administration. *Pharmacol. Biochem. Behav.* (1988). doi:10.1016/0091-3057(88)90292-4
7. Alderson, H. L., Parkinson, J. A., Robbins, T. W. & Everitt, B. J. The effects of excitotoxic lesions of the nucleus accumbens core or shell regions on intravenous heroin self-administration in rats. *Psychopharmacology (Berl).* (2001). doi:10.1007/s002130000634
8. Bossert, J. M., Gray, S. M., Lu, L. & Shaham, Y. Activation of group II metabotropic glutamate receptors in the nucleus accumbens shell attenuates context-induced relapse to heroin seeking. *Neuropsychopharmacology* (2006). doi:10.1038/sj.npp.1300977
9. Burke, D. A., Rotstein, H. G. & Alvarez, V. A. Striatal Local Circuitry: A New Framework for Lateral Inhibition. *Neuron* (2017). doi:10.1016/j.neuron.2017.09.019
10. Kravitz, A. V. *et al.* Regulation of parkinsonian motor behaviours by optogenetic control of basal ganglia circuitry. *Nature* (2010). doi:10.1038/nature09159
11. Vowles, K. E. *et al.* Rates of opioid misuse, abuse, and addiction in chronic pain. *Pain* (2015). doi:10.1097/01.j.pain.0000460357.01998.f1
12. Deroche-Gamonet, V., Belin, D. & Piazza, P. V. Evidence for addiction-like behavior in the rat. *Science (80-.).* (2004). doi:10.1126/science.1099020
13. Zimmer, B. A., Oleson, E. B. & Roberts, D. C. S. The motivation to self-administer is increased after a history of spiking brain levels of cocaine. *Neuropsychopharmacology* (2012). doi:10.1038/npp.2012.37
14. Allain, F., Minogianis, E. A., Roberts, D. C. S. & Samaha, A. N. How fast and how often: The pharmacokinetics of drug use are decisive in addiction. *Neuroscience and Biobehavioral Reviews* (2015). doi:10.1016/j.neubiorev.2015.06.012

15. American Psychiatric Association. *Diagnostic and statistical manual of mental disorders : DSM-5. American Psychiatric Association*. *DSM* (2014). doi:10.1176/appi.books.9780890425596.744053
16. Rogan, S. C. & Roth, B. L. Remote control of neuronal signaling. *Pharmacol. Rev.* (2011). doi:10.1124/pr.110.003020
17. Roth, B. L. DREADDs for Neuroscientists. *Neuron* (2016). doi:10.1016/j.neuron.2016.01.040
18. Kremer, E. J., Boutin, S., Chillon, M. & Danos, O. Canine Adenovirus Vectors: an Alternative for Adenovirus-Mediated Gene Transfer. *J. Virol.* (2009). doi:10.1128/jvi.74.1.505-512.2000
19. Yager, L. M., Garcia, A. F., Donckels, E. A. & Ferguson, S. M. Chemogenetic inhibition of direct pathway striatal neurons normalizes pathological, cue-induced reinstatement of drug-seeking in rats. *Addict. Biol.* (2019). doi:10.1111/adb.12594
20. Paxinos, G., Watson, C. R. R. & Emson, P. C. AChE-stained horizontal sections of the rat brain in stereotaxic coordinates. *J. Neurosci. Methods* (1980). doi:10.1016/0165-0270(80)90021-7
21. Gottås, A. *et al.* Levels of heroin and its metabolites in blood and brain extracellular fluid after i.v. heroin administration to freely moving rats. *Br. J. Pharmacol.* (2013). doi:10.1111/bph.12305
22. Bock, R. *et al.* Strengthening the accumbal indirect pathway promotes resilience to compulsive cocaine use. *Nat. Neurosci.* (2013). doi:10.1038/nn.3369
23. Ferguson, S. M., Norton, C. S., Watson, S. J., Akil, H. & Robinson, T. E. Amphetamine-evoked c-fos mRNA expression in the caudate-putamen: The effects of DA and NMDA receptor antagonists vary as a function of neuronal phenotype and environmental context. *J. Neurochem.* (2003). doi:10.1046/j.1471-4159.2003.01815.x
24. Guettier, J. M. *et al.* A chemical-genetic approach to study G protein regulation of β cell function in vivo. *Proc. Natl. Acad. Sci. U. S. A.* (2009). doi:10.1073/pnas.0906593106
25. Jain, S. *et al.* Chronic activation of a designer Gq-coupled receptor improves β cell function. *J. Clin. Invest.* (2013). doi:10.1172/JCI66432
26. Pardo-Garcia, T. R. *et al.* Ventral pallidum is the primary target for accumbens D1 projections driving cocaine seeking. *J. Neurosci.* (2019). doi:10.1523/JNEUROSCI.2822-18.2018
27. Gomez, J. L. *et al.* Chemogenetics revealed: DREADD occupancy and activation via converted clozapine. *Science (80-.).* (2017). doi:10.1126/science.aan2475
28. Bossert, J. M., Poles, G. C., Wihbey, K. A., Koya, E. & Shaham, Y. Differential Effects of Blockade of Dopamine D1-Family Receptors in Nucleus Accumbens Core or Shell on Reinstatement of Heroin Seeking Induced by Contextual and Discrete Cues. *J. Neurosci.* (2007). doi:10.1523/jneurosci.3926-07.2007
29. Yee, J. *et al.* Muscarinic acetylcholine receptors in the nucleus accumbens core and shell contribute to cocaine priming-induced reinstatement of drug seeking. *Eur. J. Pharmacol.* (2011).

doi:10.1016/j.ejphar.2010.10.045

30. Stefanik, M. T. *et al.* Optogenetic inhibition of cocaine seeking in rats. *Addict. Biol.* (2013). doi:10.1111/j.1369-1600.2012.00479.x
31. Heinsbroek, J. A. *et al.* Loss of Plasticity in the D2-Accumbens Pallidal Pathway Promotes Cocaine Seeking. *J. Neurosci.* (2017). doi:10.1523/JNEUROSCI.2659-16.2016
32. Guercio, L. A., Schmidt, H. D. & Pierce, R. C. Deep brain stimulation of the nucleus accumbens shell attenuates cue-induced reinstatement of both cocaine and sucrose seeking in rats. *Behav. Brain Res.* (2015). doi:10.1016/j.bbr.2014.12.025
33. Rocha, A. & Kalivas, P. W. Role of the prefrontal cortex and nucleus accumbens in reinstating methamphetamine seeking. *Eur. J. Neurosci.* (2010). doi:10.1111/j.1460-9568.2010.07134.x
34. Perry, C. J. & McNally, G. P. μ-Opioid receptors in the nucleus accumbens shell mediate context-induced reinstatement (renewal) but not primed reinstatement of extinguished alcohol seeking. *Behav. Neurosci.* (2013). doi:10.1037/a0032981
35. Guy, E. G., Choi, E. & Pratt, W. E. Nucleus accumbens dopamine and mu-opioid receptors modulate the reinstatement of food-seeking behavior by food-associated cues. *Behav. Brain Res.* (2011). doi:10.1016/j.bbr.2011.01.024
36. Ferguson, S. M. *et al.* Transient neuronal inhibition reveals opposing roles of indirect and direct pathways in sensitization. *Nat. Neurosci.* (2011). doi:10.1038/nn.2703
37. Lobo, M. K. *et al.* Cell type - Specific loss of BDNF signaling mimics optogenetic control of cocaine reward. *Science (80-.).* (2010). doi:10.1126/science.1188472
38. Barrett, A. C., Miller, J. R., Dohrmann, J. M. & Caine, S. B. Effects of dopamine indirect agonists and selective D1-like and D2-like agonists and antagonists on cocaine self-administration and food maintained responding in rats. *Neuropharmacology* (2004). doi:10.1016/j.neuropharm.2004.07.007
39. Caine, S. B., Negus, S. S., Mello, N. K. & Bergman, J. Effects of dopamine D(1-like) and D(2-like) agonists in rats that self-administer cocaine. *J. Pharmacol. Exp. Ther.* (1999).
40. Caine, S. B., Negus, S. S. & Mello, N. K. Effects of dopamine D(1-like) and D(2-like) agonists on cocaine self- administration in rhesus monkeys: Rapid assessment of cocaine dose-effect functions. *Psychopharmacology (Berl).* (2000). doi:10.1007/s002130050023
41. Crummy, E. A., Donckels, E. A., Baskin, B. M., Bentzley, B. S. & Ferguson, S. M. The impact of cocaine and heroin drug history on motivation and cue sensitivity in a rat model of polydrug abuse. *Psychopharmacology (Berl).* (2019). doi:10.1007/s00213-019-05349-2
42. Uslaner, J. *et al.* Amphetamine and cocaine induce different patterns of c-fos mRNA expression in the striatum and subthalamic nucleus depending on environmental context. *Eur. J. Neurosci.* (2001). doi:10.1046/j.0953-816X.2001.01574.x

43. Ferguson, S. M., Thomas, M. J. & Robinson, T. E. Morphine-induced c-fos mRNA expression in striatofugal circuits: Modulation by dose, environmental context, and drug history. *Neuropsychopharmacology* (2004). doi:10.1038/sj.npp.1300465
44. Rubio, F. J. *et al.* Prelimbic cortex is a common brain area activated during cue-induced reinstatement of cocaine and heroin seeking in a polydrug self-administration rat model. *Eur. J. Neurosci.* (2019). doi:10.1111/ejn.14203
45. McGlinchey, E. M., James, M. H., Mahler, S. V., Pantazis, C. & Aston-Jones, G. Prelimbic to Accumbens Core Pathway Is Recruited in a Dopamine-Dependent Manner to Drive Cued Reinstatement of Cocaine Seeking. *J. Neurosci.* (2016). doi:10.1523/jneurosci.1291-15.2016
46. Augur, I. F., Wyckoff, A. R., Aston-Jones, G., Kalivas, P. W. & Peters, J. Chemogenetic Activation of an Extinction Neural Circuit Reduces Cue-Induced Reinstatement of Cocaine Seeking. *J. Neurosci.* (2016). doi:10.1523/jneurosci.0773-16.2016
47. Reiner, D. J., Fredriksson, I., Lofaro, O. M., Bossert, J. M. & Shaham, Y. Relapse to opioid seeking in rat models: behavior, pharmacology and circuits. *Neuropsychopharmacology* (2019). doi:10.1038/s41386-018-0234-2
48. Rogers, J. L., Ghee, S. & See, R. E. The neural circuitry underlying reinstatement of heroin-seeking behavior in an animal model of relapse. *Neuroscience* (2008). doi:10.1016/j.neuroscience.2007.10.012
49. Bossert, J. M. *et al.* Role of projections from ventral medial prefrontal cortex to nucleus accumbens shell in context-induced reinstatement of heroin seeking. *J. Neurosci.* (2012). doi:10.1523/JNEUROSCI.0005-12.2012
50. Kufahl, P. R., Pentkowski, N. S., Heintzelman, K. & Neisewander, J. L. Cocaine-induced Fos expression is detectable in the frontal cortex and striatum of rats under isoflurane but not α-chloralose anesthesia: Implications for FMRI. *J. Neurosci. Methods* (2009). doi:10.1016/j.jneumeth.2009.05.012
51. Mahler, S. V. & Aston-Jones, G. S. Fos activation of selective afferents to ventral tegmental area during cue-induced reinstatement of cocaine seeking in rats. *J. Neurosci.* (2012). doi:10.1523/JNEUROSCI.2277-12.2012
52. Dayas, C. V., Liu, X., Simms, J. A. & Weiss, F. Distinct Patterns of Neural Activation Associated with Ethanol Seeking: Effects of Naltrexone. *Biol. Psychiatry* (2007). doi:10.1016/j.biopsych.2006.07.034
53. Zhao, Y. *et al.* Activation of group II metabotropic glutamate receptors attenuates both stress and cue-induced ethanol-seeking and modulates c-fos expression in the hippocampus and amygdala. *J. Neurosci.* (2006). doi:10.1523/JNEUROSCI.2384-06.2006
54. Lin, P. & Pratt, W. E. Inactivation of the nucleus accumbens core or medial shell attenuates reinstatement of sugar-seeking behavior following sugar priming or exposure to food-associated cues. *PLoS One* (2014). doi:10.1371/journal.pone.0099301

55. Chen, W. *et al.* Activation of AMPA receptor in the infralimbic cortex facilitates extinction and attenuates the heroin-seeking behavior in rats. *Neurosci. Lett.* (2016). doi:10.1016/j.neulet.2015.11.024
56. Liu, Z., Zhang, J. J., Liu, X. D. & Yu, L. C. Inhibition of CaMKII activity in the nucleus accumbens shell blocks the reinstatement of morphine-seeking behavior in rats. *Neurosci. Lett.* (2012). doi:10.1016/j.neulet.2012.05.003
57. MacLaren, D. *et al.* Clozapine N-Oxide Administration Produces Behavioral Effects in Long-Evans Rats: Implications for Designing DREADD Experiments. *eNeuro* **3**, (2016).
58. Mahler, S. V. *et al.* Designer receptors show role for ventral pallidum input to ventral tegmental area in cocaine seeking. *Nat. Neurosci.* (2014). doi:10.1038/nn.3664
59. Wunsch, A. M. *et al.* Chemogenetic inhibition reveals midline thalamic nuclei and thalamo-accumbens projections mediate cocaine-seeking in rats. *Eur. J. Neurosci.* (2017). doi:10.1111/ejn.13631
60. Wirtshafter, D. & Stratford, T. R. Chemogenetic inhibition of cells in the paramedian midbrain tegmentum increases locomotor activity in rats. *Brain Res.* (2016). doi:10.1016/j.brainres.2015.12.014
61. DiBenedictis, B. T., Olugbemi, A. O., Baum, M. J. & Cherry, J. A. DREADD-Induced Silencing of the Medial Olfactory Tubercle Disrupts the Preference of Female Mice for Opposite-Sex Chemosignals. *eNeuro* (2015). doi:10.1523/eneuro.0078-15.2015
62. Peñagarikano, O. *et al.* Exogenous and evoked oxytocin restores social behavior in the Cntnap2 mouse model of autism. *Sci. Transl. Med.* (2015). doi:10.1126/scitranslmed.3010257
63. Soumier, A. & Sibille, E. Opposing effects of acute versus chronic blockade of frontal cortex somatostatin-positive inhibitory neurons on behavioral emotionality in mice. *Neuropsychopharmacology* (2014). doi:10.1038/npp.2014.76
64. Zink, A. N., Bunney, P. E., Holm, A. A., Billington, C. J. & Kotz, C. M. Neuromodulation of orexin neurons reduces diet-induced adiposity. *Int. J. Obes.* (2018). doi:10.1038/ijo.2017.276
65. Sasaki, K. *et al.* Pharmacogenetic modulation of orexin neurons alters sleep/wakefulness states in mice. *PLoS One* (2011). doi:10.1371/journal.pone.0020360
66. Garner, A. R. *et al.* Generation of a synthetic memory trace. *Science (80-.).* (2012). doi:10.1126/science.1214985
67. Kerstetter, K. A. *et al.* Corticostriatal Afferents Modulate Responsiveness to Psychostimulant Drugs and Drug-Associated Stimuli. *Neuropsychopharmacology* (2016). doi:10.1038/npp.2015.253
68. Peters, J., LaLumiere, R. T. & Kalivas, P. W. Infralimbic Prefrontal Cortex Is Responsible for Inhibiting Cocaine Seeking in Extinguished Rats. *J. Neurosci.* (2008). doi:10.1523/jneurosci.1045-08.2008

CHAPTER 3

A CONDITIONED PLACE PREFERENCE TO HEROIN IS SIGNALED BY INCREASES IN DOPAMINE AND DIRECT PATHWAY ACTIVITY AND DECREASES IN INDIRECT PATHWAY ACTIVITY IN THE NUCLEUS ACCUMBENS

Timothy J. O'Neal, Mollie X. Bernstein, Susan M. Ferguson

Currently under review at *Neuropsychopharmacology*

ABSTRACT

Opioid addiction remains a public health crisis in the United States. Early drug use drives the development of conditioned reinforcement, in which the reinforcing properties of a drug becomes attributed to drug-associated stimuli, such as cues and contexts. Although only a subset of individuals who use opioids transition to addiction, whether this is due to innate differences in conditioned reinforcement is unknown. A central role for the nucleus accumbens (NAc) in encoding individual vulnerability to addiction has begun to emerge. In particular, direct and indirect pathway medium spiny neurons (dMSNs and iMSNs) of the NAc have been shown to bidirectionally regulate behavior, including motivation and drug-seeking, in animals expressing addiction-like phenotypes. However, whether intrinsic differences in the strength of dMSNs and iMSNs confers vulnerability to addiction remains unknown, and how the activity of dMSNs and iMSNs guides conditioned reinforcement is not clear. Moreover, despite a prominent role for dopamine in modulating NAc activity, its role in opioid reinforcement remains uncertain. Here, we integrate fiber photometry for *in vivo* monitoring of dopamine, dMSNs, and iMSNs with a heroin conditioned place preference (CPP) procedure that produces variability in conditioned reinforcement for heroin. We demonstrate a ramp in dopamine activity, activation of dMSNs, and inactivation in iMSNs in rats that develop a CPP to heroin, and a ramp in iMSN activity in rats that do not develop a heroin CPP. Moreover, we reveal innate differences in the relative strength of dMSNs and iMSNs between heroin CPP-sensitive and heroin CPP-resistant rats, with stronger dMSN and iMSN tone at baseline, respectively. Lastly, we show a central role for dopamine in the development and expression of a heroin CPP. Together, these data support the hypothesis that an imbalance in activity between dMSNs and iMSNs drives the development and expression of addictive behaviors.

INTRODUCTION

The U.S. Opioid Epidemic remains a major public health crisis, with relapse rates and overdose-related fatalities continuing to rise[1]. One critical mechanism underlying persistent drug-craving is conditioned drug reinforcement, which is the attribution of the reinforcing properties of a drug to a previously neutral stimulus (conditioned stimulus (CS); e.g., cues, contexts)[2]. Re-exposure to drug CS can reinstate drug-seeking following action/outcome devaluation[3] or prolonged abstinence[4]. The nucleus accumbens (NAc) integrates cortical and subcortical inputs to guide behavioral processes associated with addiction, including associative learning, decision making, and motivation[5–7]. The NAc is heterogeneous, and predominantly comprised of two interspersed populations of medium spiny neurons (MSNs): direct pathway MSNs (dMSNs) project to the ventral tegmental area (VTA) and primarily express the dopamine (DA) D1 receptor; and indirect pathway MSNs (iMSNs) project to the ventral pallidum (VP) and primarily express the DA D2 receptor. These cell populations can have opposing control over behavioral output, with dMSNs serving as a “go” signal to facilitate behavioral actions and iMSNs serving as a “stop” signal to suppress or terminate unwanted actions[8–11]. Emerging evidence has demonstrated a role for NAc dMSNs and iMSNs in encoding variability to the addictive effects of illicit drugs[12–16], yet whether intrinsic differences in MSN activity confer vulnerability to addiction is unknown.

Midbrain DA release into the NAc is central to the rewarding effects of illicit drugs[17], and phasic DA release into the NAc promotes drug-seeking[18]. In addition to slower modulation of dMSNs and iMSNs via activation of G-protein coupled D1 and D2 receptors, DA can rapidly modulate these neuronal populations via opening of IP_3 receptors and release of intracellular calcium (Ca^{2+})[19], a process that is integral for the propagation of Ca^{2+} waves and heterosynaptic plasticity in the NAc[20,21]. *In vivo* imaging of dMSN and iMSN Ca^{2+} activity has revealed a rapid increase in dMSN activity and a progressive decrease in iMSN activity after acute cocaine exposure[22], as well as a persistent attenuation of iMSN activity after chronic cocaine treatment[23]; all of which lead to a long-lasting predominance of dMSN over iMSN signaling. Moreover, a ramping of dMSN activity along with a concomitant decrease in iMSN activity has been observed in mice preceding entry into a context associated with cocaine treatment[24].

Targeted manipulations of dMSNs and iMSNs have demonstrated oppositional control over addictive behaviors[3,10,11]; however, it remains to be determined how dMSNs and iMSNs encode the acquisition of behaviors related to opioid addiction. Additionally, whether innate differences in relative dMSN and iMSN signaling strength confer vulnerability to addiction has not been studied. Thus, we combined fiber photometry for *in vivo* monitoring of dMSN and iMSN Ca^{2+} signaling, as well as NAc DA signaling, with a heroin conditioned place preference (CPP) procedure that produces variability in the reinforcing effects of heroin. Individual rats were classified based on their sensitivity to heroin conditioning, and basal and drug-evoked NAc

activity was examined in groups showing a preference or aversion to the heroin-paired chamber. Finally, we examined how temporally precise DA signaling and activity of dMSNs and iMSNs marks a preference or aversion to a context associated with heroin.

METHODS

Subjects

Outbred female and male Sprague-Dawley rats (*n* = 44; Envigo) were pair-housed in a humidity- and temperature-controlled vivarium, with *ad libitum* access to food and water throughout the experiments. Rats were acclimated to the vivarium for at least five days and handled for at least three days prior to any procedures. All procedures were done in accordance with the National Institutes of Health's Office of Laboratory Animal Welfare and were approved by the Seattle Children's Research Institute's Institutional Animal Care and Use Committee.

Drugs

Diamorphine HCl (heroin) was obtained through the Drug Supply Program of the National Institute on Drug Abuse (NIDA) and was dissolved in sterile saline (0.9%) to a concentration of 3 mg/ml and administered at a dose of 1 ml/kg. Buprenorphine was also obtained through the Drug Supply Program of NIDA and was dissolved in sterile saline (0.9%) to a concentration of 0.2 mg/ml and administered at a dose of 1 ml/kg.

Viral vectors

Adeno-associated viruses containing Flp recombinase (AAVrg-EF1a-flpo; #55637-AAVrg), Flp-dependent GCaMP6s (AAV8-EF1a-fDIO-GCaMP6s; #105714-AAV8), and Cre-dependent RCaMP1b (AAV1-Syn-FLEX-NES-jRCaMP1b-WPRE-SV40; #100850-AAV1) were acquired from Addgene and had titers of ≥1x10^{13} viral genomes/ml. dLight1.3b plasmid (AAV1-Syn-dLight1.3b) was acquired from Addgene (#135762) and prepared by the NAPE Molecular Genetics Resource Core. Canine adenovirus containing Cre recombinase (CAV2-Cre) had a titer of ~2.5x10^{9} viral genomes/μl and was prepared as previously described[25].

Stereotaxic surgery

Rats were anesthetized with isoflurane (3% induction, 1-2% maintenance; Patterson Veterinary) and given an injection of meloxicam (1 mg/ml, 1 ml/kg *sc*; Patterson Veterinary) for analgesia. Following head-fixation in a digital stereotax (Kopf Instruments), the skull was exposed and scored, and craniotomies were drilled above target nuclei. Viral vectors were loaded into 10 μl gas-tight syringes (Hamilton Company) and infused unilaterally into target nuclei (500 nl per virus, 100 nl/min). Coordinates (in mm, relative to Bregma[26]) were as follows: NAc [A/P +1.5, M/L +1.0, D/V -7.5], VP [A/P +0.2, M/L +2.0, D/V -8.0], VTA [A/P -5.3, M/L +0.8 D/V -8.3]. Syringes were left in place for an additional 5 min following infusion and slowly retracted to allow proper

diffusion of virus into target nuclei. Following viral infusion, fiber optic cannula (MFC_400/430-0.37_8mm_ZF2.5_FLT; >85% transmittance; Doric Lenses) were implanted in the NAc [D/V -7.4] and secured with skull screws, metabond (Patterson Dental), and dental cement.

Fiber photometry

Three-four weeks after surgery, fiber photometry recordings were performed using a multiplex photometry system (FP3001; Neurophotometrics). Three days prior to experimental recordings, rats were acclimated to branching fiberoptic patch cords (BFP4_400/440/LWMJ-0.37_3m_SMA*-4xFC; Doric Lenses) and biosensor expression was confirmed via brief (~5 min) home cage recordings. LEDs were heated at 100% power for >5min prior to recording to minimize heat-induced LED decay during recordings, then reduced to <50 μW for the duration of recordings (415 nm and 470 nm: ~12.5 μW; 560 nm: ~25 μW). Photometry recordings with a single biosensor (dLight imaging) used 2-phase cycling of 415 nm and 470 nm LEDs, and recordings with two biosensors (dual GCaMP/RCaMP imaging) used 3-phase cycling of 415 nm, 470 nm, and 560 nm LEDs. Fluorescent signals were bandpass filtered, collimated, reflected by a dichroic mirror, and focused by a 20x objective (0.40 NA) on the sensor of a CMOS camera. Signals were imaged at ~40 Hz, collected via custom-written workflows in Bonsai, and exported for off-line analysis via custom-written Python scripts.

Conditioned place preference

CPP apparatus

Behavioral sessions were conducted in custom-built acrylic chambers (TAP Plastics) with two equally sized but visually distinct chambers (15” wide x 15” long x 12” tall) and a smaller center chamber (6” wide x 15” long x 12” tall), separated from the outer chambers via removable guillotine doors (3” wide x 12” tall). The walls of the two outer chambers were covered with visually distinct wallpapers (honeycomb and zebra, both grayscale), and the floor of the entire apparatus was matte black to facilitate behavioral tracking. USB cameras (2.1mm, wide-angle; ELP) were positioned above CPP chambers and interfaced with Bonsai for motion tracking. Video streams were greyscaled and thresholded, and binary region analysis was used to detect animal position within the CPP chambers. Chambers were cleaned between sessions with 70% ethanol (w/v).

CPP procedure

Behavioral testing included an initial preference test (15 min), eight conditioning sessions (40 min each), and a final preference test (15 min). During the preference tests, the guillotine doors were removed, and subjects were placed in the center of the neutral chamber and allowed to freely explore the full apparatus. Conditioning sessions were run twice daily, beginning at 09:00 (saline) and 13:00 (heroin). During conditioning sessions, subjects received *ip* injections of saline or heroin and were immediately confined to one of the outer chambers. Pretreatment injections were given 10 min prior to injections of saline or heroin, when appropriate. Heroin

conditioning was always paired with the initially less-preferred chamber to maximize the potential for a change in preference. All behavioral testing was done during the light cycle, due to the use of visual cues for conditioning.

Immunohistochemistry

After behavioral testing, rats were deeply anesthetized with Euthasol (2 ml/kg *ip*; 3.9 mg/ml pentobarbital sodium and 0.5 mg/ml phenytoin sodium; Patterson Veterinary) and transcardially perfused with phosphate-buffered saline (PBS; pH = 7.4) followed by paraformaldehyde (PFA; 4% in PBS). Brains were extracted, fixed overnight in 4% PFA, post-fixed for >48 h in sucrose (30% in PBS), and sectioned (50 μm) with a vibrating microtome. Floating sections were washed (PBS; 3x10 min), blocked (0.25% Triton-X, 5% normal goat serum, PBS; 120 min), and incubated with primary antibodies (0.25% Triton-X, 2.5% normal goat serum, PBS; 24h) against Fos (1:800 rabbit anti-cFos, Cell Signaling #2250; RRID:AB_2247211). Sections were then washed (PBS; 3x10 min) and incubated with secondary antibodies (0.25% Triton-X, 2.5% normal goat serum, PBS; 120 min) conjugated to AF-568 (1:500 goat-anti-rabbit; Life Technologies #A11011, RRID: AB_143157). Finally, sections were washed (PBS; 3x10min), mounted on slides, and cover-slipped with mounting medium with DAPI (Vectashield). Z-stacks along the rostral/caudal axis of the NAc (A/P +2.5 through A/P +0.7) were collected with confocal microscopy (20x; Zeiss LSM 710), and Fos^+ cells were quantified using ImageJ (V1.49; NIH) and Adobe Illustrator (CC 2020). Subjects with weak viral expression ($n = 6$) or incorrect fiber placement ($n = 2$) were excluded from all analyses.

Statistical analysis

All data was collected using custom-written workflows (Bonsai V3.5.2), processed using custom-written Python scripts (V3.7.7), and analyzed using Python and GraphPad Prism (V9.0). Transitions between chambers and cumulative time spent in each chamber were scored via Bonsai, and preference was calculated as the amount of time spent in either conditioning chamber divided by the total time spent in both conditioning chambers (i.e., heroin preference = (time in heroin-paired) / (time in heroin-paired + time in saline-paired) *100). Change in preference for each chamber and final preference were analyzed using unpaired *t*-tests or two-way repeated-measures (RM) ANOVA (group x test). Sex differences in final preference were analyzed using Chi-square and Fisher's exact test (sex x group). Fos^+ cell counts along the rostral-caudal axis of the NAc were averaged into a single value per rat and analyzed using two-way ANOVA (region x group). Photometry signals were de-interleaved and corrected for photobleaching by fitting the isosbestic signal (415 nm) with a first-order exponential decay curve that was scaled and subtracted from experimental traces[27,28]. Linearized photometry traces were then converted to z-scores ($F_n - F_{mean} / F_{SD}$) using a rolling window of 10 s centered around F_n, and events were identified where $z > 2$ ($p < .05$) with a minimum inter-event interval of 1.5 s. Processed signals were aligned to transitions between chambers, and the window centered around each transition (-3 to +3) was

extracted for analysis. Transition windows were analyzed using two-way ANOVA (group x time or chamber x time), and peak activity prior to transition was analyzed using unpaired *t*-tests, two-way ANOVA (chamber x test) or linear regressions (peak signal x preference). Photometry signals during conditioning sessions were analyzed with RM ANOVA (group x treatment). Statistical significance for all analyses was set at $p < 0.05$, all ANOVAs were followed by Sidak *post-hoc* tests, and data are shown throughout as individual subjects and/or mean ± SEM.

RESULTS

Only a subset of rats prefer the chamber associated with heroin following conditioning

Male and female rats underwent a CPP procedure that included an initial preference test, four days of conditioning (saline each morning on one side, heroin each afternoon on the other side), and a final preference test (**Figure 3.1a**). We identified notable heterogeneity in preference during the final preference test (range = 21% to 68% for the heroin-paired chamber), so all subsequent analyses categorized rats based on their final preference. Two-way RM ANOVA revealed significant group x time interactions for time spent in the heroin-paired chamber ($F_{(1,15)} = 10.57$, $p = .0054$) and saline-paired chamber ($F_{(1,15)} = 4.87$, $p = .043$), with heroin-preferring (HP; $n = 9$) and saline-preferring (SP; $n = 8$) rats significantly increasing time spent in their preferred chambers during the post-test ($p < .0001$ and $p = .003$, respectively; **Figure 3.1b-3.1c**). In addition, HP rats spent significantly more time in the heroin-paired chamber during the final preference test than SP rats (unpaired *t*-test: $t_{(15)} = 5.16$, $p = .0001$; **Figure 3.1d**). No sex differences were identified in the probability of classification into either preference phenotype ($\chi^2_{(1, 17)} = 0.05$, $p > .99$), so all subsequent analyses combined both sexes. To assess the role of NAc signaling in the acquisition and expression of a heroin CPP, a separate group of rats received a pretreatment of buprenorphine (0.2 mg/kg) or vehicle prior to each conditioning session (**Figure 3.1e**). Two-way RM ANOVA revealed a significant pretreatment x time interaction for time spent in the heroin-paired chamber ($F_{(1,14)} = 5.10$, $p = .040$) but not the saline-paired chamber ($F_{(1,14)} = 0.46$, $p = .51$), with only vehicle-pretreated rats developing a significant preference for the heroin-paired chamber ($p = .0031$; **Figure 3.1f-3.1g**). In addition, rats pretreated with vehicle and buprenorphine significantly differed in their final preference for the heroin-paired chamber (unpaired *t*-test: $t_{(14)} = 3.84$, $p = .0018$; **Figure 3.1h**), with buprenorphine pretreatment preventing the development of heroin preference. After the final preference test, rats were perfused and activation of the NAc was assessed via Fos immunohistochemistry (**Figure 3.1i-3.1j**). Pretreatment with buprenorphine significantly attenuated the amount of neuronal activation in both the NAc shell and the NAc core (two-way ANOVA, main effect of group: $F_{(1,28)} = 52.25$, $p < .0001$) during the final preference test (**Figure 3.1k**), and activation of both subregions significantly correlated with final preference for the heroin-paired chamber (linear regressions: shell, $r^2 = .50$, $p = .0023$; core, $r^2 = .38$, $p = .011$; **Figure 3.1l-3.1m**).

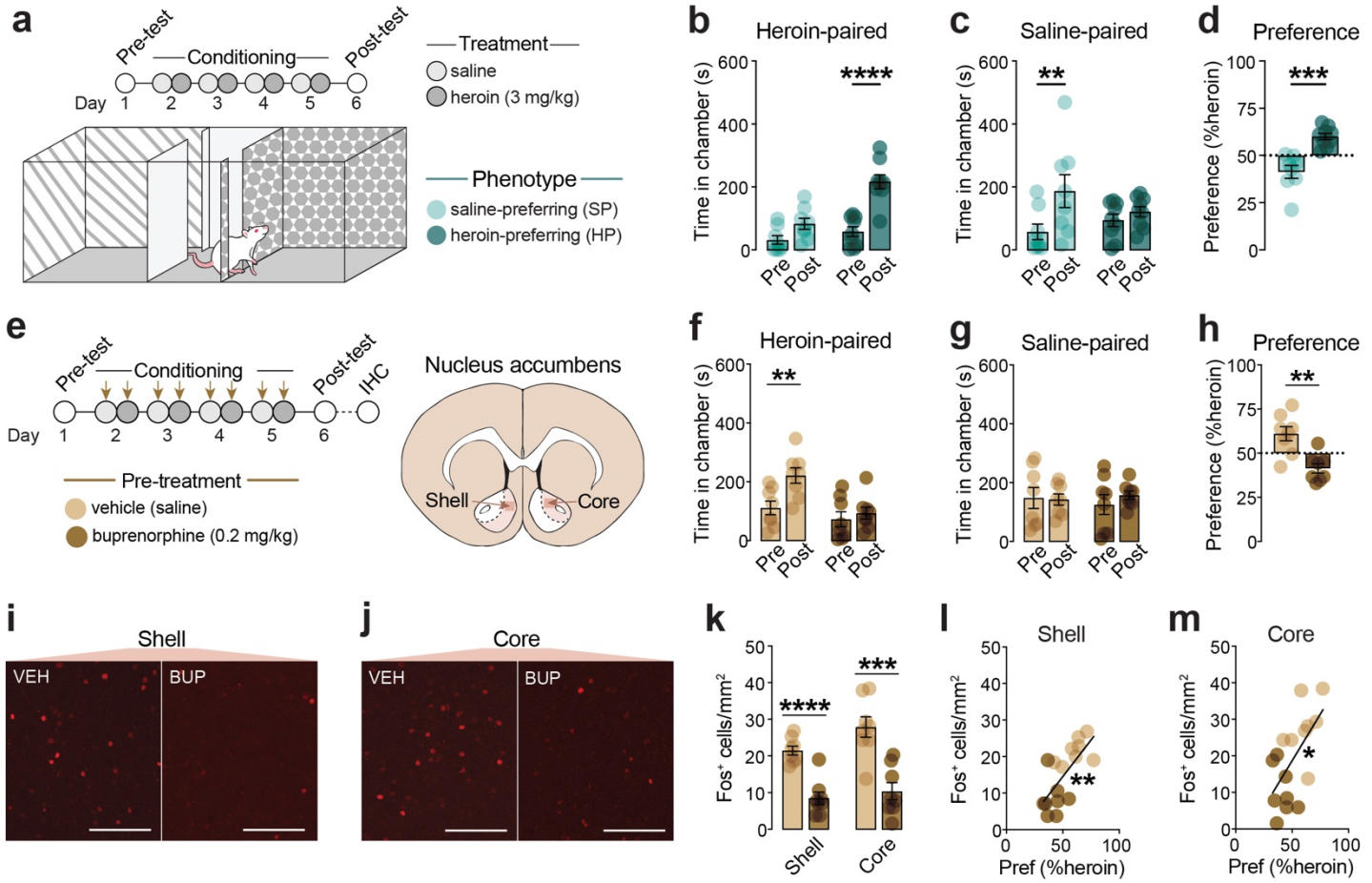

Figure 3.1 | Heroin CPP produces variable heroin preference that is blocked by buprenorphine. (**a**) Timeline of CPP procedure. Testing included an initial preference test (15 min), four days of conditioning (40 min each, 2x/day), and a final preference test (15 min). Rats were classified as saline-preferring (SP) or heroin-preferring (HP) based on final preference. (**b-c**) HP and SP rats significantly increased time spent in their preferred chambers during the post-test. (**d**) HP rats spent significantly more time in the heroin-paired chamber during the post-test than SP rats. (**e**) Timeline of buprenorphine experiment. Rats received *ip* injections of either vehicle (VEH; saline) or buprenorphine (BUP; 0.2 mg/kg) 10 min prior to each conditioning session and were perfused for Fos immunohistochemistry (IHC) after the final preference test. (**f-g**) VEH-treated rats spent significantly more time in the heroin-paired chamber during the post-test, while BUP-treated rats had no change in time spent in either chamber. (**h**) VEH-treated rats spent significantly more time in the heroin-paired chamber than BUP-treated rats. (**i-j**) Representative images of Fos staining in the NAc shell and NAc core. (**k**) BUP-pretreated rats had significantly weaker activation of the NAc shell and core than VEH-pretreated rats. (**l-m**) NAc shell and NAc core activation significantly correlated with final heroin preference. n = 8-9/group; scale bar = 0.1 mm; $^{**}p < .01$, $^{***}p < .001$, $^{****}p < .0001$

In vivo imaging of DA activity and MSN calcium activity in the NAc

In order to better understand the roles of DA and Ca^{2+} activity in the NAc in the development and expression of a heroin CPP, we next sought to monitor real-time activity dynamics over the course of the CPP procedure. To image DA activity, rats received an infusion of the dopamine sensor dLight1.3b into the NAc[29]. dLight1.3b was robustly expressed throughout the NAc, but imaging was restricted to the tip of the fiber optic in the NAc medial shell (**Figure 3.2a-3.2c**). To simultaneously image activity of dMSNs and iMSNs, a combinatorial viral approach was used to selectively target each population[12]. Rats received an infusion of different retrogradely transported recombinases into the VTA (AAVrg-flpo to target dMSNs) and VP (CAV2-Cre to target iMSNs)

along with an infusion into the NAc of a mixture of a green-shifted Ca^{2+} indicator (AAV8-fDIO-GCaMP6s) and a red-shifted Ca^{2+} indicator (AAV1-DIO-RCaMP1b). During periods of heightened neuronal activity, Ca^{2+} ions flow into dendritic spines and trigger intracellular signaling cascades, and the use of genetically-encoded Ca^{2+} indicators can be used as a proxy for neuronal signaling[30,31]. Both GCaMP6s and RcaMP1b were robustly expressed throughout the NAc, but imaging was restricted to the tip of the fiber in the NAc medial shell (**Figure 3.2d-3.2f**). Notably, GCaMP6s and RcaMP1b events occasionally occurred in tandem, similar to synchronous firing of dorsal striatal MSNs[11], but more often occurred in opposition (i.e., concomitant activation of one sensor and inactivation of the other).

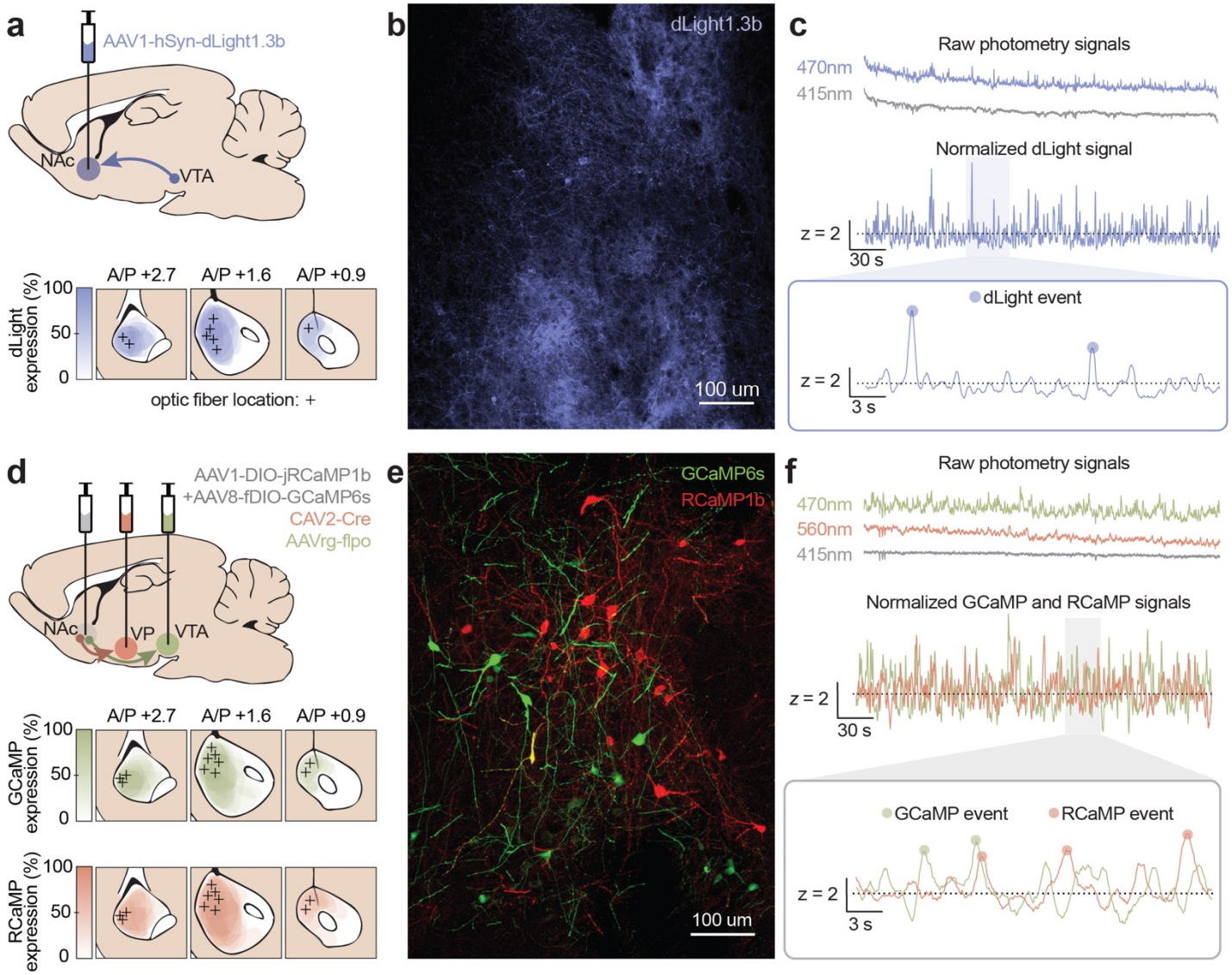

Figure 3.2 | Targeting, expression, and signal processing of DA and calcium biosensors. (**a**) Viral strategy for dLight1.3b expression in the NAc. (**b**) Representative dLight1.3b expression in the NAc. (**c**) dLight1.3b signal processing. *Top*: raw dLight1.3b (470 nm) and isosbestic (415 nm) signals; *Center*: normalized dLight1.3b signal; *Bottom*: dLight1.3b event detection. (**d**) Viral strategy for dMSN-GCaMP6s and iMSN-RCaMP1b expression. (**e**) Representative viral expression in the NAc. Green: dMSNs, red: iMSNs. (**f**) GCaMP6s and RCaMP1b signal processing. *Top*: raw GCaMP6s (470 nm), RCaMP1b (560 nm), and isosbestic (415 nm) signals; *Center*: normalized GCaMP6s and RCaMP1b signals; *Bottom*: GCaMP6s and RCaMP1b event detection.

Susceptibility to a heroin CPP is associated with intrinsic differences in the balance of activity between dMSNs and iMSNs during heroin treatment

On the first day of conditioning, there were no differences in DA activity following saline versus heroin in either group (two-way RM ANOVA, no main effect of treatment: $F_{(1,5)} = 2.50$, $p = .30$) nor were there differences between HP and SP rats (two-way RM ANOVA, no main effect of group: frequency, $F_{(1,5)} = 0.007$, $p = .93$; **Figure 3.3a**). However, there was a significant treatment x group interaction on the peak amplitude of DA events (two-way RM ANOVA: $F_{(1,5)} = 13.06$, $p = .015$), with a greater heroin-evoked than saline-evoked DA signal in HP rats ($p = .034$) and a greater heroin-evoked signal in HP rats than SP rats ($p = .013$; **Figure 3.3b**). Unlike DA activity, there was a significant main effect of group on dMSN Ca^{2+} activity (two-way RM ANOVA: $F_{(1,8)} = 14.32$, $p = .005$), whereby HP rats had greater levels of dMSN activity both at baseline ($p = .013$) and after heroin ($p = .007$) compared to SP rats (**Figure 3.3c**). Nonetheless, there were no differences in dMSN Ca^{2+} activity following saline versus heroin in either group (two-way RM ANOVA, no main effect of treatment: $F_{(1,8)} = 4.55$, $p = .066$). However, there was a significant group x drug interaction on peak dMSN Ca^{2+} activity (two-way RM ANOVA: $F_{(1,8)} = 19.43$, $p = .002$), with a greater peak dMSN signal after heroin compared to saline in HP rats but not SP rats ($p = .0052$) as well as a greater peak dMSN signal after heroin in HP rats compared to SP rats ($p = .0013$; **Figure 3.3d**). Conversely, there was a significant main effect of group on iMSN Ca^{2+} activity (two-way RM ANOVA: $F_{(1,8)} = 20.53$, $p = .002$), whereby SP rats had greater levels of iMSN activity both at baseline ($p = .013$) and after heroin ($p = .002$) compared to HP rats (**Figure 3.3e**). Nonetheless, there were no differences in iMSN Ca^{2+} activity following saline versus heroin in either group (two-way RM ANOVA, no main effect of treatment: $F_{(1,8)} = 1.09$, $p = .033$). There was also a significant group x drug interaction on peak iMSN Ca^{2+} activity (two-way RM ANOVA: $F_{(1,8)} = 5.95$, $p = .041$), with a greater peak iMSN signal following heroin versus saline in SP but not HP rats ($p = .026$) as well as a greater peak iMSN signal after heroin in SP rats compared to HP rats ($p = .015$; **Figure 3.3f**). Notably, there were no significant differences between HP and SP rats in the mean event amplitude for any signal (two-way RM ANOVAs, no main effect of group: DA, $F_{(1,5)} = 0.04$, $p = .85$; dMSNs, $F_{(1,8)} = 0.25$, $p = .63$; iMSNs, $F_{(1,8)} = 0.64$, $p = .45$), nor were there any differences following saline versus heroin in either group (two-way RM ANOVAs, no main effect of treatment: DA, $F_{(1,5)} = 1.85$, $p = .23$; dMSNs, $F_{(1,8)} = 0.69$, $p = .43$; iMSNs, $F_{(1,8)} = 2.05$, $p = .19$).

On the fourth day of conditioning, there was a significant group x treatment interaction on the frequency of DA events (two-way RM ANOVA: $F_{(1,5)} = 10.77$, $p = .022$), whereby heroin increased levels of DA activity compared to saline in HP but not SP rats ($p = .019$). In addition, the frequency of heroin-induced DA events was significantly greater in HP rats compared to SP rats *(*$p = .003$; **Figure 3.3g**). However, there were no differences in the peak amplitude of DA signals following heroin versus saline (two-way RM ANOVA, no main effect of treatment: $F_{(1,5)} = 0.05$, $p = .83$), nor were there differences in the peak amplitude of DA signals between HP and SP rats (two-way RM ANOVA, no main effect of group: $F_{(1,5)} = 0.09$, $p = .77$; **Figure 3.3h**).

Similar to the first day of conditioning, there was a significant main effect of group on dMSN Ca^{2+} activity (two-way RM ANOVA: $F_{(1,8)} = 16.81$, $p = .003$), with greater levels of dMSN activity in HP rats after saline ($p = .019$) and heroin ($p = .045$) compared to SP rats (**Figure 3.3i**). Nonetheless, there were no differences in dMSN Ca^{2+} activity following saline versus heroin in either group (two-way RM ANOVA, no main effect of treatment: $F_{(1,8)} = 2.69$, $p = .14$). In addition, there was no significant difference in the peak amplitude of dMSN events between HP and SP rats (two-way RM ANOVA, no main effect of group: $F_{(1,8)} = 0.06$, $p = .81$) nor were there differences in the peak amplitude of dMSN events following saline versus heroin in either group (two-way RM ANOVA, no main effect of treatment: $F_{(1,8)} = 0.33$, $p = .58$; **Figure 3.3j**). In contrast to the changes in dMSN activity, there was a significant main effect of group on iMSN Ca^{2+} activity (two-way RM ANOVA: $F_{(1,8)} = 13.21$, $p = .007$), with greater levels of iMSN activity in SP rats after saline ($p = .019$) and heroin ($p = .003$) compared to HP rats (**Figure 3.3k**). However, there were no differences in iMSN Ca^{2+} activity following saline versus heroin in either group (two-way RM ANOVA, no main effect of treatment: $F_{(1,8)} = 0.08$, $p = .79$). In addition, there were no significant differences in the peak amplitude of iMSN events between HP and SP rats (two-way RM ANOVA, no main effect of group: $F_{(1,8)} = 2.36$, $p = .16$), and there were no differences in the peak amplitude of iMSN events following saline versus heroin in either group (two-way RM ANOVA, no main effect of treatment: $F_{(1,8)} =$

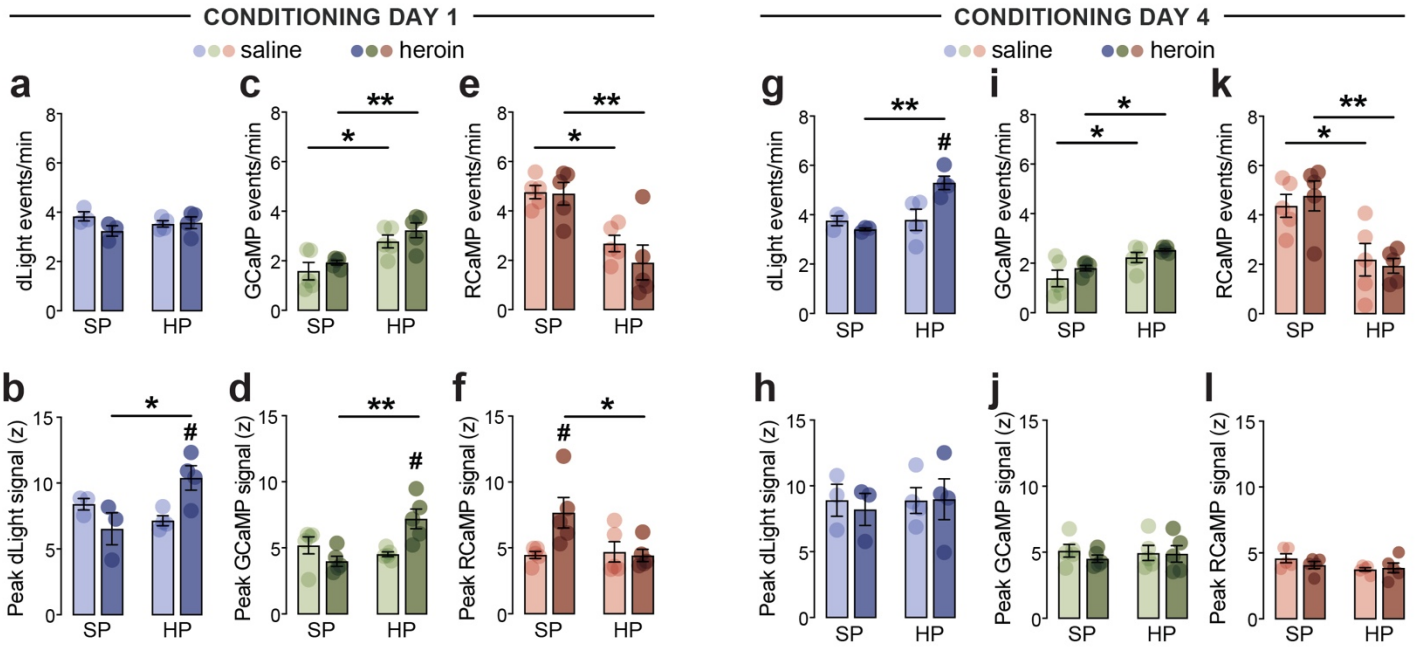

Figure 3.3 | HP rats and SP rats have basal and heroin-evoked differences in NAc activity. (**a-f**) Frequency and peak amplitude of NAc signals on the first day of conditioning. (**a-b**) The frequency of DA signals was similar for SP and HP rats, but heroin evoked a significantly greater peak DA signal in HP rats. (**c-d**) The frequency of dMSN signals was significantly greater for HP rats than SP rats after saline and heroin, and heroin evoked a significantly greater peak dMSN signal in HP rats. (**e-f**) The frequency of iMSN signals was significantly greater for SP rats than HP rats after saline and heroin, and heroin evoked a significantly greater peak iMSN signal in SP rats. (**g-l**) Frequency and peak amplitude of NAc signals on the fourth day of conditioning. (**g-h**) The frequency of DA signals was significantly greater for HP rats after heroin, but the peak DA signal was similar after both treatments. (**i-j**) The frequency of dMSN signals was significantly greater for HP rats than SP rats after saline and heroin, but the peak dMSN signal was similar after both treatments. (**k-l**) The frequency of iMSN signals was significantly greater for SP rats than HP rats after saline and heroin, but the peak iMSN signal was similar after both treatments. *$p < .05$ (SP vs HP), **$p < .01$(SP vs HP), #$p < .05$ (saline vs heroin)

0.66, $p = .44$; **Figure 3.3l**). Similar to the first day of conditioning, there were no significant differences between HP and SP rats in the mean event amplitude for any signal (two-way RM ANOVAs, no main effect of group: DA, $F_{(1,5)} = 0.05$, $p = .84$; dMSN, $F_{(1,8)} = 0.05$, $p = .83$; iMSN, $F_{(1,8)} = 0.19$, $p = .67$), nor were there any differences following saline versus heroin in either group (two-way RM ANOVAs, no main effect of treatment: DA, $F_{(1,5)} = .17$, $p = .70$; dMSN, $F_{(1,8)} = 0.85$, $p = .38$; iMSN, $F_{(1,8)} = 0.02$, $p = .90$).

Amplified DA and dMSN activity and decreased iMSN activity accompany a heroin CPP

Prior to any conditioning, there were no differences in DA activity, dMSN activity, or iMSN activity between HP and SP rats when initially exploring the CPP apparatus (unpaired *t*-tests: $t < 0.75$, $p > .49$; **Figure S3.1**). During the final preference test, however, HP rats developed a strong motivational signal that preceded entry into the heroin-paired chamber. A two-way RM ANOVA revealed a significant test x chamber interaction on peak DA signaling for HP rats ($F_{(1,3)} = 15.38$, $p = .03$), with an increase in peak DA signaling when entering the heroin-paired chamber ($p = .045$; **Figure 3.4a**). Conversely, there was no difference in peak DA signaling for SP rats (two-way RM ANOVA, no main effect of test: $F_{(1,2)} = 0.16$, $p = .72$; **Figure 3.4b**). Unlike DA activity, however, two-way RM ANOVAs found significant test x chamber interactions on peak dMSN Ca^{2+} activity for both HP rats ($F_{(1,4)} = 20.82$, $p = .01$) and SP rats ($F_{(1,4)} = 7.96$, $p = .047$), with a significant increase in peak dMSN signaling for HP rats entering the heroin-paired chamber ($p = .040$; **Figure 3.4c**) and a near-significant increase for SP rats entering the saline-paired chamber ($p = .052$; **Figure 3.4d**). Interestingly, there was a significant main effect of test on peak iMSN Ca^{2+} activity for HP rats (two-way RM ANOVA: $F_{(1,4)} = 85.64$, $p = .0008$), with significantly weaker iMSN signaling when entering the heroin-paired chamber ($p = .046$; **Figure 3.4e**). Additionally, there was a significant test x chamber interaction on peak iMSN Ca^{2+} activity for SP rats (two-way RM ANOVA: $F_{(1,4)} = 15.35$, $p = .017$), with significantly greater iMSN signaling when entering the heroin-paired chamber ($p = .019$; **Figure 3.4f**).

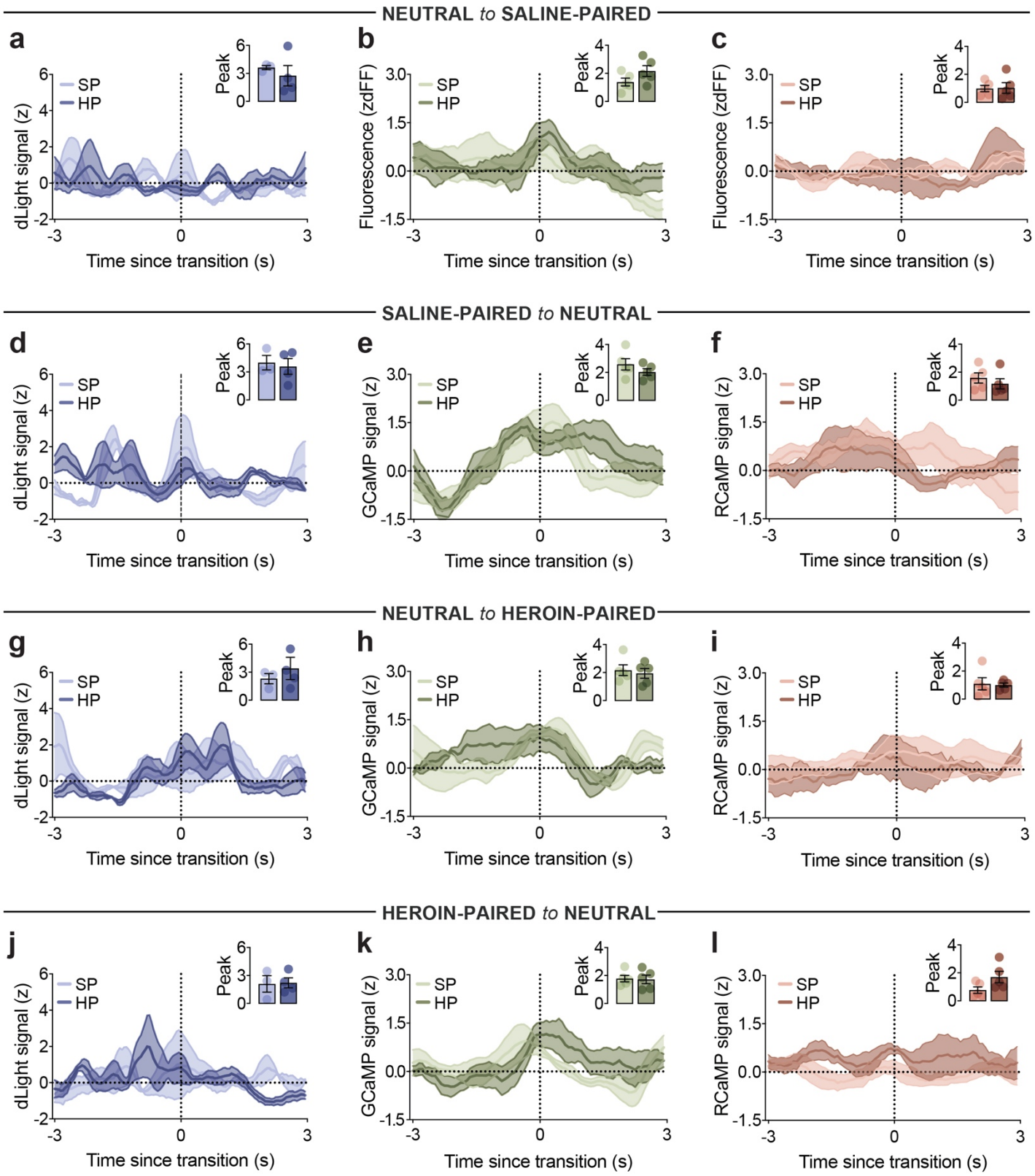

Figure S3.1 | **HP and SP rats have similar patterns of NAc activity prior to conditioning.** DA, dMSN, and iMSN signals during transitions from (**a-c**) the neutral chamber to the saline-paired chamber, (**d-f**) the saline-paired chamber back to the neutral chamber, (**g-i**) the neutral chamber to the heroin-paired chamber, and (**j-l**) the heroin-paired chamber back to the neutral chamber. Insets: peak signals during transitions. DA signals, dMSN signals, and iMSN signals were similar for HP and SP rats during all transitions prior to any conditioning.

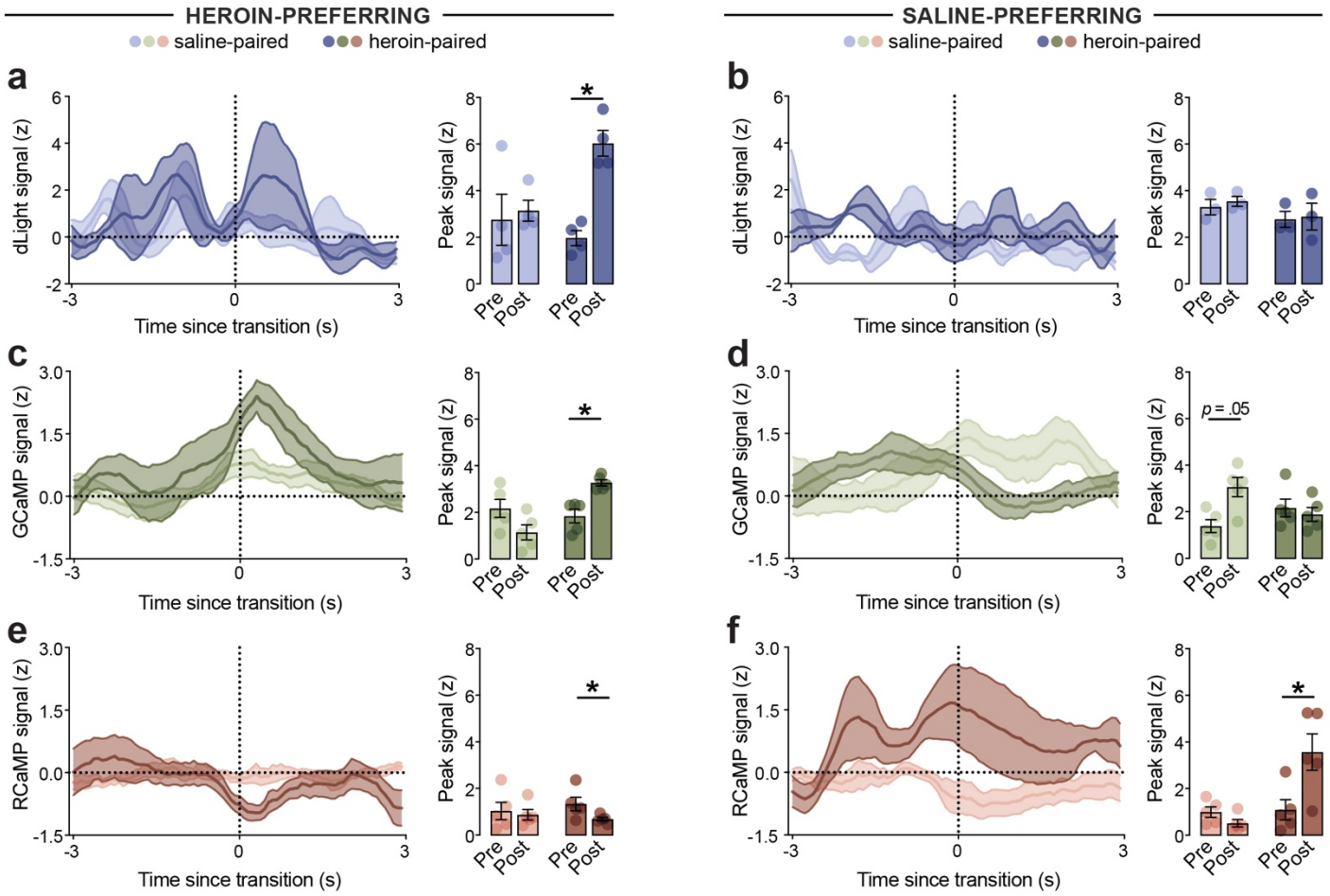

Figure 3.4 | **Enhanced DA and dMSN signals and weakened iMSN signals accompany a heroin CPP.** (**a**) HP rats had a significant increase in peak DA when entering the heroin-paired chamber in the final preference test. (**b**) Peak DA signals were unchanged for SP rats for both chambers during the final preference test. (**c**) HP rats had a significant increase in peak dMSN activity when entering the heroin-paired chamber during the final preference test. (**d**) SP rats had a near-significant increase in peak dMSN activity when entering the saline-paired chamber during the final preference test. (**e**) HP rats had a non-significant reduction in peak iMSN activity when entering the heroin-paired chamber during the final preference test. (**f**) SP rats had a significant increase in peak iMSN signal when entering the heroin-paired chamber during the final preference test. n = 3-5/group; *$p < .05$

Heroin conditioning enhances DA and dMSN activity in HP rats, but enhances iMSN activity in SP rats

Given the differential activity patterns for HP and SP rats entering their preferred side during the final preference test, we next sought to examine differences between groups during transitions into the same chamber. When entering the heroin-paired chamber, the peak pre- to post-test DA signal was significantly greater in HP rats compared to SP rats (unpaired t-test: $t_{(5)} = 3.14$, $p = .026$), and the peak DA signal preceding entry was significantly and positively correlated with final heroin preference (linear regression: $r^2 = .73$, $p = .014$; **Figure 3.5a**). Similarly, HP rats had a significantly greater increase in peak pre- to post-test dMSN Ca^{2+} activity during entry than SP rats (unpaired t-test: $t_{(8)} = 2.45$, $p = .040$), and peak dMSN activity was significantly and positively correlated with final heroin preference (linear regression: $r^2 = .48$, $p = .027$; **Figure 3.5b**). Conversely, SP rats had a significantly greater increase in peak pre- to post-test iMSN Ca^{2+} activity

during entry than HP rats (unpaired *t*-test: $t_{(8)} = 2.96$, $p = .018$), and peak iMSN activity preceding entry significantly and negatively correlated with final heroin preference (linear regression: $r^2 = .45$, $p = .034$; **Figure 3.5c**). When exiting the heroin-paired chamber, the peak pre- to post-test DA signal was significantly greater in SP rats than HP rats (unpaired *t*-test: $t_{(5)} = 3.19$, $p = .024$), and peak DA activity preceding exit significantly and negatively correlated with final heroin preference (linear regression: $r^2 = .91$, $p = .0008$; **Figure 3.5d**). Similarly, the peak pre- to post-test dMSN Ca^{2+} signal preceding exit was significantly greater for SP rats than HP rats (unpaired *t*-test: $t_{(8)} = 2.64$, $p = .029$), and peak dMSN activity preceding exit significantly and negatively correlated with final heroin preference (linear regression: $r^2 = .48$, $p = .027$; **Figure 3.5e**). Interestingly, the peak pre- to post-test iMSN Ca^{2+} signal preceding exit was significantly greater for SP rats than HP rats (unpaired *t*-test: $t_{(8)} = 2.78$, $p = .024$), although peak iMSN activity preceding exit was not significantly correlated with final heroin preference (linear regression: $r^2 = .12$, $p = .32$; **Figure 3.5f**). When entering the saline-paired chamber, there was no significant difference in the peak pre- to post-test DA signal between SP and HP rats (unpaired *t*-test: $t_{(5)} = 0.85$, $p = .43$), and DA activity preceding entry was not correlated with final saline preference (linear regression: $r^2 = .05$, $p = .64$; **Figure 3.5g**). However, the peak pre- to post-test dMSN Ca^{2+} signal preceding entry was significantly greater for SP rats than HP rats (unpaired *t*-test: $t_{(8)} = 3.56$, $p = .007$), and peak dMSN activity preceding entry significantly and positively correlated with final saline preference (linear regression: $r^2 = .48$, $p = .026$; **Figure 3.5h**). Moreover, the peak pre- to post-test iMSN Ca^{2+} signal preceding entry was significantly weaker for SP rats than HP rats (unpaired *t*-test: $t_{(8)} = 3.07$, $p = .015$), though there was no significant correlation between peak iMSN activity preceding entry and final saline preference (linear regression: $r^2 = .16$, $p = .26$; **Figure 3.5i**). Finally, when exiting the saline-paired chamber there were no significant pre- to post-test differences for HP or SP rats (unpaired *t*-tests: DA, $t_{(5)} = 0.09$, $p = .93$; dMSN, $t_{(8)} = 0.47$, $p = .65$; iMSN, $t_{(8)} = 0.48$, $p = .65$), and there was no relationship between final saline preference and peak signaling (linear regressions: DA, $r^2 = .11$, $p = .48$; dMSN, $r^2 = .07$, $p = .44$; iMSN, $r^2 = .09$, $p = .39$) preceding entry (**Figure 3.5j-3.5l**).

Figure 3.5 | Entry to a preferred heroin context is accompanied by enhanced DA and dMSN signaling and weakened iMSN signaling. (**a-c**) Entry to the heroin-paired chamber in the final preference test. (**a**) HP rats had a significantly greater increase in DA signaling than SP rats that was positively correlated with heroin preference. (**b**) HP rats had a significantly greater increase in dMSN signaling than SP rats that was positively correlated with heroin preference. (**c**) SP rats had a significantly greater increase in iMSN signaling than HP rats that was inversely correlated with heroin preference. (**d-f**) Exit from the heroin-paired chamber in the final preference test. (**d**) SP rats had a significantly greater increase in DA signaling than HP rats that was inversely correlated with heroin preference. (**e**) SP rats had a significantly greater increase in dMSN signaling than HP rats that was inversely correlated with heroin preference. (**f**) SP rats had a significantly greater increase in iMSN signaling than HP rats that was uncorrelated with heroin preference. (**g-i**) Entry to the saline-paired chamber in the final preference test. (**g**) HP and SP rats had peak DA signaling that was comparable to the initial preference test and uncorrelated with saline preference. (**h**) SP rats had a significantly greater increase in dMSN signaling than HP rats that was positively correlated with saline preference. (**i**) SP rats had a significantly greater decrease in iMSN signaling than HP rats that was uncorrelated with saline. (**j-m**) Exit from to the saline-paired chamber in the final preference test. (**j**) DA signals, (**k**) dMSN signals, and (**l**) iMSN signals were comparable for both HP and SP rats, relative to the initial preference test. $n = 3$-5/group; $^*p < .05$, $^{**}p < .01$ (SP vs HP)

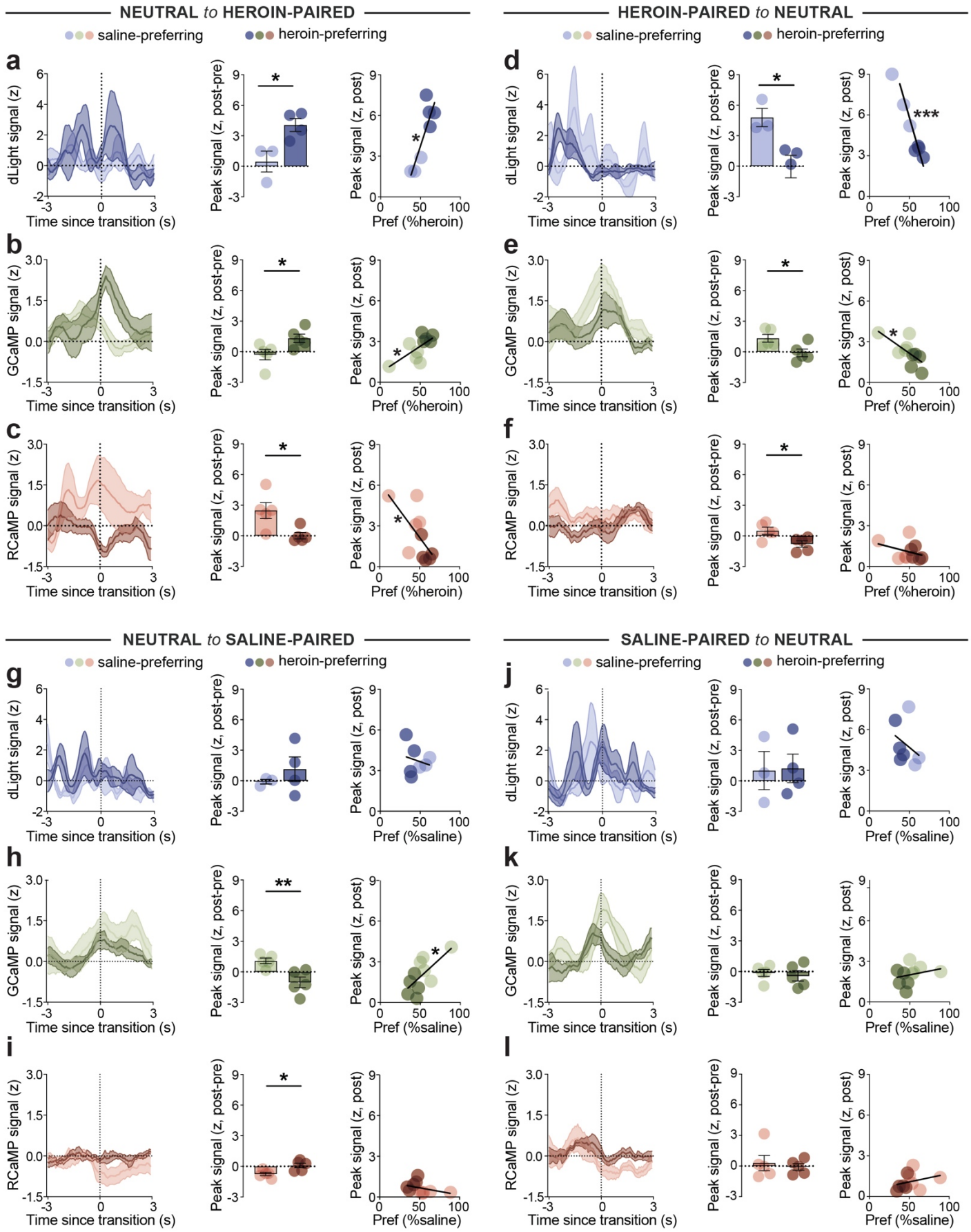

Figure 3.5 | Entry to a preferred heroin context is accompanied by enhanced DA and dMSN signaling and weakened iMSN signaling. See previous page for complete legend.

DISCUSSION

Using fiber photometry coupled with a heroin CPP procedure, we demonstrate that expression of a CPP for heroin is signaled in the NAc by an increase in both DA and dMSN signaling, and a decrease in iMSN signaling. These findings are in accordance with the hypothesis that an imbalance in signaling between the accumbal direct and indirect pathways drives addictive behaviors[12]. We also identified stark differences in the balance of activity between the direct and indirect pathways of heroin-preferring (HP) and saline-preferring (SP) rats prior to any drug exposure, with stronger direct pathway tone in HP rats, and stronger indirect pathway tone in SP rats. Together, these data reveal a central role for the NAc in the acquisition and expression of the reinforcing effects of heroin.

Dopaminergic modulation in the NAc contributes to heroin conditioning

While the contribution of DA to the rewarding effects of most potentially addictive drugs (e.g., psychostimulants, nicotine) is well-established[17], the role of DA in opioid reward is more complicated[32]. Opioids increase phasic DA release, and both D1 receptor blockade and D2 receptor deletion blocks morphine reward[33–36]. However, bilateral 6-OHDA lesions of the NAc can block or have no effect on morphine reward[34,36], and chronic blockade of both D1 and D2 receptors potentiates the rewarding effects of low doses of heroin[37]. In our experiments, we found that pretreatment with buprenorphine blocked the development of a heroin CPP and associated Fos activity in the NAc. Although buprenorphine weakly activates mu opioid receptors to mildly elevate DA release, it also prevents heroin from binding to the same receptors and driving larger phasic DA release[38]. Thus, buprenorphine administration prior to each conditioning session would produce comparably low levels of DA release in both chambers, preventing the acquisition of a strong conditioned response to heroin. We also observed two striking effects during conditioning that only occurred in rats that developed a strong preference for the heroin-paired chamber: a significant increase in peak DA signaling during the first day of conditioning, and a significant increase in the frequency of DA signals on the final day of conditioning. Further, we found a significant increase in DA signaling preceding entry into the heroin-paired chamber during the final preference test, but only in rats that preferred the heroin-paired chamber. On the other hand, DA signaling was relatively unchanged by heroin in rats that did not develop a heroin preference, and DA signaling during the final preference test for those rats was unchanged relative to the initial preference test. Thus, these data support the idea that DA signaling in the NAc is important for the development of conditioned reinforcement to opioids.

An imbalance in accumbal activity influences sensitivity to heroin conditioning

Importantly, the ability of DA to alter overall accumbal activity is dependent not only on dopaminergic modulation of individual MSNs but also on the network implications of such modulation. Although dMSNs and iMSNs can be differentiated according to their downstream targets (VTA and VP, respectively), both subtypes

of MSNs are heavily interconnected in a local microcircuit of lateral inhibition within the NAc[39]. Indeed, although dMSNs are more likely to collateralize with other dMSNs than iMSNs[40], D2 receptor-mediated disinhibition of iMSN lateral inhibition onto dMSNs is necessary for the locomotor sensitizing effects of cocaine[41]. An imbalance between dMSNs and iMSNs can thereby shape the ability of DA to modulate accumbal activity, with the overall balance in signaling guiding vulnerability to the reinforcing effects of drugs.

Perhaps the strongest evidence in support of a role for a balance of activity in the NAc in encoding vulnerability to behaviors related to heroin addiction was our finding of basal differences in dMSN and iMSN signaling strength between rats that were sensitive or resistant to developing a CPP to heroin following drug treatment. Prior to any heroin exposure, HP rats had slightly stronger dMSN activity than SP rats, but SP rats had >2x stronger iMSN activity than HP rats. Surprisingly, this pattern was observed throughout conditioning and was unchanged by heroin exposure. In fact, initial heroin exposure seemed to exacerbate the signaling imbalance, increasing peak dMSN signaling in HP rats and increasing iMSN signaling in SP rats. These differences in the relative balance of MSN activity between groups was also evident during the final preference test. Specifically, when entering the heroin-paired side, HP rats had strong activation of dMSNs and inactivation of iMSNs, whereas SP rats had strong activation of iMSNs but not dMSNs. Notably, these results are in-line with previous reports of strengthened excitatory inputs onto iMSNs of addiction-resistant mice[16], and provide evidence that iMSNs suppress drug-associated behaviors. Moreover, these findings are in agreement with previous reports showing enhanced dMSN activity preceding entry into a cocaine-paired context[24], supporting a role for dMSNs in driving drug reinforcement across drug classes.

Conclusions

Together, these data highlight a central role for dMSNs and iMSNs, along with NAc DA activity, in encoding individual vulnerability to the reinforcing effects of heroin. Importantly, we reveal innate differences in the relative strength of dMSNs and iMSNs between individuals sensitive to versus resistant to the conditioned reinforcement produced by heroin. Future work will further examine the role of dMSNs and iMSNs in encoding individual vulnerability to other facets of opioid addiction, with a particular focus on differences in excitability from prominent glutamatergic nuclei, such as the medial prefrontal cortex.

ACKNOWLEDGMENTS

We thank Dr. John Neumaier and Dr. Michelle Kelly for providing the CAV2-Cre virus and the UW Molecular Genetics Resource Core (P30DA048736) for producing the AAV1-dLight1.3b virus. This work was supported by grants from the National Institute on Drug Abuse (F31DA047012 to TJO, R01DA036582 to SMF) and the UW Alcohol and Drug Abuse Institute (ADAI-0138 to TJO).

REFERENCES

1. Hedegaard, H., Miniño, A. M. & Warner, M. Drug Overdose Deaths in the United States, 1999-2017. *NCHS Data Brief* (2018).
2. Everitt, B. J., Giuliano, C. & Belin, D. Addictive behaviour in experimental animals: Prospects for translation. *Philosophical Transactions of the Royal Society B: Biological Sciences* (2018). doi:10.1098/rstb.2017.0027
3. Shaham, Y., Shalev, U., Lu, L., De Wit, H. & Stewart, J. The reinstatement model of drug relapse: History, methodology and major findings. *Psychopharmacology* (2003). doi:10.1007/s00213-002-1224-x
4. Grimm, J. W., Hope, B. T., Wise, R. A. & Shaham, Y. Incubation of cocaine craving after withdrawal. *Nature* (2001). doi:10.1038/35084134
5. Gerfen, C. R. & Surmeier, D. J. Modulation of Striatal Projection Systems by Dopamine. *Annu. Rev. Neurosci.* (2011). doi:10.1146/annurev-neuro-061010-113641
6. Calabresi, P., Picconi, B., Tozzi, A., Ghiglieri, V. & Di Filippo, M. Direct and indirect pathways of basal ganglia: A critical reappraisal. *Nature Neuroscience* (2014). doi:10.1038/nn.3743
7. Koob, G. F. & Volkow, N. D. Neurobiology of addiction: a neurocircuitry analysis. *The Lancet Psychiatry* (2016). doi:10.1016/S2215-0366(16)00104-8
8. Kravitz, A. V. *et al.* Regulation of parkinsonian motor behaviours by optogenetic control of basal ganglia circuitry. *Nature* (2010). doi:10.1038/nature09159
9. Albin, R. L., Young, A. B. & Penney, J. B. The functional anatomy of basal ganglia disorders. *Trends Neurosci.* (1989). doi:10.1016/0166-2236(89)90074-X
10. Macpherson, T., Morita, M. & Hikida, T. Striatal direct and indirect pathways control decision-making behavior. *Frontiers in Psychology* (2014). doi:10.3389/fpsyg.2014.01301
11. Cui, G. *et al.* Concurrent activation of striatal direct and indirect pathways during action initiation. *Nature* (2013). doi:10.1038/nature11846
12. O'Neal, T. J., Nooney, M. N., Thien, K. & Ferguson, S. M. Chemogenetic modulation of accumbens direct or indirect pathways bidirectionally alters reinstatement of heroin-seeking in high- but not low-risk rats. *Neuropsychopharmacology* **45**, 1251–1262 (2020).
13. Volkow, N. D. *et al.* Brain DA D2 receptors predict reinforcing effects of stimulants in humans: Replication study. *Synapse* (2002). doi:10.1002/syn.10137
14. Belin, D., Mar, A. C., Dalley, J. W., Robbins, T. W. & Everitt, B. J. High impulsivity predicts the switch to compulsive cocaine-taking. *Science (80-.).* (2008). doi:10.1126/science.1158136
15. Nader, M. A. *et al.* PET imaging of dopamine D2 receptors during chronic cocaine self-administration in monkeys. *Nat. Neurosci.* (2006). doi:10.1038/nn1737
16. Bock, R. *et al.* Strengthening the accumbal indirect pathway promotes resilience to compulsive cocaine use. *Nat. Neurosci.* (2013). doi:10.1038/nn.3369

17. Crummy, E. A., O'Neal, T. J., Baskin, B. M. & Ferguson, S. M. One Is Not Enough: Understanding and Modeling Polysubstance Use. *Frontiers in Neuroscience* **14**, (2020).
18. Phillips, P. E. M., Stuber, G. D., Helen, M. L. A. V., Wightman, R. M. & Carelli, R. M. Subsecond dopamine release promotes cocaine seeking. *Nature* (2003). doi:10.1038/nature01476
19. Swapna, I., Bondy, B. & Morikawa, H. Differential Dopamine Regulation of Ca2+ Signaling and Its Timing Dependence in the Nucleus Accumbens. *Cell Rep.* (2016). doi:10.1016/j.celrep.2016.03.055
20. Plotkin, J. L. *et al.* Regulation of dendritic calcium release in striatal spiny projection neurons. *J. Neurophysiol.* (2013). doi:10.1152/jn.00422.2013
21. Bailey, C. H., Giustetto, M., Huang, Y. Y., Hawkins, R. D. & Kandel, E. R. Is Heterosynaptic modulation essential for stabilizing hebbian plasiticity and memory. *Nat. Rev. Neurosci.* (2000). doi:10.1038/35036191
22. Luo, Z., Volkow, N. D., Heintz, N., Pan, Y. & Du, C. Acute cocaine induces fast activation of D1 receptor and progressive deactivation of D2 receptor striatal neurons: In vivo optical microprobe [Ca 2+] i imaging. *J. Neurosci.* (2011). doi:10.1523/JNEUROSCI.2369-11.2011
23. Park, K., Volkow, N. D., Pan, Y. & Du, C. Chronic cocaine dampens dopamine signaling during cocaine intoxication and unbalances D1 over D2 receptor signaling. *J. Neurosci.* (2013). doi:10.1523/JNEUROSCI.1935-13.2013
24. Calipari, E. S. *et al.* In vivo imaging identifies temporal signature of D1 and D2 medium spiny neurons in cocaine reward. *Proc. Natl. Acad. Sci. U. S. A.* (2016). doi:10.1073/pnas.1521238113
25. Kremer, E. J., Boutin, S., Chillon, M. & Danos, O. Canine Adenovirus Vectors: an Alternative for Adenovirus-Mediated Gene Transfer. *J. Virol.* (2009). doi:10.1128/jvi.74.1.505-512.2000
26. Paxinos, G., Watson, C. R. R. & Emson, P. C. AChE-stained horizontal sections of the rat brain in stereotaxic coordinates. *J. Neurosci. Methods* (1980). doi:10.1016/0165-0270(80)90021-7
27. Martianova, E., Aronson, S. & Proulx, C. D. Multi-fiber photometry to record neural activity in freely-moving animals. *J. Vis. Exp.* (2019). doi:10.3791/60278
28. Proulx, C. D. *et al.* A neural pathway controlling motivation to exert effort. *Proc. Natl. Acad. Sci. U. S. A.* (2018). doi:10.1073/pnas.1801837115
29. Patriarchi, T. *et al.* Ultrafast neuronal imaging of dopamine dynamics with designed genetically encoded sensors. *Science (80-.).* (2018). doi:10.1126/science.aat4422
30. Yasuda, R. *et al.* Imaging calcium concentration dynamics in small neuronal compartments. *Sci. STKE* (2004). doi:10.1126/stke.2192004pl5
31. Osanai, M., Yamada, N. & Yagi, T. Long-lasting spontaneous calcium transients in the striatal cells. *Neurosci. Lett.* (2006). doi:10.1016/j.neulet.2006.04.012
32. Badiani, A., Belin, D., Epstein, D., Calu, D. & Shaham, Y. Opiate versus psychostimulant addiction: The differences do matter. *Nature Reviews Neuroscience* (2011). doi:10.1038/nrn3104

33. Johnson, S. W. & North, R. A. Opioids excite dopamine neurons by hyperpolarization of local interneurons. *J. Neurosci.* (1992). doi:10.1523/jneurosci.12-02-00483.1992
34. Shippenberg, T. S., Bals-Kubik, R. & Herz, A. Examination of the neurochemical substrates mediating the motivational effects of opioids: Role of the mesolimbic dopamine system and D-1 vs. D-2 dopamine receptors. *J. Pharmacol. Exp. Ther.* (1993).
35. Maldonado, R. *et al.* Absence of opiate, rewarding effects in mice lacking dopamine D2 receptors. *Nature* (1997). doi:10.1038/41567
36. Sellings, L. H. L. & Clarke, P. B. S. Segregation of amphetamine reward and locomotor stimulation between nucleus accumbens medial shell and core. *J. Neurosci.* (2003). doi:10.1523/jneurosci.23-15-06295.2003
37. Stinus, L. *et al.* Chronic flupentixol treatment potentiates the reinforcing properties of systemic heroin administration. *Biol. Psychiatry* (1989). doi:10.1016/0006-3223(89)90052-8
38. Isaacs, D. P. *et al.* Buprenorphine is a weak dopamine releaser relative to heroin, but its pretreatment attenuates heroin-evoked dopamine release in rats. *Neuropsychopharmacol. Reports* (2020). doi:10.1002/npr2.12139
39. Burke, D. A., Rotstein, H. G. & Alvarez, V. A. Striatal Local Circuitry: A New Framework for Lateral Inhibition. *Neuron* (2017). doi:10.1016/j.neuron.2017.09.019
40. Taverna, S., Ilijic, E. & Surmeier, D. J. Recurrent collateral connections of striatal medium spiny neurons are disrupted in models of Parkinson's disease. *J. Neurosci.* (2008). doi:10.1523/JNEUROSCI.5493-07.2008
41. Dobbs, L. K. K. *et al.* Dopamine Regulation of Lateral Inhibition between Striatal Neurons Gates the Stimulant Actions of Cocaine. *Neuron* (2016). doi:10.1016/j.neuron.2016.04.031

CHAPTER 4

SEX DIFFERENCES IN HEROIN SENSITIZATION AND HEROIN SEEKING IN FEMALE & MALE RATS

Timothy J. O'Neal, Zackari D. Murphy, Susan M. Ferguson

In preparation for submission to XX

ABSTRACT

The opioid crisis in the US is a public health emergency, and overdose-related deaths have continued to rise, driven largely by heroin-related overdoses in women. Clinical studies have consistently found women to be more vulnerable to opioid addiction than men, yet the vast majority of preclinical research into opioid addiction has focused almost exclusively on males. Gaining insight into the neurobiological mechanisms underlying differences in addiction vulnerability between sexes is imperative and will require renewed focus on sex differences in preclinical models of addiction. Thus, we sought to characterize differences between female and male rats in two behavioral models: locomotor sensitization, to assess differences in the sensitizing effects of heroin; and intermittent-access self-administration, to assess differences in heroin intake, heroin seeking, the motivation to take heroin, and cue-induced relapse to heroin seeking. We demonstrate that despite greater basal locomotor activity in females, both female and male rats sensitize to the effects of repeated heroin. However, the locomotor response sensitizes above basal activity levels in a greater proportion of males than females. Further, although subsets of female and male rats develop low or high-risk addiction phenotypes, the development of a high-risk phenotype occurs in a greater proportion of females than males. Moreover, high-risk females exhibit significantly greater heroin seeking than males, both during acute periods of drug-unavailability and during extinction training. Together, these findings reveal that male rats may be more sensitive to the sensitizing effects of heroin, while female rats may be more sensitive to the development of an addiction-like phenotype after self-administration.

INTRODUCTION

Opioid addiction is a chronic, relapsing disorder, characterized by periods of drug intake, withdrawal, and drug craving[1]. The ongoing opioid epidemic in the United States has resulted in nearly half a million deaths since 1999, and overdose-related deaths during the early months of the COVID-19 pandemic were more than 40% greater than the same time in 2019[2,3]. Although men have historically been more likely to die of a fatal opioid overdose, the death rate has been rising faster in women than men, driven largely by increased heroin use[4]. Indeed, sex is a critical biological variable and is known to influence vulnerability to a range of psychiatric disorders, including anxiety[5], depression[6], and addiction[7]. Women are more likely to be prescribed and misuse prescription opioids than men, contributing to an increased likelihood of an opioid use disorder diagnosis[8–12]. Additionally, women initiate drug use at a lower age, escalate drug intake at a faster rate, maintain intake at a higher dose, experience shorter periods of abstinence, and are more susceptible to relapse than men[13–16]. Despite this robust clinical literature, there is a profound male bias in preclinical research, particularly in neuroscience where single-sex studies of males outnumber those of females 5.5 to 1, even as meta-analyses demonstrate comparable variability between females and males across neuroscience research[17,18].

Funding agencies have attempted to reconcile this bias by mandating the inclusion of both sexes in all preclinical research[19], yet significant disparities remain in preclinical studies of addiction. Moreover, there are notable discrepancies in reports of sex differences, particularly in studies of opioid addiction. Some studies suggest faster acquisition of opioid self-administration and greater motivation for opioids in females than males[20,21], while others report no differences[22,23]. Similarly, some studies report greater heroin self-administration by female rats[24], while others report no sex differences in heroin, fentanyl, or oxycodone self-administration[23,25–28]. Lastly, while females and males do not differ in forced (i.e., food choice-based) abstinence after heroin self-administration[25], females have greater perseverative responding during extinction training than males after intermittent-access fentanyl self-administration[24]. Importantly, however, no differences between females and males have been observed in the somatic symptoms of opioid withdrawal or in opioid-induced analgesia.[29] Thus, it appears that sex differences may be more related to the appetitive and motivational properties of opioids.

Given clinical reports of greater vulnerability to opioid addiction among women[8–12] and the ongoing opioid crisis, it is imperative to understand the neurobiological mechanisms underlying sex differences in the addictive effects of opioids. Thus, in the present study we first investigated sex differences in sensitivity to the locomotor sensitizing effects of heroin, used as a proxy for neurobiological adaptations arising from repeated drug exposure[30], Next, we investigated sex differences in heroin seeking and heroin taking behaviors using an intermittent-access self-administration procedure. Intermittent-access self-administration produces individual

variability in the expression of addiction behaviors[31,32], allowing both general comparisons between sexes as well as comparisons within each severity phenotype.

METHODS

Subjects

Outbred female and male Sprague-Dawley rats (Envigo) were pair-housed in a humidity- and temperature-controlled vivarium, with *ad libitum* access to food and water throughout testing. Rats were acclimated to the vivarium for at least five days and handled for at least three days prior to any procedures. Behavioral testing was done at the beginning of the dark cycle (lights off at 19:00). All procedures were done in accordance with the National Institutes of Health's Office of Laboratory Animal Welfare and were approved by Seattle Children's Research Institute's Institutional Animal Care and Use Committee.

Drugs

Diamorphine HCl (heroin) was obtained through the Drug Supply Program of the National Institute on Drug Abuse (NIDA) and was dissolved in sterile saline (0.9% NaCl). For sensitization experiments, heroin was prepared at a dose of 2 mg/ml and administered *ip* at a volume of 1 ml/kg. For self-administration experiments, individual heroin syringes were prepared based on body weight for administration of 0.075 mg/kg heroin per infusion (50 μl/infusion delivered over 2.8 s).

Heroin psychomotor sensitization

Sensitization apparatus

Behavioral testing was done in locomotor activity boxes (San Diego Instruments) equipped with infrared beam breaks for monitoring locomotion, recorded by consecutive beam breaks and collected in 15s bins (PAS; San Diego Instruments). The floors of locomotor chambers were filled with ~1 cup of fresh bedding prior to each session, and chambers were cleaned daily with 70% ethanol.

Sensitization procedure

Psychomotor sensitization was done as previously described[33], with minor changes. Testing included an initial habituation phase (3 days, 30 min/day) followed by a sensitization phase (9 days, 30 min/day). During habituation, all subjects received an injection of saline and were immediately placed in locomotor chambers for activity monitoring. During sensitization, subjects received an injection of saline or heroin and were immediately placed in locomotor chambers for activity monitoring.

Heroin self-administration

Catheter surgeries

Jugular catheterization surgeries were done as previously described[31,34]. Rats were anesthetized with isoflurane (4-5% induction, 1-2% maintenance; Patterson Veterinary) and received an injection of meloxicam (1 mg/ml, 1 ml/kg *sc*; Patterson Veterinary) prior to surgery for analgesia. The right jugular vein was isolated, and a custom-made silastic tubing catheter (ID = 0.51 mm, OD = 0.94 mm, length = 100 mm) was implanted, tied in place with non-absorbable silk sutures, and attached subcutaneously to a back-mounted port. Following surgery, catheters were flushed daily with a mixture of gentamicin (5 mg/ml) and heparin (3 U/ml) in sterile saline (0.2 ml/day, *iv*) to maintain patency. Catheter patency was checked prior to the first day of self-administration and following the final progressive ratio test with an infusion of brevital sodium (10 mg/ml in sterile saline, 0.05 – 0.2 ml/infusion, *iv*; Methohexital sodium, Patterson Veterinary); rats that became ataxic within 5 seconds of infusion were considered to have maintained patency. Rats that lost patency or whose catheters were damaged (n = 14) prior to the beginning of extinction training were excluded from all analyses.

Self-administration apparatus

Behavioral testing was conducted in standard self-administration chambers equipped with two retractable levers, two white cue lights located above each lever, a house light, and a grid floor (MedAssociates). White cue lights were located on the front wall of the chamber above the levers for localized illumination, while the house light was located near the top of the back wall to illuminate the entire chamber. A syringe pump located outside each chamber was connected to a swivel within each chamber to permit *iv* drug infusions. Self-administration chambers were cleaned daily after each session with 70% ethanol.

Self-administration procedure

Intermittent-access (IntA) heroin self-administration employed a procedure that results in individual variability of addiction severity, as previously described[31]. Each self-administration (SA) session (6 h/day, 10 days) consisted of 12 repeating drug-available (DA; 5 min) and drug-unavailable (DU; 25 min) blocks. Daily IntA SA sessions were signaled by extinction of house lights and extension of two levers into the chamber: lever presses on the active lever resulted in drug delivery (FR1, 0.075 mg/kg/infusion over 2.8 s) and illumination of the cue light (3 s) over the drug lever, while lever presses on the inactive lever had no consequences. At the end of each DA block, house lights re-illuminated to signal the beginning of the DU block and levers remained extended to monitor drug-seeking. Following IntA SA, rats underwent a progressive ratio (PR) test in which the number of lever presses required for an infusion increased with each successive infusion (5, 10, 20, 45, 65, 85, 115, 145, 165, 185, 215, 245) until either 30 min passed without an infusion or 6 h total had elapsed[34]. Next, rats underwent daily extinction sessions (60 min/day, 9 days) during which lever presses no longer resulted in cue presentation or drug delivery. Finally, rats underwent a cue-induced reinstatement test (60 min), during which the drug-paired cue light was presented at the beginning of the session and active lever presses resulted in further cue presentations but no drug delivery.

Addiction severity classification

Six behavioral measures were collected and used to classify individual rats according to their overall addiction severity: (1) *Intake*, calculated as the total number of heroin infusions taken during IntA SA; (2) *Consistency*, calculated as the cumulative percentage of DA blocks across all IntA sessions in which at least one infusion was self-administered; (3) *Seeking*, calculated as the cumulative number of active presses during DU blocks across all IntA sessions; (4) *Motivation*, calculated as the breakpoint during PR testing; (5) *Extinction*, calculated as the total number of active lever presses during extinction training; and (6) *Relapse*, calculated as the total number of active lever presses during cue-induced reinstatement. The raw values for each behavior were converted to z-scores by subtracting the group mean from the individual values and dividing by the standard deviation of the group[35]. Individual z-scores for each animal were then combined to give a cumulative addiction severity score (SS), which was used to classify rats into low-risk ($SS < -1$), moderate-risk ($-1 \leq SS \leq 1$), and high-risk ($SS > 1$).

Statistical analysis

Behavioral data was collected using automated procedures (San Diego Instruments and MedAssociates) and analyzed using GraphPad Prism (V9.0). Locomotor activity was compared via unpaired two-tailed *t*-tests (female vs male) or two-way repeated-measures ANOVAs (time x sex or time x drug). Addiction severity metrics were compared using two-way repeated-measures ANOVAs (time x severity) or two-way ANOVAs (severity x sex). All ANOVAs were followed by Sidak's *post-hoc* tests, and statistical significance was set at $p < .05$ for all comparisons. Data are shown throughout as individual subjects and/or mean ± SEM.

RESULTS

Female and male rats are sensitive to the locomotor sensitizing effects of heroin

To assess differences in the sensitizing effects of heroin, female and male rats underwent a heroin sensitization procedure that has previously been shown to induce locomotor sensitization in male rats[33]. Testing included three days of habituation, in which all rats received an injection of saline and were placed in locomotor boxes for 30 min, followed by nine days of sensitization, in which rats received daily injections of either saline or heroin and were placed in locomotor boxes for 30 min (**Figure 4.1a**). A two-way ANOVA revealed a significant sex x time interaction on locomotor activity on the last day of habituation (Day 0: $F_{(29, 870)} = 1.93$, $p = .0025$; **Figure 4.1b**), with significantly greater basal locomotion in females versus males (unpaired *t*-test: $t_{(30)} = 5.45$, $p < .0001$; **Figure 4.1c**), consistent with previous reports[36]. On the first day of sensitization, heroin significantly reduced locomotion in both female rats (two-way ANOVA, main effect of drug: $F_{(1,14)} = 12.59$, $p = .0032$; **Figure 4.1d**) and male rats (two-way ANOVA, main effect of drug: $F_{(1,14)} = 20.92$, $p = .0004$; **Figure 4.1e**). On the ninth day of sensitization, however, whereas heroin-treated females had comparable

levels of locomotion to saline-treated females (two-way RM ANOVA, no main effect of drug: $F_{(1,14)} = 0.56$, $p = .47$; **Figure 4.1f**), heroin-treated males had significantly greater locomotion than saline-treated males (two-way RM ANOVA, drug x time interaction: $F_{(29,406)} = 1.76$, $p = .0096$; **Figure 4.1g**), suggesting sex differences in the sensitizing effects of heroin. To characterize the sensitizing effects of heroin in both sexes, locomotor activity was compared on the ninth day of sensitization with the first day of sensitization for saline- and heroin-treated rats. Two-way ANOVAs revealed a significant drug x time interaction for both females ($F_{(1,14)} = 9.51$, $p = .0081$; **Figure 4.1h**) and males ($F_{(1,14)} = 12.03$, $p = .0038$; **Figure 4.1i**), with significantly greater locomotion for heroin-treated females ($p < .0001$) and males ($p < .0001$) after repeated heroin exposure compared to initial heroin

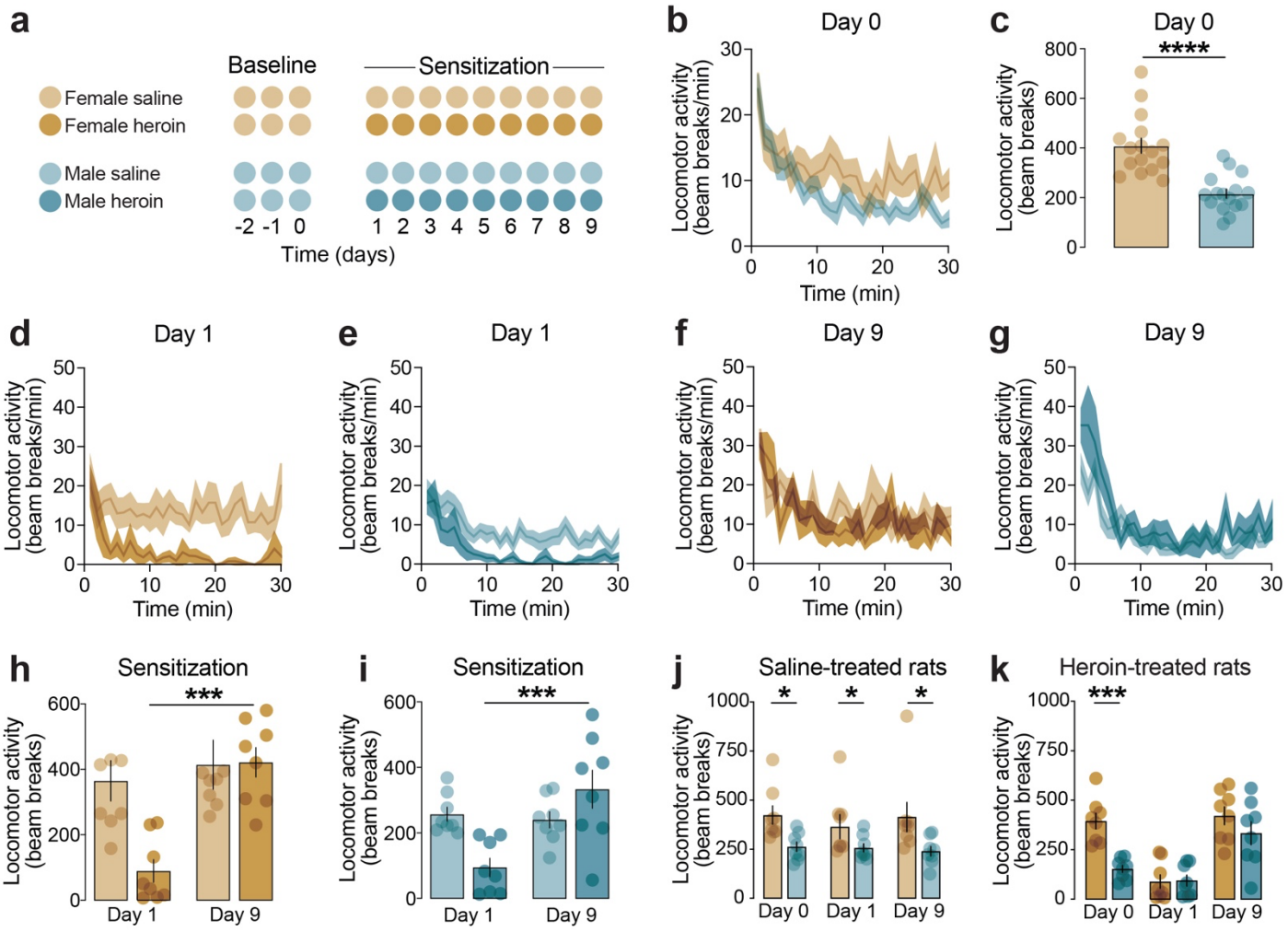

Figure 4.1 | Female and male rats sensitize to the locomotor effects of heroin. (**a**) Timeline of sensitization procedure. Testing included a baseline phase (30 min/day) following injections of saline and a sensitization phase (30 min/day) following injections of either saline or heroin (2 mg/kg, *ip*). (**b-c**) Baseline sex differences in locomotor activity. Female rats had significantly greater locomotor activity during the baseline phase than male rats. (**d-g**) Time course of the locomotor effects of heroin on (**d-e**) the first day of sensitization and (**f-g**) the ninth day of sensitization. (**h-i**) Development of heroin sensitization. Heroin-treated females and males significantly increased their locomotor response to heroin following completion of the sensitization phase. (**j**) Persistent sex differences in saline-treated rats. Saline-treated females had significantly greater locomotor activity than saline-treated males throughout testing. (**k**) Acute sex differences in heroin-treated rats. Female rats had significantly greater locomotor activity during baseline, but heroin-treated female and male rats had similar locomotor activity throughout sensitization. $n = 8$/group; $^{*}p < .05$, $^{***}p < .001$, $^{****}p < .0001$

exposure. Moreover, whereas saline-treated females had greater locomotion than males throughout testing (two-way ANOVA, main effect of sex: $F_{(1,14)} = 9.79$, $p = .007$; **Figure 4.1j**), heroin-treated females had significantly greater activity only during habituation (two-way ANOVA, sex x time interaction: $F_{(2,28)} = 7.42$, $p = .002$; **Figure 4.1k**). Thus, despite basal differences in locomotor activity, both female and male rats appear sensitive to the locomotor sensitizing effects of heroin.

Subsets of female and male rats develop an addiction-like phenotype after heroin self-administration

To further examine sex differences in the behavioral effects of heroin, female and male rats underwent an intermittent-access (IntA) heroin self-administration procedure that produces subsets of addiction-sensitive ("high-risk") and addiction-resistant ("low-risk") rats[31]. IntA sessions included twelve 5-min drug available (DA) blocks on an FR1 schedule separated by 25-min drug unavailable (DU) blocks. Following IntA training, rats underwent a PR test, extinction training, and a cue-induced reinstatement test (**Figure 4.2a**). Six behavioral metrics were collected throughout testing and used to classify individual rats as high- or low-risk for the expression of addictive behaviors. During IntA self-administration, two-way ANOVAs of daily heroin intake revealed significant severity x day interactions for both females ($F_{(12,201)} = 2.21$, $p = .012$; **Figure 4.2b**) and males ($F_{12,183)} = 1.89$, $p = .038$; **Figure 4.2c**), with high-risk rats escalating their intake significantly more than low-risk rats. Accordingly, there was a significant main effect of severity on cumulative heroin intake ($F_{(1,34)} = 31.01$, $p < .0001$; **Figure 4.2d**), though females and males within each severity group had comparable intake (no severity x sex interaction: $F_{(1,34)} = 1.57$, $p = .22$). However, a two-way ANOVA of intake consistency (i.e., percent of DA blocks with drug intake) revealed a significant severity x sex interaction ($F_{(1,34)} = 4.11$, $p = .041$), with low-risk males taking heroin significantly more often than low-risk females ($p = .002$; **Figure 4.2e**). During IntA self-administration, two-way ANOVAs of daily heroin seeking (i.e., presses during DU blocks) revealed significant severity x day interactions for both females ($F_{(12,200)} = 2.51$, $p = .004$; **Figure 4.2f**) and males ($F_{(12,201)} = 2.08$, $p = .019$; **Figure 4.2g**), with high-risk rats escalating heroin seeking significantly more than low-risk rats. Interestingly, there was a significant severity x sex interaction on total heroin seeking during IntA sessions ($F_{(1,37)} = 7.99$, $p = .008$), with high-risk females actively seeking heroin during cued unavailability significantly more than high-risk males ($p = .0006$; **Figure 4.2h**). During progressive ratio testing, high-risk rats had significantly greater motivation to work for heroin than low-risk rats (two-way ANOVA, main effect of severity: $F_{(1,34)} = 29.02$, $p < .0001$; **Figure 4.2i**), though females and males within each severity group had comparable motivation (no severity x sex interaction: $F_{(1,34)} = 0.18$, $p = .68$). During extinction training, two-way ANOVAs of perseverative drug seeking revealed significant severity x day interactions for both females ($F_{(8,96)} = 5.36$, $p < .0001$; **Figure 4.2j**) and males ($F_{(8,96)} = 2.31$, $p = .026$; **Figure 4.2k**), with high risk rats continuing to respond on the active lever despite the action/outcome devaluation during extinction. Similar to heroin seeking during IntA sessions, there was a significant severity x sex interaction on total heroin seeking during extinction training ($F_{(1,24)} = 6.26$, $p = .019$), with high-risk females continuing to seek heroin significantly more than high-risk males

(p = .022; **Figure 4.2l**). Lastly, during cue-induced reinstatement testing, high-risk rats had significantly greater responding on the previously drug-paired lever in response to cue presentation than low-risk rats (two-way

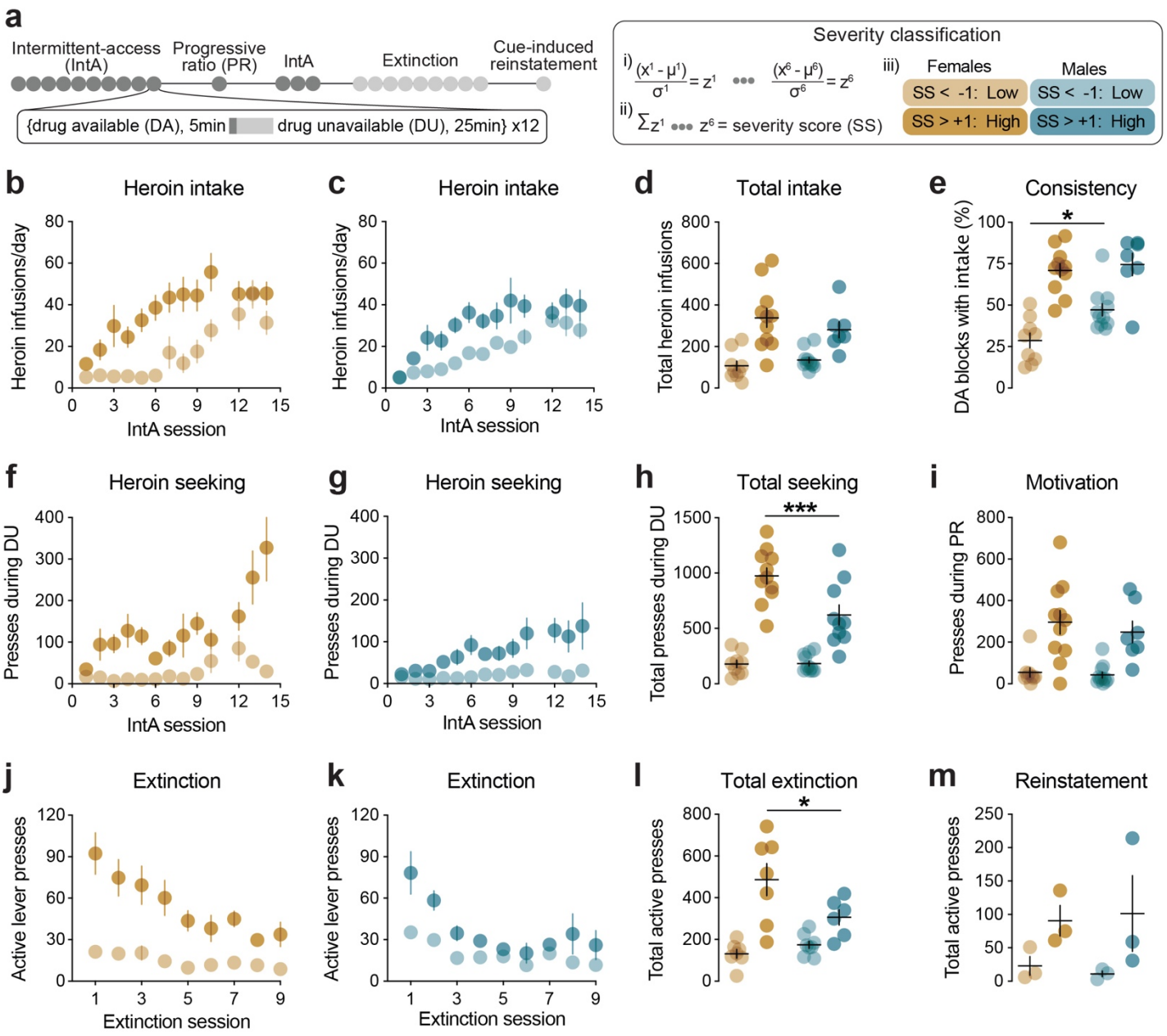

Figure 4.2 | Female and male rats develop addiction-like behaviors after heroin self-administration. (**a**) Timeline of self-administration procedure and severity classification. *Left*: dark grey: periods of drug availability (DA); light gray: periods of drug unavailability (DU). *Right*: (i) raw behavioral data were converted to z-scores, (ii) z-scores were combined to give a cumulative severity score (SS), and (iii) individual rats were classified as low-risk (SS < -1; light orange/blue) or high-risk (SS > +1; dark orange/blue). (**b-d**) High-risk rats self-administered significantly more heroin than low-risk rats, but there were no sex differences within each severity phenotype. (**e**) Low-risk males self-administered heroin during significantly more DA blocks than low-risk females. (**f-g**) High-risk rats pressed the drug-paired lever during DU blocks significantly more than low-risk rats, and (**h**) high-risk females had greater cumulative heroin seeking during DU blocks than high-risk males. (**i**) High-risk rats had greater motivation for heroin than low-risk rats during PR testing, but there were no sex differences within each severity group. (**j-k**) High-risk rats pressed the drug-paired lever during extinction sessions significantly more than low-risk rats, and (**l**) high-risk females had greater cumulative heroin seeking during extinction than high-risk males. (**m**) High-risk rats had greater cue-induced reinstatement of heroin seeking than low-risk rats, but there were no sex differences within each severity group. n = 3-12/group; *p < .05, ***p < .001

ANOVA, main effect of severity: $F_{(1,8)} = 6.26$, $p = .037$; **Figure 4.2m**), though females and males within each group did not differ (no severity x sex interaction: $F_{(1,8)} = 0.13$, $p = .73$).

DISCUSSION

Using locomotor sensitization and self-administration procedures, we sought to characterize sex differences in the behavioral effects of heroin in female and male rats. In assessing the locomotor sensitizing effects of heroin, we demonstrate that although female rats have greater baseline locomotor activity than male rats, both sexes significantly increase their locomotor response to heroin after repeated exposure. However, the locomotor response sensitized beyond baseline levels more often in males than females (**Figure 4.3a**). Similarly, we demonstrate that intermittent-access heroin self-administration produces subsets of female and male rats that are either low-risk or high-risk for the development of addiction-like behaviors. Surprisingly, we found that within the high-risk phenotype, females exhibit significantly greater heroin seeking than male, while within the low-risk phenotype, males self-administer heroin at a greater frequency than females. Moreover, the majority of female rats expressed a high-risk phenotype, whereas the majority of male rats expressed a low-risk phenotype (**Figure 4.3b**). Together, these data demonstrate subtle, though notable, differences in heroin addiction between female and male rats.

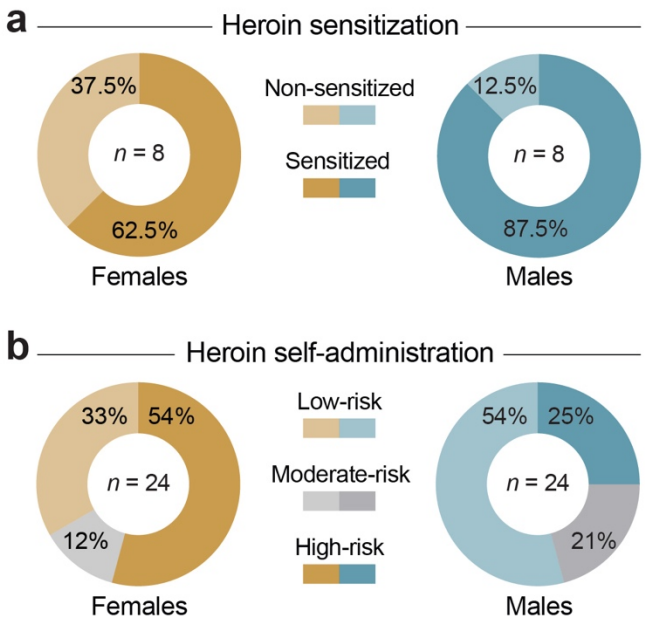

Figure 4.3 | Summary of sex differences in heroin sensitization and self-administration. (**a**) Proportion of female and male rats that sensitized to the effects of heroin (i.e., had greater locomotor activity after the ninth day of heroin relative to habituation). Male rats were more likely to sensitize to the effects of heroin than female rats. (**b**) Proportion of female and male rats that developed an addiction-like phenotype. Female rats were more likely to develop a high-risk phenotype after heroin self-administration than male rats.

Repeated exposure to drugs of abuse leads to an increase in the locomotor-stimulating effects of the drug, which is believed to reflect drug-induced neuroplastic changes in neural circuitry[30,37]. In our study, we found that males were more sensitive to the effects of repeated heroin administration that females. However, females have previously been shown to be more sensitive to the sensitizing effects of cocaine and amphetamine than males[38–41], a difference that is blocked by female ovariectomy[41–43] and enhanced by estradiol treatment[44,45]. Psychostimulants directly enhance striatal dopamine signaling via disruption of dopamine transport[46], and robust sex differences have been established in the regulatory mechanisms controlling dopamine signaling[47]. Importantly, while opioids and psychostimulants both enhance midbrain dopamine release into the nucleus

accumbens, they do so via distinct mechanisms, with opioids disinhibiting midbrain dopamine neurons via inhibition of local and distal inhibitory projections[46]. Thus, it is possible that differences in the regulation of dopamine synthesis, release, and reuptake attributes increased sensitivity to the sensitizing effects of psychostimulants but not opioids in females.

Past studies on sex differences in opioid self-administration have yielded conflicting results[20–23]. Notably, these studies used classic short- or long-access self-administration procedures, focusing on differences between but not within sexes. In our study, we report the development of an addiction-like phenotype following intermittent-access self-administration in a greater proportion of females than males, with significantly greater heroin seeking in high-risk females than high-risk males. However, we did not identify any differences in heroin intake, the escalation of intake, or the motivation to take heroin between females and males in either severity group. This is again in contrast with psychostimulant studies that have reported greater total intake, increased escalation, and higher motivation in females compared to males[14], an effect that is blocked by ovariectomy and restored by estradiol treatment[48]. Conversely, estradiol has no effect on the acquisition or maintenance of heroin self-administration in females[23,49], and estradiol treatment has no effect on cue-induced reinstatement of heroin seeking[50]. Together, these data indicate a role for hormonal regulation of behaviors associated with psychostimulants but not opioids. Unfortunately, estrous cycle was not monitored for the experiments described here, so the influence of ovarian hormone levels on sex differences in heroin seeking cannot be determined.

CONCLUSIONS

We report subtle though notable sex differences in the behavioral effects of heroin in female and male rats. Both female and male rats significantly increase their behavioral response to repeated heroin exposure, but a greater proportion of males sensitizes beyond their basal activity levels than females. Conversely, subsets of both female and male rats develop an addiction-like phenotype after intermittent-access heroin self-administration, but a greater proportion of females develop a high-risk phenotype, and high-risk females engage in significantly more heroin seeking than high-risk males.

ACKNOWLEDGMENTS

This work was supported by grants from the National Institute on Drug Abuse (F31DA047012 to TJO, R01DA036582 to SMF).

REFERENCES

1. Koob, G. F. & Volkow, N. D. Neurobiology of addiction: a neurocircuitry analysis. *The Lancet Psychiatry* (2016). doi:10.1016/S2215-0366(16)00104-8
2. CDC. Provisional Drug Overdose Death Counts. *Centers for Disease Control* (2019).
3. CDC. *Overdose Deaths Accelerating During COVID-19*. (2020).
4. Marsh, J. C., Park, K., Lin, Y. A. & Bersamira, C. Gender differences in trends for heroin use and nonmedical prescription opioid use, 2007–2014. *J. Subst. Abuse Treat.* (2018). doi:10.1016/j.jsat.2018.01.001
5. Donner, N. C. & Lowry, C. A. Sex differences in anxiety and emotional behavior. *Pflugers Archiv European Journal of Physiology* (2013). doi:10.1007/s00424-013-1271-7
6. Piccinelli, M. & Wilkinson, G. Gender differences in depression. Critical review. *British Journal of Psychiatry* (2000). doi:10.1192/bjp.177.6.486
7. Becker, J. B., McClellan, M. L. & Reed, B. G. Sex differences, gender and addiction. *Journal of Neuroscience Research* (2017). doi:10.1002/jnr.23963
8. Hemsing, N., Greaves, L., Poole, N. & Schmidt, R. Misuse of prescription opioid medication among women: A scoping review. *Pain Research and Management* (2016). doi:10.1155/2016/1754195
9. Mazure, C. M. & Fiellin, D. A. Women and opioids: something different is happening here. *The Lancet* (2018). doi:10.1016/S0140-6736(18)31203-0
10. Huhn, A. S., Berry, M. S. & Dunn, K. E. Review: Sex-Based Differences in Treatment Outcomes for Persons With Opioid Use Disorder. *American Journal on Addictions* (2019). doi:10.1111/ajad.12921
11. Koons, A. L., Rayl Greenberg, M., Cannon, R. D. & Beauchamp, G. A. Women and the Experience of Pain and Opioid Use Disorder: A Literature-based Commentary. *Clin. Ther.* (2018). doi:10.1016/j.clinthera.2017.12.016
12. Hirschtritt, M. E., Delucchi, K. L. & Olfson, M. Outpatient, combined use of opioid and benzodiazepine medications in the United States, 1993–2014. *Prev. Med. Reports* (2018). doi:10.1016/j.pmedr.2017.12.010
13. Zilberman, M., Tavares, H. & El-Guebaly, N. Gender Similarities and Differences: The Prevalence and Course of Alcohol- and Other Substance-Related Disorders. *Journal of Addictive Diseases* (2003). doi:10.1300/J069v22n04_06
14. Becker, J. B. & Hu, M. Sex differences in drug abuse. *Frontiers in Neuroendocrinology* (2008). doi:10.1016/j.yfrne.2007.07.003
15. Randall, C. L. *et al.* Telescoping of landmark events associated with drinking: A gender comparison. *J. Stud. Alcohol* (1999). doi:10.15288/jsa.1999.60.252
16. Zachry, J. E., Johnson, A. R. & Calipari, E. S. Sex Differences in Value-Based Decision Making Underlie Substance Use Disorders in Females. *Alcohol and Alcoholism* (2019). doi:10.1093/alcalc/agz052

17. Becker, J. B., Prendergast, B. J. & Liang, J. W. Female rats are not more variable than male rats: A meta-analysis of neuroscience studies. *Biol. Sex Differ.* (2016). doi:10.1186/s13293-016-0087-5
18. Beery, A. K. & Zucker, I. Sex bias in neuroscience and biomedical research. *Neuroscience and Biobehavioral Reviews* (2011). doi:10.1016/j.neubiorev.2010.07.002
19. Clayton, J. A. & Collins, F. S. NIH to balance sex in cell and animal studies. *Nature* (2014). doi:10.1038/509282a
20. Carroll, M. E., Morgan, A. D., Lynch, W. J., Campbell, U. C. & Dess, N. K. Intravenous cocaine and heroin self-administration in rats selectively bred for differential saccharin intake: Phenotype and sex differences. *Psychopharmacology (Berl).* (2002). doi:10.1007/s00213-002-1030-5
21. Cicero, T. J., Aylward, S. C. & Meyer, E. R. Gender differences in the intravenous self-administration of mu opiate agonists. *Pharmacol. Biochem. Behav.* (2003). doi:10.1016/S0091-3057(02)01039-0
22. Lynch, W. J. & Carroll, M. E. Sex differences in the acquisition of intravenously self-administered cocaine and heroin in rats. *Psychopharmacology (Berl).* (1999). doi:10.1007/s002130050979
23. Stewart, J., Woodside, B. & Shaham, Y. Ovarian hormones do not affect the initiation and maintenance of intravenous self-administration of heroin in the female rat. *Psychobiology* (1996). doi:10.3758/BF03331967
24. Bakhti-Suroosh, A., Towers, E. B. & Lynch, W. J. A buprenorphine-validated rat model of opioid use disorder optimized to study sex differences in vulnerability to relapse. *Psychopharmacology (Berl).* (2021).
25. Venniro, M., Zhang, M., Shaham, Y. & Caprioli, D. Incubation of Methamphetamine but not Heroin Craving after Voluntary Abstinence in Male and Female Rats. *Neuropsychopharmacology* (2017). doi:10.1038/npp.2016.287
26. Reiner, D. J. *et al.* Role of projections between piriform cortex and orbitofrontal cortex in relapse to fentanyl seeking after palatable food choice-induced voluntary abstinence. *J. Neurosci.* (2020). doi:10.1523/JNEUROSCI.2693-19.2020
27. Fredriksson, I. *et al.* Effect of the dopamine stabilizer (-)-OSU6162 on potentiated incubation of opioid craving after electric barrier-induced voluntary abstinence. *Neuropsychopharmacology* (2020). doi:10.1038/s41386-020-0602-6
28. Bossert, J. M. *et al.* In a Rat Model of Opioid Maintenance, the G Protein–Biased Mu Opioid Receptor Agonist TRV130 Decreases Relapse to Oxycodone Seeking and Taking and Prevents Oxycodone-Induced Brain Hypoxia. *Biol. Psychiatry* (2020). doi:10.1016/j.biopsych.2020.02.014
29. Kimbrough, A. *et al.* Oxycodone self-administration and withdrawal behaviors in male and female Wistar rats. *Psychopharmacology (Berl).* (2020). doi:10.1007/s00213-020-05479-y
30. Everitt, B. J., Giuliano, C. & Belin, D. Addictive behaviour in experimental animals: Prospects for translation. *Philosophical Transactions of the Royal Society B: Biological Sciences* (2018).

doi:10.1098/rstb.2017.0027

31. O'Neal, T. J., Nooney, M. N., Thien, K. & Ferguson, S. M. Chemogenetic modulation of accumbens direct or indirect pathways bidirectionally alters reinstatement of heroin-seeking in high- but not low-risk rats. *Neuropsychopharmacology* **45**, 1251–1262 (2020).
32. Zimmer, B. A., Oleson, E. B. & Roberts, D. C. S. The motivation to self-administer is increased after a history of spiking brain levels of cocaine. *Neuropsychopharmacology* (2012). doi:10.1038/npp.2012.37
33. Morrison, J., Thornton, V. & Ranaldi, R. Chronic intermittent heroin produces locomotor sensitization and long-lasting enhancement of conditioned reinforcement. *Pharmacol. Biochem. Behav.* (2011). doi:10.1016/j.pbb.2011.04.020
34. Yager, L. M., Garcia, A. F., Donckels, E. A. & Ferguson, S. M. Chemogenetic inhibition of direct pathway striatal neurons normalizes pathological, cue-induced reinstatement of drug-seeking in rats. *Addict. Biol.* (2019). doi:10.1111/adb.12594
35. Bock, R. *et al.* Strengthening the accumbal indirect pathway promotes resilience to compulsive cocaine use. *Nat. Neurosci.* (2013). doi:10.1038/nn.3369
36. Smethells, J. R., Greer, A., Dougen, B. & Carroll, M. E. Effects of voluntary exercise and sex on multiply-triggered heroin reinstatement in male and female rats. *Psychopharmacology (Berl).* (2020). doi:10.1007/s00213-019-05381-2
37. Stewart, J. & Badiani, A. Tolerance and sensitization to the behavioral effects of drugs. in *Behavioural Pharmacology* (1993). doi:10.1097/00008877-199308000-00003
38. Davis, B. A., Clinton, S. M., Akil, H. & Becker, J. B. The effects of novelty-seeking phenotypes and sex differences on acquisition of cocaine self-administration in selectively bred High-Responder and Low-Responder rats. *Pharmacol. Biochem. Behav.* (2008). doi:10.1016/j.pbb.2008.03.008
39. Camp, D. M. & Robinson, T. E. Susceptibility to sensitization. I. Sex differences in the enduring effects of chronic d-amphetamine treatment on locomotion, stereotyped behavior and brain monoamines. *Behav. Brain Res.* (1988). doi:10.1016/0166-4328(88)90008-3
40. Harrod, S. B., Booze, R. M., Welch, M., Browning, C. E. & Mactutus, C. F. Acute and repeated intravenous cocaine-induced locomotor activity is altered as a function of sex and gonadectomy. *Pharmacol. Biochem. Behav.* (2005). doi:10.1016/j.pbb.2005.08.005
41. Van Haaren, F. & Meyer, M. E. Sex differences in locomotor activity after acute and chronic cocaine administration. *Pharmacol. Biochem. Behav.* (1991). doi:10.1016/0091-3057(91)90054-6
42. Camp, D. M. & Robinson, T. E. Susceptibility to sensitization. II. The influence of gonadal hormones on enduring changes in brain monoamines and behavior produced by the repeated administration of d-amphetamine or restraint stress. *Behav. Brain Res.* (1988). doi:10.1016/0166-4328(88)90009-5
43. Sircar, R. & Kim, D. Female gonadal hormones differentially modulate cocaine-induced behavioral sensitization in Fischer, Lewis, and Sprague-Dawley rats. *J. Pharmacol. Exp. Ther.* (1999).

44. Forgie, M. L. & Stewart, J. Sex differences in amphetamine-induced locomotor activity in adult rats: Role of testosterone exposure in the neonatal period. *Pharmacol. Biochem. Behav.* (1993). doi:10.1016/0091-3057(93)90555-8
45. Peris, J., Decambre, N., Coleman-Hardee, M. L. & Simpkins, J. W. Estradiol enhances behavioral sensitization to cocaine and amphetamine-stimulated striatal [3H]dopamine release. *Brain Res.* (1991). doi:10.1016/0006-8993(91)91706-7
46. Crummy, E. A., O'Neal, T. J., Baskin, B. M. & Ferguson, S. M. One Is Not Enough: Understanding and Modeling Polysubstance Use. *Frontiers in Neuroscience* **14**, (2020).
47. Zachry, J. E. *et al.* Sex differences in dopamine release regulation in the striatum. *Neuropsychopharmacology* (2020). doi:10.1038/s41386-020-00915-1
48. Lynch, W. J., Roth, M. E., Mickelberg, J. L. & Carroll, M. E. Role of estrogen in the acquisition of intravenously self-administered cocaine in female rats. *Pharmacol. Biochem. Behav.* (2001). doi:10.1016/S0091-3057(01)00455-5
49. Roth, M. E., Casimir, A. G. & Carroll, M. E. Influence of estrogen in the acquisition of intravenously self-administered heroin in female rats. *Pharmacol. Biochem. Behav.* (2002). doi:10.1016/S0091-3057(01)00777-8
50. Vazquez, M., Frazier, J. H., Reichel, C. M. & Peters, J. Acute ovarian hormone treatment in freely cycling female rats regulates distinct aspects of heroin seeking. *Learn. Mem.* (2020). doi:10.1101/lm.050187.119

CHAPTER 5
CONCLUSIONS & FUTURE DIRECTIONS

Timothy J. O'Neal, Abigail Schindler, Whitney Heavner, Stephen E. P. Smith, Susan M. Ferguson

SUMMARY OF MAIN FINDINGS

The goal of this thesis was to combine modern techniques for cell type-specific monitoring and manipulation of neuronal activity with classical behavioral models to gain an understanding of the role of NAc dMSNs and iMSNs in encoding individual vulnerability to heroin addiction. In Chapter 2, I described an intermittent-access heroin self-administration procedure that produces individual variability in the development of addiction-like behaviors, allowing for classification of individual subjects into either high- or low-risk for addiction. By combining this model with dual viral-mediated gene transfer of excitatory or inhibitory DREADDs, I demonstrated a selective role for dMSNs and iMSNs in driving and suppressing, respectively, cue-induced reinstatement of heroin-seeking in high-risk rats. In Chapter 3, I described a heroin conditioned place preference procedure that produces individual variability in conditioned reinforcement for heroin, allowing for classification of individual subjects into either heroin-sensitive or heroin-resistant. By combining this model with targeted expression of biosensors for *in vivo* monitoring of dopamine activity, dMSN activity, and iMSN activity, I demonstrated a robust rise in dopamine and dMSN activity and a fall in iMSN activity for heroin-sensitive rats, as well as a ramp in iMSN activity in heroin-resistant rats during exposure to a heroin-paired CS. Moreover, I identified innate differences in the relative strength of dMSN and iMSN activity prior to drug exposure in heroin-sensitive and heroin-resistant rats, with a stronger dMSN tone in heroin-sensitive rats and a stronger iMSN tone in heroin-resistant rats. In Chapter 4, I described an investigation into sex differences in sensitivity to the behavioral effects of heroin using heroin locomotor sensitization and intermittent-access heroin self-administration procedures. In these experiments, I identified an increased sensitivity to the sensitizing effects of heroin in male rats, along with an increased sensitivity to the development of a high-risk addiction phenotype in female rats, driven largely by greater levels of heroin seeking.

Regulation of heroin taking and heroin seeking by accumbens dMSNs and iMSNs

In Chapter 2, I sought to establish the role of NAc dMSNs and iMSNs in mediating heroin seeking and heroin taking, with a particular focus of the role of these two neuronal populations in regulating these behaviors in rats expressing an addictive-like phenotype. This was accomplished via the use of an intermittent-access heroin

self-administration procedure, developed to highlight individual differences in addiction severity. Unlike traditional short- and long-access self-administration procedures that allow continuous access to drug (with the exception of brief time-out periods between infusions), intermittent-access self-administration procedures alternate short periods of drug availability with longer periods of drug unavailability. The difference in how these sessions are structured produces notably different pharmacokinetic profiles. Short- and long-access sessions are characterized by an initial loading phase, with subjects taking multiple infusions to reach their desired level of "high", followed by a maintenance phase, with subjects taking occasional infusions to maintain that level[1]. Intermittent-access sessions are characterized by spikes in brain drug concentration separated by long periods in which brain drug concentration returns to baseline[2,3]. As a result, the motivation to take drug has been shown to be greater after intermittent-access than after short- or long-access self-administration[3–5], and intermittent- but not long-access self-administration results in substantial individual variability in the development of addiction-like behaviors[6,7]. Researchers have taken advantage of this variability by modeling the DSM criteria for addiction in rats, with subsets of rats expressing an addiction-resilient phenotype or an addiction-like phenotype, with increased motivation to take drug, greater drug intake, more persistent drug seeking, and a higher propensity towards cue-induced reinstatement of drug seeking[6–9]. Moreover, following intermittent-access self-administration, subjects exhibit stronger incubation of craving[9,10], a phenomenon where drug craving progressively increases over the course of abstinence[11–13].

Using an intermittent-access procedure for heroin self-administration in concert with additional behavioral tests for assessing the motivation for heroin (via progressive ratio testing) and the ability of a heroin-associated stimulus to reinstate heroin seeking after action/outcome devaluation (via cue-induced reinstatement testing), the role of NAc dMSNs and iMSNs in controlling these behaviors in low- and high-risk rats was examined using bidirectional DREADD manipulations. This included the separate use of inhibitory $G_{i/o}$-coupled DREADDs (hM4Di) and excitatory $G_{q/11}$-coupled DREADDs (hM3Dq) in each cell type, to gain insight into the effect of inactivation and activation of each cell type, respectively. Despite ample evidence demonstrating DREADD-induced modulation of neuronal activity[14,15], I validated the utility of these tools in dMSNs and iMSNs by altering novelty-evoked Fos activation in the NAc[16], with an increase in Fos after dMSN activation or iMSN inactivation and a decrease in Fos after dMSN inactivation of iMSN activation. This Fos data provided support for the overarching hypothesis of my thesis: that the balance in signaling between dMSNs and iMSNs is a major predictor for the initiation of goal-directed actions. To test this in the context of addiction, four groups of rats (dMSN-hM4Di, dMSN-hM3Dq, iMSN-hM4Di, iMSN-hM3Dq) underwent the intermittent-access procedure outlined above, with each subject receiving two progressive ratio tests and two cue-induced reinstatement tests: one following injection of clozapine-N-oxide (CNO) to activate DREADDs, and one following injection of vehicle as a control. While these manipulations failed to alter the motivation to self-administer heroin

(discussed below), there was a selective bidirectional modulation of cue-induced relapse of heroin seeking in high-risk rats: altering the balance in favor of the indirect pathway (dMSN-hM4Di or iMSN-hM3Dq) reduced heroin seeking, whereas altering the balance in favor of the direct pathway (dMSN-hM3Dq or iMSN-hM4Di) enhanced heroin seeking. The finding that heroin seeking could be bidirectionally modulated in high-risk rats is consistent with a role for activation of glutamatergic projections from the prefrontal cortex to the NAc[17–19] and enhanced glutamate release in the NAc during presentation of heroin-associated cues in promoting reinstatement of drug seeking[20,21]. Moreover, the finding that heroin seeking could not be promoted in low-risk rats suggests the emergence of neuroplastic adaptations attributing resilience to the presentation of heroin-associated cues. Abstinence from drug taking (via either extinction training or incubation of craving) has been shown to both alter protein translation and upregulate Ca^{2+} permeable AMPA receptors in the NAc[22,23] and potentiate excitatory inputs to the NAc[24], contributing to enhanced excitability of the NAc. However, whereas abstinence from cocaine taking potentiates excitatory inputs to dMSNs of all mice, these inputs are selectively potentiated onto iMSNs of mice expressing an addiction-resilient phenotype[25]. Moreover, the AMPA to NMDA ratio (a proxy for neuronal excitability) is upregulated in dMSNs of mice that continue cocaine seeking during extinction, but upregulated in iMSNs of mice that refrain from cocaine seeking during extinction[26]. This suggests a direct role for neuroadaptations of dMSNs in the persistence of drug seeking, but a role for neuroadaptations of iMSNs in promoting resilience to drug seeking during abstinence.

Surprisingly, chemogenetic modulation of dMSNs and iMSNs had no effect on the motivation to self-administer heroin, regardless of addiction phenotype. Both dMSNs and iMSNs are activated by presentation of food-associated cues at the start of a progressive ratio test[27], activation of either dMSNs or iMSNs increases the motivation for food pellets[28,29], and inhibition of either population during cue presentation decreases the motivation for food pellets[27]. While this suggests a cooperative role for dMSNs and iMSNs in facilitating motivation, other research indicates a more nuanced, reward-specific role for MSNs in motivation. Activation of iMSNs reduces cocaine self-administration, whereas inactivation of iMSNs enhances the motivation to self-administer cocaine in mice[25]. Moreover, inactivation of dMSNs in the dorsal striatum has no effect on the motivation to self-administer cocaine in rats[8]. The progressive ratio procedure used in my intermittent-access experiments was adapted from this latter study, with a greater cost for both initial and subsequent infusions (5, 10, 20, 30, 45… as opposed to 1, 2, 4, 6, 9….)[30]. While useful for identifying differences in motivation between rats expressing an addiction-like versus addiction-resilient phenotype, it is possible that the use of this exaggerated schedule of reinforcement prevented subtle changes in motivation caused by our DREADD manipulations. However, a recent study using iMSN-D2 receptor knock-out mice demonstrated selective deficits in action initiation and the willingness to work for food rewards under high contingencies[31]. This study involved the genetic deletion of D2 receptors from all iMSNs (i.e., those in the NAc and dorsal striatum)[31], so it

is possible that repeating our manipulation in the dorsal striatum would have an effect on the motivation to self-administer heroin under our progressive ratio contingency. Notably, rats trained to sequentially self-administer heroin and cocaine have significantly greater motivation for cocaine than heroin[32], and cocaine and morphine have opposite effects on iMSNs, with cocaine increasing and morphine decreasing Fos activation[33,34]. Thus, while the circuitry of drug seeking is relatively conserved across drug classes[35,36], regulation of drug taking appears to be dependent on multiple factors, including the type of drug and the reinforcement contingency.

Regulation of conditioned heroin reinforcement by accumbens dMSNs and iMSNs

In Chapter 3, I sought to expand on the findings that dMSNs and iMSNs selectively regulated heroin seeking in high-risk rats by investigating the role of these neuronal populations in conditioned heroin reinforcement, with a particular focus on how dMSN and iMSN signaling differed at baseline and after heroin conditioning in heroin-preferring and heroin-resistant rats. This was accomplished by designing a heroin conditioned place preference (CPP) procedure that was optimized for the development of a heroin preference[37] and incorporating *in vivo* recordings of neuronal activity via fiber photometry throughout testing. Unlike self-administration procedures, CPP involves researcher-administered (i.e., non-contingent) drug delivery. Although this method precludes analysis of individual differences based on volitional drug taking and drug seeking, it holds the amount of drug exposure constant across all subjects. Thus, individual differences in responsiveness to the same amount of heroin could be compared between animals that developed a preference for versus an aversion to heroin. Moreover, the inclusion of fiber photometry recordings prior to any heroin exposure allowed investigation into intrinsic differences in dMSN and iMSN signaling in rats that would later prefer or be resistant to the effects of heroin. Studies using targeted manipulation of dMSNs and iMSNs have emphasized their oppositional control over behavioral output[38–41], and others have shown divergent neuroplastic adaptations in dMSNs and iMSNs in addiction-like and addiction-resistant subjects[25,26,42]. Yet an outstanding question remains whether the signaling balance between dMSNs and iMSNs in drug-naïve individuals contribute to future addiction vulnerability. Consistent with a previous report showing greater iMSN activity than dMSN activity in drug-naïve mice[43], the activity of iMSNs was generally greater than the activity of dMSNs in our drug-naïve rats. However, after retrospective categorization of individual rats based on sensitivity to heroin reinforcement, some dramatic differences were identified between heroin-sensitive and heroin-resistant rats. Prior to any drug exposure, heroin-sensitive rats had roughly equal signaling between dMSNs and iMSNs, but heroin-resistant rats had ~2x greater iMSN signaling than dMSN signaling, indicating a pre-existing signaling imbalance that predicts future addiction vulnerability. Indeed, this imbalance not only persisted throughout testing, but was acutely magnified by heroin exposure: heroin significantly increased peak dMSN signaling in heroin-sensitive rats, but significantly increased peak iMSN signaling in heroin-resistant rats. Moreover, when entering the heroin-paired chamber after heroin conditioning, heroin-sensitive and heroin-resistant rats had a

significant rise in dMSN and iMSN activity, respectively, indicating activation of the “go” and “stop” pathway in rats that were sensitive to and resistant to the reinforcing effects of heroin, respectively.

In addition to basal differences in the strength of dMSNs and iMSNs in heroin-sensitive and heroin-resistant rats, we also differences in the dopaminergic response to heroin between these groups. Heroin-sensitive rats had a stronger peak DA response during the first day of heroin conditioning than heroin-resistant rats, and the frequency of DA events was significantly greater after the fourth day of heroin conditioning in heroin-sensitive but not heroin-resistant rats. Additionally, only heroin-sensitive rats had a robust rise in DA signaling preceding entry into the heroin-paired chamber following heroin conditioning, though heroin-resistant rats had a similar rise in DA preceding exit from the heroin-paired chamber, suggesting an aversion rather than an indifference to heroin in heroin-resistant rats. Notably, although opioids activate VTA DA neurons and increase DA release into the NAc[36], whether DA is necessary for opioid reward has remained an outstanding question[35]. D1 receptor blockade or D2 receptor deletion block morphine reward[44–46], but bilateral 6-OHDA lesions of the NAc can either block or have no effect on morphine reward[44,46], and chronic blockade of both D1 and D2 receptors can potentiate the rewarding effects of heroin[47]. Nevertheless, our data demonstrates selective, robust DA signaling during conditioned heroin reinforcement in heroin-sensitive but not heroin-resistant rats, supporting a role for DA in opioid reward. Moreover, pretreatment with buprenorphine prior to each conditioning session prevented the acquisition of a heroin CPP and activation of the NAc during exploration of the CPP apparatus post-conditioning. Buprenorphine, a partial mu opioid receptor agonist, weakly activates mu opioid receptors in the VTA to mildly elevate DA release, but also prevents heroin from binding to drive larger phasic DA release[48]. Together, these data support a role for DA signaling in the development of heroin preference, but only in heroin-sensitive individuals.

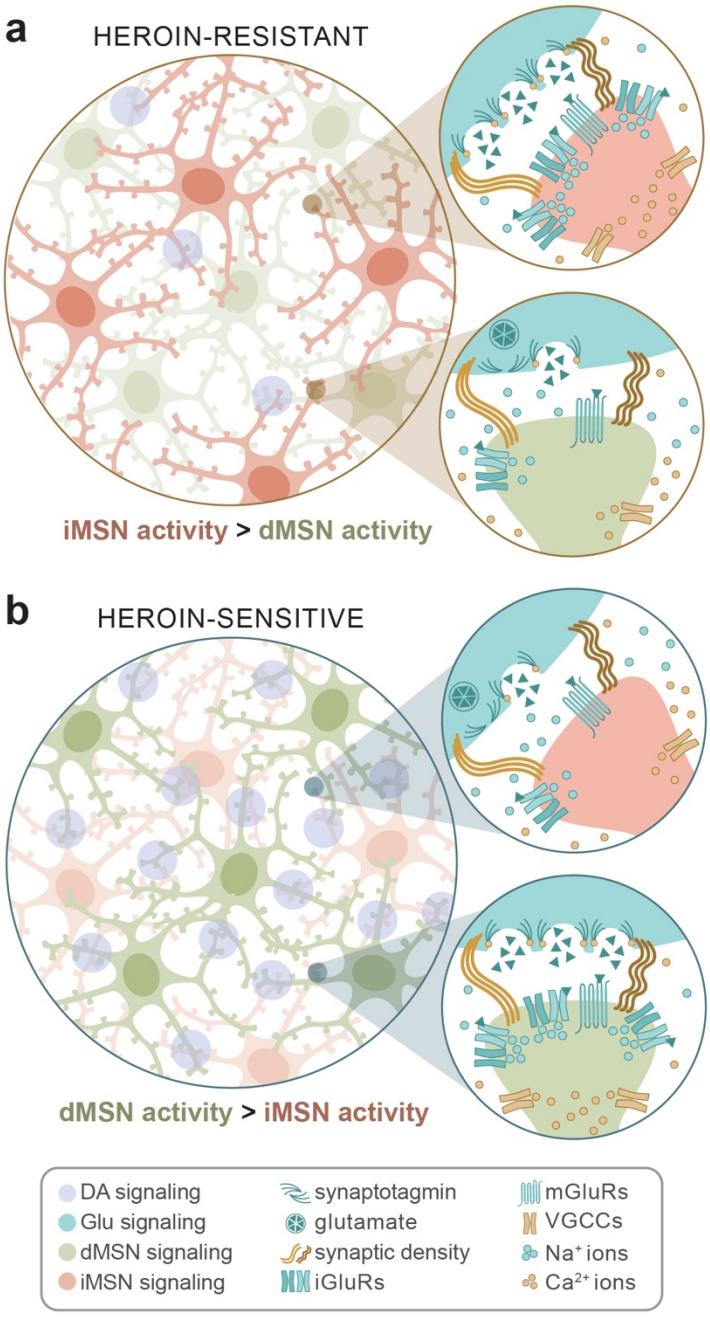

Figure 5.1 I Proposed model of addiction severity encoding in the NAc. (**a**) Heroin-resistant individuals have prominent iMSN signaling, weaker dMSN signaling, and weak DA signaling in response to drug-associated stimuli, and drug exposure increases excitability of iMSNs to suppress the development of addictive behaviors. (**b**) Heroin-sensitive individuals have prominent dMSN signaling, weaker iMSN signaling, and strong DA signaling in response to drug-associated stimuli, and drug exposure increases excitability of dMSNs to facilitate the development of addictive behaviors.

Conclusions

In summary, the experiments presented in this thesis describe a role for dMSNs and iMSNs in encoding and signaling individual vulnerability to heroin seeking and heroin reinforcement in rats (**Figure 5.1**). These results build on a rich existing literature describing bidirectional regulation of motivated behaviors by these two neuronal populations and offer some insight into how these neuronal populations respond to opioids differently than other rewards. Moreover, we provide evidence of intrinsic differences in the signaling strength of dMSNs and iMSNs between individuals sensitive to versus resistant to heroin reinforcement, suggesting individual vulnerability to addiction is at least partially due to basal differences in NAc signaling.

FUTURE DIRECTIONS

Using machine learning to predict individual vulnerability to heroin addiction

The vast majority of preclinical addiction research approaches addiction through a lens of homogeneity, with all drug-exposed rats being grouped together and treated as a monolith. While useful for answering specific questions, this becomes problematic when attempting to translate findings into a broader understanding of addiction. In Chapter 2, we described a model for classifying addiction severity in rats following intermittent-access heroin self-administration. Using that model, we showed that chemogenetic modulation of dMSNs or iMSNs is sufficient to modulate cue-induced heroin seeking in high-risk but not low-risk rats. The inability to modulate heroin seeking in low-risk rats suggests that neuroplasticity

within the NAc is necessary during early self-administration sessions to produce a high-risk phenotype. To investigate this, we developed a model for predicting future addiction severity after the initial days of self-administration, before differences in low- and high-risk rats begin to emerge.

Self-administration data from male and female Sprague-Dawley rats (n = 118) was used to train and validate a machine learning model. Six metrics were extracted from the first five days of intermittent-access self-administration and used for modeling: (1) *Loading infusions*, calculated as the number of infusions taken during the first block of drug availability each day; (2) *Total infusions*, calculated as the total number of infusions taken each day; (3) *Consistency*, calculated as the cumulative percentage of drug available blocks with drug intake; (4) *Seeking*, calculated as the cumulative presses on the drug-paired lever during cued drug unavailability; (5) *Latency*, calculated as the latency to the first infusion each day; and (6) *Inter-infusion interval*, calculated as the average delay between successive infusions during each drug available block. Data from 85% of subjects was used for training the model, while the other 15% was set aside for validation. The performance of six models was compared: logistic regression, random forest, linear support vector, k-nearest neighbors, gradient boosting, and adaptive boosting. All six models performed reasonably well, but logistic regression was found to have the greatest sensitivity, precision, and accuracy. Moreover, this model successfully predicted the severity of >80% of subjects in the validation dataset (**Figure 5.2**). Moving forward, we hope to implement this model in concert with targeted optogenetic stimulation of excitatory inputs to the NAc (e.g., PFC, amygdala, thalamus) coincident with drug delivery/CS presentation to either enhance (future low-risk) or suppress (future high-risk) drug CS encoding and alter the future severity of individual subjects.

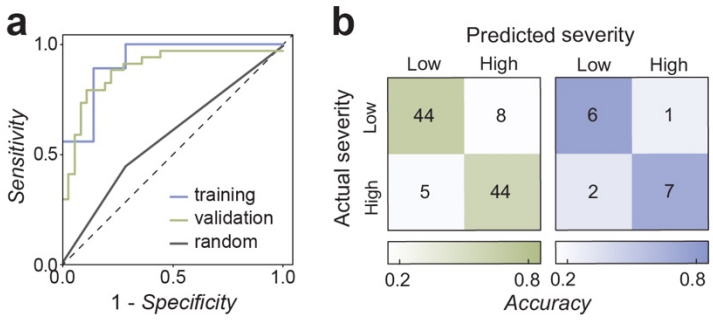

Figure 5.2 I Machine learning model for predicting addiction severity. Training dataset was used to define predictive logistic regression model using cross-validation (k = 10). (**a**) AUC-ROC curves. ROC curves show model performance across all classification thresholds, while AUC shows probability of correct severity prediction. (**b**) Confusion matrices for training dataset (left; n = 101 rats) and validation dataset (right; n = 16 rats). *Top-left*: true negative (TN); *Top-right*: false positive (FP); *Bottom-left*: false negative (FN); *Bottom-right*: true positive (TP). Sensitivity = TP/(TP+FN); Specificity = TN/(TN+FP); Accuracy = (TP+TN)/(total).

Using sensitivity to respiratory depression as a biomarker for heroin addiction

Over the past two decades, there has been a marked change in opioid use patterns in the US. The early 2000s saw a dramatic rise in overall opioid use, driven by abuse of prescription opioids (e.g., oxycontin). By 2010, opioid use began to plateau, but overdose-related mortality continued to escalate. This has been attributed to changes in supply of prescription opioids that led opioid-dependent individuals to transition to cheaper, highly

potent opioids such as heroin and fentanyl. Overdose deaths are now at historic levels, and viable options for long-term treatment of opioid addiction remain limited. Understanding the mechanisms that mediate individual vulnerability to opioid addiction will be critical to gaining control of the ongoing opioid epidemic. Recent research identified a bimodal distribution in acute morphine-induced respiratory depression in drug-naïve mice[49], suggesting innate differences in opioid sensitivity in a subset of individuals. Here, we sought to examine whether initial heroin-induced respiratory depression in drug-naïve rats would predict future addiction severity.

Basal respiratory frequency and opioid-induced respiratory depression were assessed using *in vivo* whole-body plethysmography in custom-built chambers (diameter: 15 cm; height: 22 cm) under normoxic conditions (5.8 psi, ~1.5 LPM oxygen). After baseline recordings (10 min), male Sprague-Dawley rats (n = 8) were given *ip* injections of saline or heroin (2 mg/kg) and returned to chambers for an additional 45 min. Plethysmography chambers were calibrated using 1 ml syringes, and signals were collected using pClamp (v10.4; Molecular Devices, Sunnyvale, CA) as differential pressure changes relative to equally pressurized chambers. Signals were analyzed using ClampFit (v10; Molecular Devices), and rapid high amplitude events (>5 Hz), indicative of grooming, were excluded from analysis. Rats then underwent intermittent-access heroin self-administration as described previously, though all sessions were run during the light cycle to accommodate parallel experiments. As a result, this cohort of rats had a more homogenous severity distribution than rats allowed to self-administer in the dark cycle: 7/8 rats were classified as low-risk and only 1/8 was classified as high-risk, limiting analyses between the two severity phenotypes. Additional plethysmography sessions were conducted the day after progressive ratio and cued-reinstatement testing, to investigate the effects of heroin self-administration and abstinence, respectively, on respiratory rate. Retrospective analysis of initial heroin-induced respiratory depression revealed that the rat who would develop the most high-risk behaviors during self-administration had negligible respiratory depression, relative to a representative low-risk rat (**Figure 5.3**). Moreover, basal respiratory rate for all rats was significantly lower following heroin self-administration, but it rebounded after a period of abstinence. However, acute heroin exposure caused similar respiratory changes in drug-naïve rats, after self-administration, and after abstinence, indicating a lack of tolerance in the systems controlling respiration. Future research will draw from these preliminary findings to fully characterize the effects of heroin on respiratory rate in addiction-sensitive vs addiction-resistant rats, potentially offering insight into a respiratory biomarker for predicting future addiction risk.

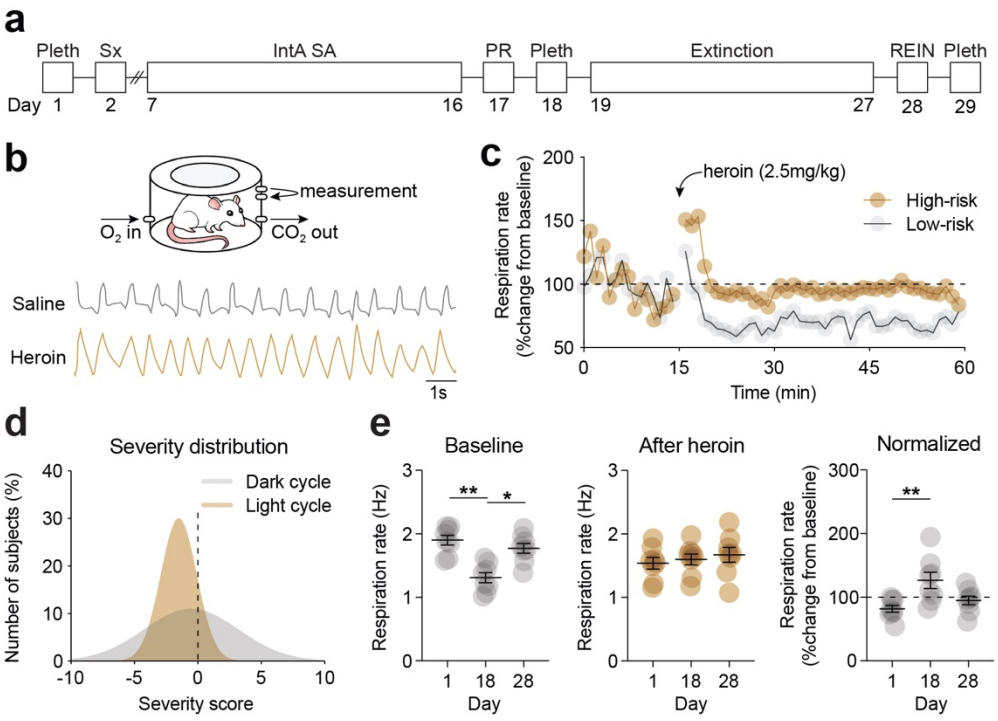

Figure 5.3 I Heroin-induced respiratory depression. (**a**) Timeline for plethysmography (Pleth) recordings during intermittent-access heroin self-administration (IntA SA). (**b**) Pleth setup and representative recordings on day 1. (**c**) Pleth recordings following initial heroin exposure (day 1) in rats that develop addiction-like (high-risk) and addiction-resistant (low-risk) phenotypes. (**d**) Distribution of severity scores following light cycle vs dark cycle IntA SA. (**e**) Respiratory frequency prior to IntA SA (day 1), following PR testing (day 18), and following reinstatement (day 29). *$p < .05$, **$p < .01$

Using a synaptic tag to examine heroin-induced disruptions in synaptic architecture

Exposure to drugs of abuse profoundly alters synaptic plasticity of both dMSNs and iMSNs, and specific changes in neuronal excitability are believed to contribute to the transition to addiction. In particular, changes in accumbal glutamate levels and expression of proteins linked to excitatory signaling (e.g., ionotropic and metabotropic glutamate receptors, cation channels) have been reported following repeated exposure to drugs of abuse. However, due to technical limitations, a full understanding of how drugs of abuse alter plasticity of dMSNs and iMSNs has remained unknown. Here, we worked to validate a recombinant synaptic TAG protein developed by Dr. Steve Smith in rats by targeting it selectively to dMSNs or iMSNs. The TAG construct contains three domains: (1) an extracellular, membrane-spanning truncated human CD4 protein, (2) a green fluorescent protein, and (3) a PSD95 mutant lacking the PZD 1 and 2 domains. mRNA for this construct gets transported to dendrites prior to translation, and the TAG protein expresses perisynaptically to prevent disruption of synaptic transmission. Sprague-Dawley rats underwent stereotaxic surgery for viral delivery of AAV8-DIO-TAG-GFP (500 nl) into the NAc along with CAV2-Cre (500 nl) into the VTA or VP to target dMSNs or iMSNs, respectively. Surgeries were done as previously described, and >3 weeks passed to allow sufficient levels of viral transfection. Subjects were then deeply anesthetized with Euthasol (2 ml/kg *ip*; Patterson Veterinary) and transcardially perfused with ice-cold phosphate-buffered saline (PBS; pH = 7.4). Brains were rapidly extracted, and the NAc was dissected and submerged in HEPES buffer (4 mM with 0.32 M sucrose and protease inhibitors). Next, P2 synaptosomes were prepared from isolated NAc tissue and isolated via flow cytometry using anti-CD4 metallic beads. Purified synaptosomes were then imaged via electron microscopy or

processed for mass spectroscopy analysis. A subset of subjects was perfused with 4% PFA after PBS, and brains were processed for immunohistochemistry using antibodies targeted to CD4.

Confocal imaging revealed substantial overlap between the anti-CD4 antibody and GFP tag for rats selectively expressing the TAG in dMSNs, and the subcellular localization of the TAG was in accordance with preliminary data in cultured neurons (**Figure 5.4**). Moreover, purified synaptosomes were enriched in synaptic material (e.g., synaptosomes, post-synaptic density) and depleted of waste material (e.g., mitochondria). Following these pilot experiments, a full cohort of rats (n = 32) was injected with TAG targeting dMSNs or iMSNs, and subsequently underwent heroin sensitization prior to synaptosome isolation. Additional experiments are underway to further validate the selectivity of the TAG virus and to analyze proteomic data from rats that underwent heroin sensitization.

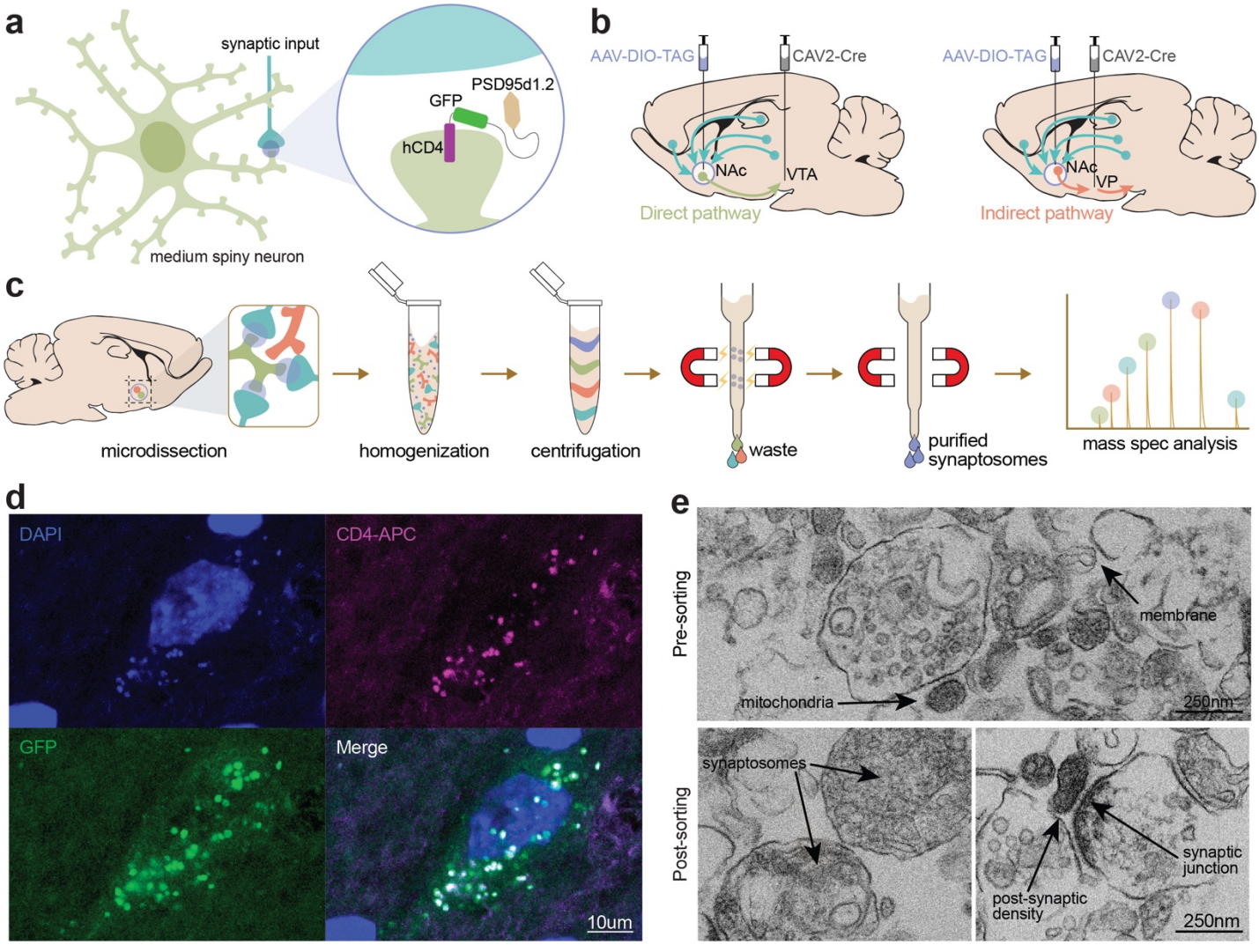

Figure 5.4 I **A recombinant TAG for synaptosome analysis.** (**a**) Schematic of TAG construct. (**b**) Viral strategy for recombinant TAG expression in dMSNs (left) and iMSNs (right). (**c**) Protocol for isolation of purified synaptosomes. (**d**) Immunohistochemical detection of the TAG's GFP and CD4 sequences in a dMSN. (**e**) Electron micrographs of an iMSN synaptosome prep prior to and following purification.

REFERENCES

1. Ahmed, S. H., Walker, J. R. & Koob, G. F. Persistent increase in the motivation to take heroin in rats with a history of drug escalation. *Neuropsychopharmacology* (2000). doi:10.1016/S0893-133X(99)00133-5
2. Allain, F., Minogianis, E. A., Roberts, D. C. S. & Samaha, A. N. How fast and how often: The pharmacokinetics of drug use are decisive in addiction. *Neuroscience and Biobehavioral Reviews* (2015). doi:10.1016/j.neubiorev.2015.06.012
3. Zimmer, B. A., Oleson, E. B. & Roberts, D. C. S. The motivation to self-administer is increased after a history of spiking brain levels of cocaine. *Neuropsychopharmacology* (2012). doi:10.1038/npp.2012.37
4. Kawa, A. B., Allain, F., Robinson, T. E. & Samaha, A. N. The transition to cocaine addiction: the importance of pharmacokinetics for preclinical models. *Psychopharmacology (Berl).* (2019). doi:10.1007/s00213-019-5164-0
5. Kawa, A. B., Bentzley, B. S. & Robinson, T. E. Less is more: prolonged intermittent access cocaine self-administration produces incentive-sensitization and addiction-like behavior. *Psychopharmacology (Berl).* (2016). doi:10.1007/s00213-016-4393-8
6. Garcia, A. F., Webb, I. G., Yager, L. M., Seo, M. B. & Ferguson, S. M. Intermittent but not continuous access to cocaine produces individual variability in addiction susceptibility in rats. *Psychopharmacology (Berl).* (2020). doi:10.1007/s00213-020-05581-1
7. Deroche-Gamonet, V., Belin, D. & Piazza, P. V. Evidence for addiction-like behavior in the rat. *Science (80-.).* (2004). doi:10.1126/science.1099020
8. Yager, L. M., Garcia, A. F., Donckels, E. A. & Ferguson, S. M. Chemogenetic inhibition of direct pathway striatal neurons normalizes pathological, cue-induced reinstatement of drug-seeking in rats. *Addict. Biol.* (2019). doi:10.1111/adb.12594
9. Fragale, J. E., James, M. H. & Aston-Jones, G. Intermittent self-administration of fentanyl induces a multifaceted addiction state associated with persistent changes in the orexin system. *Addict. Biol.* (2020). doi:10.1111/adb.12946
10. Nicolas, C. *et al.* Incubation of Cocaine Craving After Intermittent-Access Self-administration: Sex Differences and Estrous Cycle. *Biol. Psychiatry* (2019). doi:10.1016/j.biopsych.2019.01.015
11. Theberge, F. R. M. *et al.* Association of time-dependent changes in mu opioid receptor mRNA, but not BDNF, TrkB, or MeCP2 mRNA and protein expression in the rat nucleus accumbens with incubation of heroin craving. *Psychopharmacology (Berl).* (2012). doi:10.1007/s00213-012-2784-z
12. Shalev, U., Morales, M., Hope, B., Yap, J. & Shaham, Y. Time-dependent changes in extinction behavior and stress-induced reinstatement of drug seeking following withdrawal from heroin in rats. *Psychopharmacology (Berl).* (2001). doi:10.1007/s002130100748

13. Venniro, M., Zhang, M., Shaham, Y. & Caprioli, D. Incubation of Methamphetamine but not Heroin Craving after Voluntary Abstinence in Male and Female Rats. *Neuropsychopharmacology* (2017). doi:10.1038/npp.2016.287
14. Roth, B. L. DREADDs for Neuroscientists. *Neuron* (2016). doi:10.1016/j.neuron.2016.01.040
15. Ferguson, S. M. *et al.* Transient neuronal inhibition reveals opposing roles of indirect and direct pathways in sensitization. *Nat. Neurosci.* (2011). doi:10.1038/nn.2703
16. Ferguson, S. M., Norton, C. S., Watson, S. J., Akil, H. & Robinson, T. E. Amphetamine-evoked c-fos mRNA expression in the caudate-putamen: The effects of DA and NMDA receptor antagonists vary as a function of neuronal phenotype and environmental context. *J. Neurochem.* (2003). doi:10.1046/j.1471-4159.2003.01815.x
17. McGlinchey, E. M., James, M. H., Mahler, S. V., Pantazis, C. & Aston-Jones, G. Prelimbic to Accumbens Core Pathway Is Recruited in a Dopamine-Dependent Manner to Drive Cued Reinstatement of Cocaine Seeking. *J. Neurosci.* (2016). doi:10.1523/jneurosci.1291-15.2016
18. Rocha, A. & Kalivas, P. W. Role of the prefrontal cortex and nucleus accumbens in reinstating methamphetamine seeking. *Eur. J. Neurosci.* (2010). doi:10.1111/j.1460-9568.2010.07134.x
19. Rubio, F. J. *et al.* Prelimbic cortex is a common brain area activated during cue-induced reinstatement of cocaine and heroin seeking in a polydrug self-administration rat model. *Eur. J. Neurosci.* (2019). doi:10.1111/ejn.14203
20. Peters, J. & De Vries, T. J. Glutamate mechanisms underlying opiate memories. *Cold Spring Harb. Perspect. Med.* (2012). doi:10.1101/cshperspect.a012088
21. LaLumiere, R. T. & Kalivas, P. W. Glutamate Release in the Nucleus Accumbens Core Is Necessary for Heroin Seeking. *J. Neurosci.* (2008). doi:10.1523/jneurosci.5129-07.2008
22. Werner, C. T., Stefanik, M. T., Milovanovic, M., Caccamise, A. & Wolf, M. E. Protein translation in the nucleus accumbens is dysregulated during cocaine withdrawal and required for expression of incubation of cocaine craving. *J. Neurosci.* (2018). doi:10.1523/JNEUROSCI.2412-17.2018
23. Wang, J. *et al.* Cascades of homeostatic dysregulation promote incubation of cocaine craving. *J. Neurosci.* (2018). doi:10.1523/JNEUROSCI.3291-17.2018
24. Ebner, S. R., Larson, E. B., Hearing, M. C., Ingebretson, A. E. & Thomas, M. J. Extinction and Reinstatement of Cocaine-seeking in Self-administering Mice is Associated with Bidirectional AMPAR-mediated Plasticity in the Nucleus Accumbens Shell. *Neuroscience* (2018). doi:10.1016/j.neuroscience.2018.05.043
25. Bock, R. *et al.* Strengthening the accumbal indirect pathway promotes resilience to compulsive cocaine use. *Nat. Neurosci.* (2013). doi:10.1038/nn.3369
26. Roberts-Wolfe, D., Bobadilla, A. C., Heinsbroek, J. A., Neuhofer, D. & Kalivas, P. W. Drug refraining and

seeking potentiate synapses on distinct populations of accumbens medium spiny neurons. *J. Neurosci.* (2018). doi:10.1523/JNEUROSCI.0791-18.2018

27. Natsubori, A. *et al.* Ventrolateral striatal medium spiny neurons positively regulate food-incentive, goal-directed behavior independently of D1 and D2 selectivity. *J. Neurosci.* (2017). doi:10.1523/JNEUROSCI.3377-16.2017
28. Soares-Cunha, C. *et al.* Activation of D2 dopamine receptor-expressing neurons in the nucleus accumbens increases motivation. *Nat. Commun.* (2016). doi:10.1038/ncomms11829
29. Soares-Cunha, C. *et al.* Nucleus accumbens microcircuit underlying D2-MSN-driven increase in motivation. *eNeuro* (2018). doi:10.1523/ENEURO.0386-18.2018
30. Richardson, N. R. & Roberts, D. C. S. Progressive ratio schedules in drug self-administration studies in rats: A method to evaluate reinforcing efficacy. *Journal of Neuroscience Methods* (1996). doi:10.1016/0165-0270(95)00153-0
31. Augustin, S. M., Loewinger, G. C., O'Neal, T. J., Kravitz, A. V. & Lovinger, D. M. Dopamine D2 receptor signaling on iMSNs is required for initiation and vigor of learned actions. *Neuropsychopharmacology* (2020). doi:10.1038/s41386-020-00799-1
32. Crummy, E. A., Donckels, E. A., Baskin, B. M., Bentzley, B. S. & Ferguson, S. M. The impact of cocaine and heroin drug history on motivation and cue sensitivity in a rat model of polydrug abuse. *Psychopharmacology (Berl).* (2019). doi:10.1007/s00213-019-05349-2
33. Uslaner, J. *et al.* Amphetamine and cocaine induce different patterns of c-fos mRNA expression in the striatum and subthalamic nucleus depending on environmental context. *Eur. J. Neurosci.* (2001). doi:10.1046/j.0953-816X.2001.01574.x
34. Ferguson, S. M., Thomas, M. J. & Robinson, T. E. Morphine-induced c-fos mRNA expression in striatofugal circuits: Modulation by dose, environmental context, and drug history. *Neuropsychopharmacology* (2004). doi:10.1038/sj.npp.1300465
35. Badiani, A., Belin, D., Epstein, D., Calu, D. & Shaham, Y. Opiate versus psychostimulant addiction: The differences do matter. *Nature Reviews Neuroscience* (2011). doi:10.1038/nrn3104
36. Crummy, E. A., O'Neal, T. J., Baskin, B. M. & Ferguson, S. M. One Is Not Enough: Understanding and Modeling Polysubstance Use. *Frontiers in Neuroscience* **14**, (2020).
37. Bardo, M. T., Rowlett, J. K. & Harris, M. J. Conditioned place preference using opiate and stimulant drugs: A meta-analysis. *Neurosci. Biobehav. Rev.* (1995). doi:10.1016/0149-7634(94)00021-R
38. Kravitz, A. V. *et al.* Regulation of parkinsonian motor behaviours by optogenetic control of basal ganglia circuitry. *Nature* (2010). doi:10.1038/nature09159
39. Albin, R. L., Young, A. B. & Penney, J. B. The functional anatomy of basal ganglia disorders. *Trends Neurosci.* (1989). doi:10.1016/0166-2236(89)90074-X

40. Macpherson, T., Morita, M. & Hikida, T. Striatal direct and indirect pathways control decision-making behavior. *Frontiers in Psychology* (2014). doi:10.3389/fpsyg.2014.01301
41. Cui, G. *et al.* Concurrent activation of striatal direct and indirect pathways during action initiation. *Nature* (2013). doi:10.1038/nature11846
42. Hearing, M. C. *et al.* Reversal of morphine-induced cell-type-specific synaptic plasticity in the nucleus accumbens shell blocks reinstatement. *Proc. Natl. Acad. Sci. U. S. A.* (2016). doi:10.1073/pnas.1519248113
43. Calipari, E. S. *et al.* In vivo imaging identifies temporal signature of D1 and D2 medium spiny neurons in cocaine reward. *Proc. Natl. Acad. Sci. U. S. A.* (2016). doi:10.1073/pnas.1521238113
44. Shippenberg, T. S., Bals-Kubik, R. & Herz, A. Examination of the neurochemical substrates mediating the motivational effects of opioids: Role of the mesolimbic dopamine system and D-1 vs. D-2 dopamine receptors. *J. Pharmacol. Exp. Ther.* (1993).
45. Maldonado, R. *et al.* Absence of opiate, rewarding effects in mice lacking dopamine D2 receptors. *Nature* (1997). doi:10.1038/41567
46. Sellings, L. H. L. & Clarke, P. B. S. Segregation of amphetamine reward and locomotor stimulation between nucleus accumbens medial shell and core. *J. Neurosci.* (2003). doi:10.1523/jneurosci.23-15-06295.2003
47. Stinus, L. *et al.* Chronic flupentixol treatment potentiates the reinforcing properties of systemic heroin administration. *Biol. Psychiatry* (1989). doi:10.1016/0006-3223(89)90052-8
48. Isaacs, D. P. *et al.* Buprenorphine is a weak dopamine releaser relative to heroin, but its pretreatment attenuates heroin-evoked dopamine release in rats. *Neuropsychopharmacol. Reports* (2020). doi:10.1002/npr2.12139
49. Wei, A. D. & Ramirez, J. M. Presynaptic Mechanisms and KCNQ Potassium Channels Modulate Opioid Depression of Respiratory Drive. *Front. Physiol.* (2019). doi:10.3389/fphys.2019.01407